LA-13665-MS

Approved for public release;
distribution is unlimited.

Development of a General Shocked-Materials-Response Description for Simulations

Los Alamos
NATIONAL LABORATORY

Los Alamos National Laboratory is operated by the University of California for the United States Department of Energy under contract W-7405-ENG-36.

An Affirmative Action/Equal Opportunity Employer

This report was prepared as an account of work sponsored by an agency of the United States Government. Neither The Regents of the University of California, the United States Government nor any agency thereof, nor any of their employees, makes any warranty, express or implied, or assumes any legal liability or responsibility for the accuracy, completeness, or usefulness of any information, apparatus, product, or process disclosed, or represents that its use would not infringe privately owned rights. Reference herein to any specific commercial product, process, or service by trade name, trademark, manufacturer, or otherwise, does not necessarily constitute or imply its endorsement, recommendation, or favoring by The Regents of the University of California, the United States Government, or any agency thereof. The views and opinions of authors expressed herein do not necessarily state or reflect those of The Regents of the University of California, the United States Government, or any agency thereof. Los Alamos National Laboratory strongly supports academic freedom and a researcher's right to publish; as an institution, however, the Laboratory does not endorse the viewpoint of a publication or guarantee its technical correctness.

LA-13665-MS

Issued: July 2000

Development of a General Shocked-Materials-Response Description for Simulations

Steven M. Valone

Los Alamos
NATIONAL LABORATORY
Los Alamos, New Mexico 87545

Table of Contents

I. Abstract and Introduction I-1

II. The Case for Shattering Fragmentation II-1

III. Topical Summaries

1. Equations of State.....III-1
2. Stress-Strain Constitutive Modeling.....III-3
3. Shock Dynamics and Hugoniot Behavior.....III-4
4. Fracture, Spall, and Strength.....III-5
5. Fragmentation.....III-7
6. Reaction Dynamics.....III-8
7. Shocked Porous Media.....III-11
8. Phase Transitions in Shocked Materials.....III-17
9. Multiphase Flow.....III-18

IV. Recommendations.....IV-1

V. Annotated Bibliography.....V-1

Appendix A. References for Porous and/or Polymeric Materials.....VI-1

Appendix B. List of Acronyms.....VII-1

Development of a General Shocked-Materials-Response Description for Simulations

by

Steven M. Valone

Abstract

This report outlines broad modeling issues pertaining to polymeric materials behavior under detonation conditions. Models applicable system wide are necessary to cope with the broad range of polymers and complex composite forms that can appear in Laboratory weapons systems. Nine major topics are discussed to span the breadth of materials, forms, and physical phenomena encountered when shocking polymers and foams over wide ranges of temperatures, pressures, shock strengths, confinement conditions, and geometries. The recommendations for directions of more intensive investigation consider physical fidelity, computational complexity, and application over widely varying physical conditions of temperature, pressure, and shock strength.

I. Introduction

The goal of this overview is to outline the broadest features of polymer materials modeling under shock conditions. The polymer materials range from foams to elastomers to rubbers. They may be present as a layer of material or as a component of a composite. The range of pertinent shock strengths covers the full spectrum from weak impact-driven shocks to explosively driven strong shocks to superdetonation. The main emphasis though is on explosively driven strong shocks with the explosive being a granular heterogeneous one. How an explosively driven shock wave interacts with binders, foams, and polymer composites is the major interest of this overview.

This overview is not intended as a technical review in which the detailed pros and cons of each model are discussed and independently tested. There is an extensive literature on each topic covered here with multiple reviews available to the interested reader. It is impossible to attempt a comprehensive review of each. Consequently, important past work that is already in use or has since been surpassed by other models and concepts may not appear. Also, work related to polymer-aging issues is only included if it seems plausible for the related models to be transcribed to strong-shock conditions.

Instead, this report is intended as a guide for developing the physical submodels needed within comprehensive simulation codes required to perform the Laboratory mission. The submodels need to cover a wide range of physical conditions and forms. For instance, models that treat both foamed and fully dense polymers or that treat porous materials under strong-shock conditions regardless of the constituent material of the foam are the targets of this overview. To complicate the situation further, the submodels vary widely as to their physical-vs.-empirical content. Ultimately, scientifically well founded submodels are the most desirable for making the predictions needed to execute the Laboratory mission, but what level of physical fidelity can be accommodated in the near term will need to be determined separately. When available, comments from the literature about the “computational difficulty” or “numerical robustness” of a model are noted.

Most of our attention will be devoted to the strong-shock regime. Strictly speaking, a distinction should be made between detonation and superdetonation fronts, but we shall do so only when such a distinction is required to clarify the discussion. The generic situation of concern may be viewed schematically in Fig. I-1 which pertains to an unsupported, explosively driven shock. The detonation wave drives the state of the material ahead of the detonation front along the reactant Hugoniot, going from the low-pressure, high-specific-volume state to the high-pressure, low-specific-volume state. The maximum in the reactant Hugoniot is referred to as the von Neumann (vN) spike.

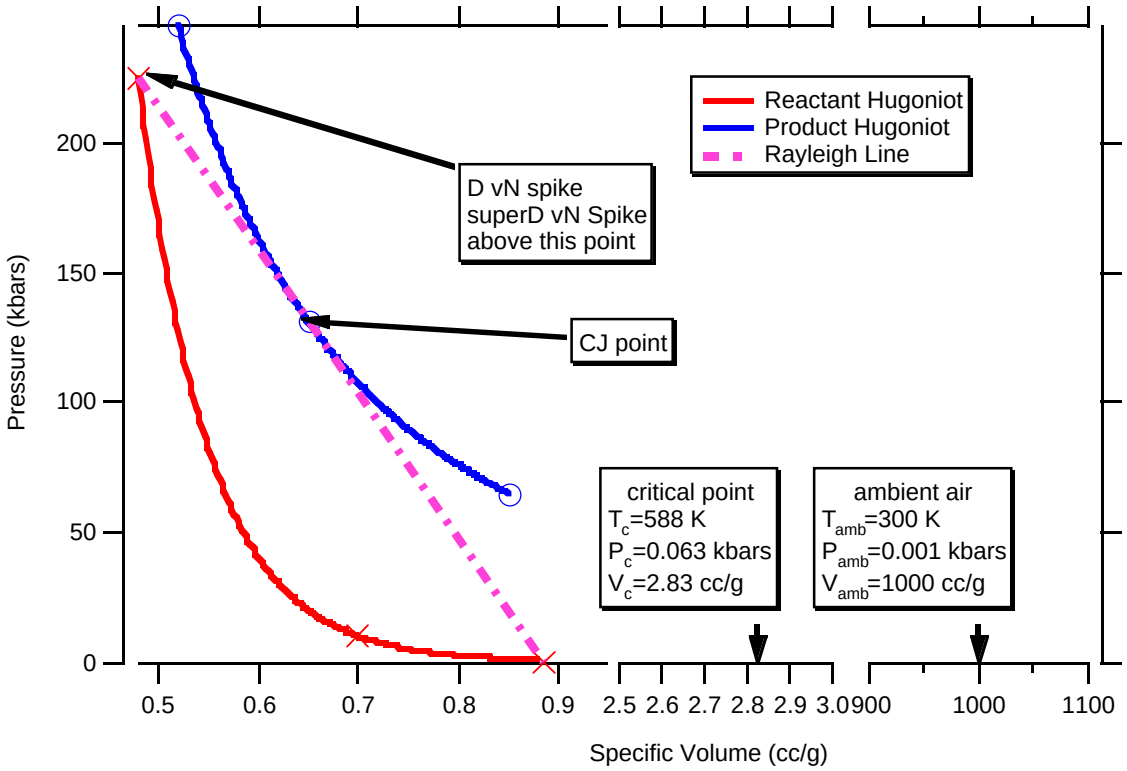

Figure I-1. This figure is a schematic in the pressure-volume (P-V) plane of nitromethane Hugoniot states for reactants and products in an unsupported shock. Also shown are the von Neumann (vN) spike and Chapman-Jouguet (CJ) point for the detonation (D) front. The vN spike for the superdetonation (SD) front is indicated as occurring at higher pressure and lower specific volume compared to the detonation front. The regions of most intense interest are immediately before the vN spike on the reactant Hugoniot and between the vN spike and the CJ point on the product Hugoniot along the Rayleigh line.

Before the detonation reaches the pressure spike, compaction and compression processes occur which are thought to be central to initiation of explosive reactions leading to deflagration and/or detonation. The main portion of the chemical reaction proceeds after the pressure peak but before the CJ point, giving rise to the temperature spike and subsequent release behavior. The details of the transition between these two points, also known as a Rayleigh line, are among the most difficult to measure. The product Hugoniot between the CJ point and the lowest-pressure, highest-specific-volume point represents the release behavior of the detonation.

"Compaction" means both the compaction of high-melting explosive (HMX) grains in a plastic-bonded explosive (PBX) as part of the detonation process and the collapse of pores in the HMX grains and/or polymers. It occurs in the "elastic" preshock region before the vN pressure spike. This issue of exactly what compaction does in an explosively driven shock and how it promotes or retards the ignition of the HMX grains has been studied extensively in recent work by Asay and coworkers [3B] and Bdzil and coworkers [9B]. Fig. I-2 is a re-creation of one of their figures illustrating the basic structure of a detonation wave near the front.

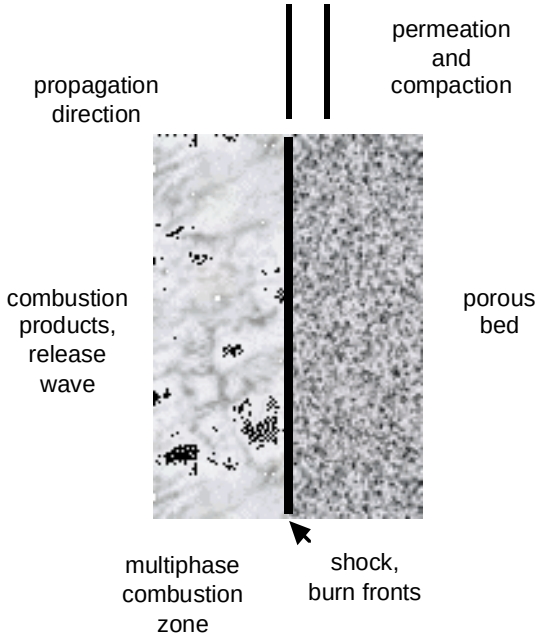

Figure I-2. This illustration shows the key zones of a detonation front in a heterogeneous, solid explosive. (This figure is based on information from Asay et al. [3B]).

The influence of a binder on the compaction process is only now being explored in any detail. Figure 2 also notes the complex, multiphase combustion zone followed by the release wave which is comprised of reaction products.

An outline of chemical reaction stages associated with the burn front and combustion zones of Fig. I-2, particularly that developed by Tarver [6CC] based on the Zel'dovich-von Neumann-Doring (ZND) model, is recreated in Fig. I-3.

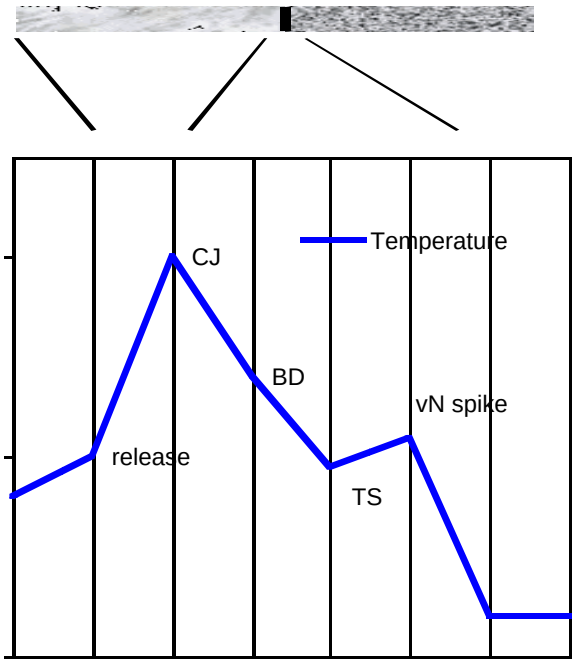

Figure I-3. Stages of chemical reaction in equilibrium and nonequilibrium Zel'dovich, von Neumann, Doring (ZND and NEZND) models of a self-sustaining detonation as explained by Tarver [6CC] in a spatial distribution plot. The stages are the pre-shock front, including compaction; the transition state (TS); the vibrational excitation/bond dissociation (BD); and the Chapman-Jouguet (CJ) state. The TS is endothermic. The direction of propagation is from left to right. The bar at the top is a reduced version of Figure I-2, relating it to this figure.

The intent of this overview is to delineate the responses of polymeric materials in compaction, reaction, and release. Particular emphasis will be placed on the most general features of their behavior. These behaviors may be categorized in terms of compression, reaction/degradation, fragmentation/release, and ionicity. As an aside, there are classes of high-temperature binary reactions for which no discussion in the explosives literature has been found to date.

Reaction and release zones, occupying the region behind the vN spike, entail a complex interplay of chemistry, fragmentation, and energy dissipation coupled to large gradients in pressure and temperature. Note that Asay et al. [3B] view this region as being intrinsically multiphase. Historically though, the bulk of the modeling effort understandably ignores the details of these interactions in favor of capturing the larger-scale behaviors. The region behind the CJ point is ordinarily thought of as having reached some stage of equilibrium. The sense of equilibrium referred to here is a very localized one. In terms of the larger-scale behavior of an unsupported shock, the system at the CJ point is still very far from equilibrium. The release behavior certainly entails condensation of solid reaction byproducts and perhaps fragmentation of solid PBX. Throughout this region, the mix is at high temperatures and pressures which are very difficult to diagnose and characterize, reaching thermodynamically supercritical values. The behavior of released supercritical fluids is addressed below in Section 2.

A central issue spanning all of the above information concerns the extent of nonequilibrium behavior under given shock-strength and confinement conditions. Of primary importance are explosively driven shocks with no confinement or limited confinement so that release and expansion are permitted. While there is still some debate as to the influence of poor equations of state (EOSs) and/or poor constitutive relations on a detonation model, there is a broad consensus on the importance of heterogeneity in general and the two-phase, multicomponent nature of compaction, reaction, and release in particular.

While the detailed nature of nonequilibrium effects for particular explosives and polymers is not yet completely clear, general behavior most often revolves around transfer processes between phases or components with different transport and thermodynamic properties rather than within a given phase. As a result, presently, the dominant approach is to assume that local thermodynamic equilibrium exists separately for each phase, but may or may not exist between the phases depending on the zone being examined and the specifics of the shock and confinement conditions.

In weaker shocks related to damage and insult situations, the extent of disequilibrium behavior will generally be much less. The immediate concern of this report pertains to strong-shock behavior. The influence of history on strong-shock behavior necessarily plays a secondary role. As the strong-shock modeling matures and as weapons systems age further, these influences will become more important.

This overview covers nine areas as indicated by the division of references below: (1) Equations of State, (2) Stress-Strain Constitutive Models, (3) Shock Dynamics and Hugoniot Behavior, (4) Fracture and Strength, (5) Fragmentation, (6) Reaction Dynamics, (7) Shocked Porous Media, (8) Phase Transitions in Shocked Materials, and (9) Multiphase Flow. References are denoted accordingly. Only a broad treatment of any one topic is attempted as each topic is a discipline in itself with a huge literature. The general notion of fragmentation—and, more specifically, shattering—will be discussed first because it seems to be a somewhat novel concept in the context of explosive materials behavior on the release side of the shock front. The general discussion of individual topics will follow. Section V is an annotated bibliography; Appendix A provides references for porous and/or polymeric materials; and Appendix B is a list of acronyms.

II. The Case for Shattering Fragmentation

Damage, failure, and fragmentation processes govern the distribution of shock energy between internal molecular degrees of freedom and the macroscopic convective motion of fragments. In heterogeneous explosives, fragmentation is seen in the release zone of the detonation wave [1S, p. 57]. Here we will focus primarily on fragmentation processes which would predominate in an explosively driven shock that is not too confined. Numerous theories about fragmentation have been applied to nonenergetic materials under shock loading in the past as represented in the sample of this type of work cited in Secs. V.4 and V.5. Partitioning of energy within the fragment-size distribution is crucial to successful modeling of the fragmentation process in nonenergetic materials. In energetic materials, there are more partitions among which to distribute energy, specifically, in reacted and unreacted solids and gases. Inhomogeneities in the form of turbulence [3P, 6BB-6DD, 9D, 9O], might also contribute to detonation behavior, especially in the bond-dissociation and CJ states noted in Fig. I-3 and during the release stages. Inhomogeneities have long been considered an essential source of nonequilibrium effects. Treating the release portion of the wave as a two-phase flow is somewhat different from the common practice for modeling the release wave of explosively driven shocks as a completely gaseous fluid.

A recent calculation possibly indicative of such effects in solid explosives is suggested by the results plotted in Fig. II-1, reproduced from [2L]. The experimental contours of the displacement fields for PBX-9501 show greater spatial dispersion and asymmetry than the corresponding simulation.

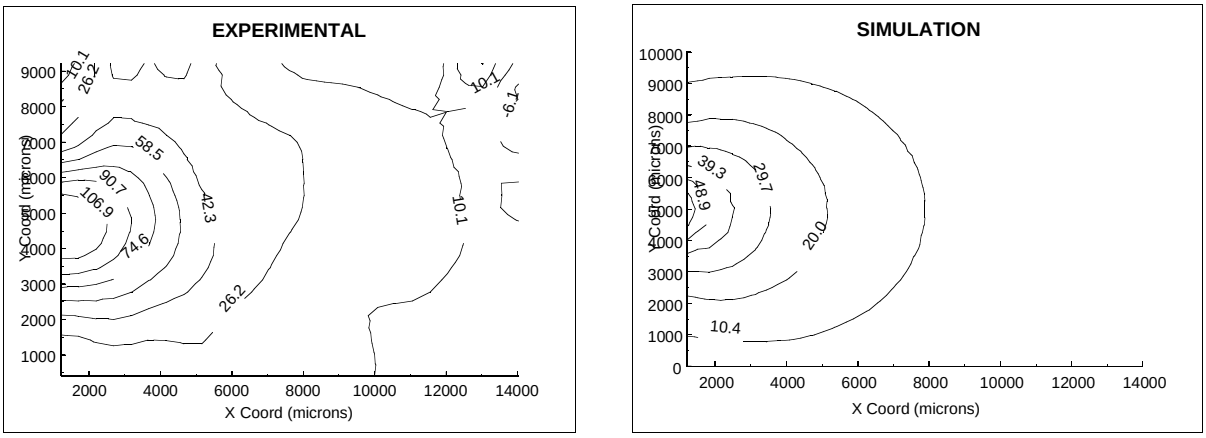

Figure II-1. These illustrations show displacement fields of PBX-9501. The panel at left represents the measured values from laser-fluorescence speckle photography. The panel at right represents the calculated values from the ViscoSCRAM constitutive model in a DYNA3D simulation code. Both are reproduced from [2L], with permission. The contours are in arbitrary units of mass density.

This difference suggests the possibility that not enough energy from the HMX reaction is being deposited as kinetic energy into the products in the early stages of release, the region after the CJ point, as shown in Fig. I-1.

When energy is deposited into a material, it can be distributed among several channels. If there is a fragmentation process associated with the energy deposition, two of the most prominent channels for partitioning that energy are evaporation and convective motion of the center of mass of a fragment. The typical assumption of most simulations is that the detonation energy is deposited instantaneously into gasification of the products. Here we make the case that there is a fragmentation channel for the reaction products as well.

Fragmentation in its most general terms can be classified into two modes, normal and shattering, according to the mass or volume distribution of the fragments. For instance, evaporating water is fragmenting normally. Bulk water changes into monomeric units (i. e., vapor) which have a dimension much smaller than

that of the macroscopic body. In shattering, a plate dropped on the floor from a sufficient height, for example, breaks into pieces that follow a power-law distribution [5J]:

$$W(V) \sim V^{-\alpha-1}. \qquad \text{(II-1)}$$

where W is the probability of finding a fragment of volume V, and α is the critical exponent for the process, which can also be thought of as being related to a fractal dimension. So, in this sense, the relationship between normal fragmentation and shattering may be considered a phase transition. The volume of the fragments covers the full spectrum of volumes or masses from those of the original body to those of the monomer.

One of the most cited works in the field, the investigation of Oddershede et al. [5T], provided some of the most suggestive evidence at that time for the generality of power-law mass distributions, with respect to dimensionality, for the fragment masses. The general form discussed is the dimensional scaling relation for the mass probability, p(a, m), of finding a fragment of mass m in the distribution. If the mass is scaled by the length a, then

$$p(a, m) = a^{-\beta}\, p(m)\ . \qquad \text{(II-2)}$$

All of the dimensional dependence is captured in the exponent β. For most three-dimensional objects, its value falls between 2.4 and 2.6. Most experimenters discuss the integrated form, giving the probability of finding a fragment greater than mass m,

$$P(m) = 1/m \int_m^\infty dm'\, p(a, m') \qquad \text{(II-3)}$$

which, for this overview, is given the specific form

$$P(m) = c\, m^{-\beta}\, e^{-m/m_0} \qquad \text{(II-4)}$$

where c is a scale factor and m_0 is the mass of the monomer. Objects of different dimensionality are fragmented (broken), and the transitions to three-dimensional fragmentation from initially quasi-one- and quasi-two-dimensional modes can be observed.

This concept of a power-law distribution for the fragment masses falls into the broad category of statistical models of failure, fragmentation, and/or spallation. Statistical, stochastic, and kinetic models appear frequently in the failure and fragmentation literature. However, it does not appear that shattering behavior itself—and particularly the current conception which has come to light only since 1993—has been applied to understanding the behavior of polymeric and other nonenergetic materials in explosives and shocks.

Even more recently, we have come to realize that **supercritical fluids also shatter**. It is natural to think of brittle materials shattering. It seems alien to think of supercritical fluids shattering, but they *can* shatter when they are released from their supercritical state. Heat a frying pan, drop a small quantity of water into it, and observe as the water breaks into droplets. If this is a pure shattering process, the water droplets splatter in the same power-law distribution that can be applied to brittle materials. The whole body of the small quantity dropped is superheated and fragments in unison before the energy can be dissipated through evaporation. Experiments at the molecular level for this regime have been performed by Raz, Levine, and coworkers [5J, 5K, 5U]. In their work, small clusters of ammonia molecules impacted a solid surface at carefully controlled velocities. Whenever the impact velocity was above a critical value, the clusters shattered into fragments with a mass distribution given by Eq. (II-2). Cluster size ranged from 2 through 100 molecules. The critical shattering-transition velocity became sharp for clusters as small as 10 molecules. The critical velocity can be thought of as corresponding to both a critical temperature and pressure as well as to the point at which the cluster heats uniformly on the time scale defined by evaporation.

The significance of fragmentation mode to shock propagation is that it affects the partitioning of impact or chemical energy between dissipative and convective channels. Shattering dissipates more energy through

kinetic energy, and hence through convection of the fragments; evaporation dissipates energy into internal degrees of freedom. This distinction is consistent with the very recent radiographic evidence for the mass distribution of fragments of impacted PBX-9501 shown in Fig. II-1. Note that the contours for the experiment vs. the simulation differ by approximately a factor of 2, indicating greater convection in the experiment. Moreover, typical shock temperatures and pressures, even well behind the CJ point, greatly exceed thermodynamic critical temperatures and pressures for typical high-explosive (HE) materials of 0.02-0.10 kbars and 400-1100 K [8L]. For instance, critical specific volumes, pressures, and temperatures for nitromethane are 2.84 cm^3/g, 0.0631 kbars, and 588 K [1MM]; for HMX they are 3.05 cm^3/g, 0.0339 kbars, and 1031 K [1NN]. Critical constants for polymeric materials are typically in the same range. By comparison, critical constants for zinc are 0.498 cm^3/g, 2.90 kbars, and 3170 K [1R].

Increased kinetic energy in the fragments means greater viscous heating of the surrounding gas, which is most commonly modeled as a Stokes term in the momentum equation for the solid phase. The whole two-phase phenomenon might be treated as a dusty-gas model [9C, 9I-9J]. A somewhat more general treatment for granular explosives is given by Asay et al. [3B, 9B]. However, only unreacted material is treated as two-phase flow in their work. The suggestion here: Also treat the reacted material as a two-phase flow until the energy has been dissipated below the shattering threshold and the duration has reached the time constant for complete dissociation of the reaction products. In thermal detonations, vapor-driven explosions, and spallation impacts [5F, 9D–9F], it is customary to simulate the fluid fragmentation as a separate process. In those cases, however, the fragmentation process is due to Rayleigh-Taylor (RT) instabilities, which evolve on a different time scale and have different physical origins than shattering processes.

The scenario conceived of here is that some fraction of the post-vN zone will shatter and then continue to dissipate. In this scenario, if the resulting fragments are, in themselves, sufficiently energetic (i. e., above some critical point) they will continue to shatter. Below the threshold energy, they may evaporate, liquefy, or solidify. Subsequent collisions among fragments may cause one or both to return to a shattering state. For fragments of explosive material, there may be additional heat production from a chemical reaction, which will contribute further to shattering.

Three other aspects are worth mentioning.

- First, the Oddershede model [5T] predicts that the exponent characterizing the larger-mass end of the fragment distribution will be quasi-two-dimensional, and the exponent for the smaller masses will be quasi-three-dimensional.

- Second, in our scenario, it may be more accurate to think of evaporation and shattering as competing. Shattering as explored to date in the literature ignores the presence of gaseous products. We need to modify the simple picture presented in the literature.

- Third, we must consider ionization processes. Shear induces ionization in both energetic and nonenergetic materials. The more polar the chemical bonds in the material, the more ionization occurs. Shear appears in several modes in a shocked heterogeneous explosive: by uniaxial compression at the front, by convective velocity differences in the multiphase flows, and by the full range of instabilities at material interfaces, crystalline defects in HMX, or foam pores.

  Fragments may also become ionized in the shattering process itself. The results reported by Saunders [5V] on charged clusters predict that multiply-charged clusters will experience a “Coulomb explosion”—one of his terms for shattering. The critical mass required to maintain stability increases with increasing charge, and it is the smaller masses, at a given level of charging, that are unstable. Fortunately, should this phenomenon prove critical, the work of Saunders and the larger molecular-clusters community strongly suggests that the liquid-drop model will perform very well for Los Alamos National Laboratory (LANL) purposes.

An important aspect of this thesis is the sequence of events in an explosion. The suggestion that shattering fragmentation may be a significant process is consistent with the general scenarios put forth by Asay et al. [3B, 9B] and Tarver [6CC, 6DD]. Based on their scenarios, shattering fragmentation models could be used both in the compaction stage of a brittle granular HMX explosive and in the release wave after the initial temperature rise, which, when combined with still-high pressure, places the products in a supercritical fluid state. A balance occurs between the internal energy of the different-size fragments and the entropy embodied by the isomeric conformations of the fragments. Specifically, Raz et al. [5H, 5K, 5U] argue for applying a maximum-entropy formalism, which, operationally, would replace the inequality constraints commonly used in two-phase flow models to bound the behavior of the exchange processes between phases.

The experiments of Raz et al. [5H, 5K, 5U] may be thought of as nanoscale flyer-plate experiments in which the fragmentation of the flyer plate itself is monitored through mass spectrometry. The level of control over the cluster sizes, both before and after impact, and the energy measurements on them are stellar. The results speak both to the general concept of power-law mass distribution in shattered materials, and, more especially, to the shattering behavior of supercritical fluids on release.

Closure is an essential element of any two-phase flow model. The choice of a fragmentation model for two-phase flow influences the closure relationship among thermodynamic properties of different phases. However, as laid out by Baer and Nunziato [9A, 9I-9J], there is no uniquely defined closure relationship connecting the transformation between the phases. The Baer-Nunziato presentation of the ambiguity goes as follows:

For two-phase, one-dimensional flow, one has five variables to describe each phase—temperature (T), pressure (P), density (ρ), velocity (v), and volume fraction (ϕ): a total of 10 variables to solve for. Each phase is governed by three conservation equations and an EOS. The volume fraction is constrained to sum to unity. This fact is well-defined in nine equations.

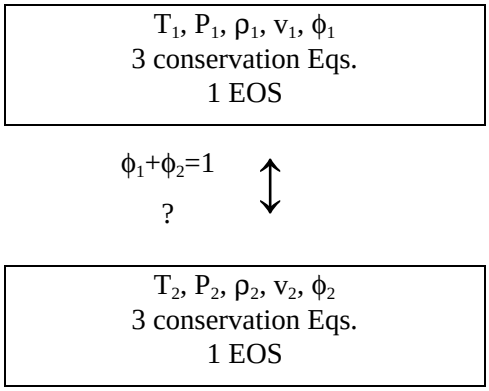

Figure II-2. This illustration is a depiction of the relationship between numbers of equations and numbers of system variables in two-phase, one-dimensional flow.

The tenth equation, represented by the question mark in Fig. II-2, has been and is still open for discussion. The most popular choice is to specify how the volume fractions exchange between the two phases. In fact, a favorite choice for that process is a variation of the Carroll-Holt pore-collapse (CH) model [7F]. The upshot of the discussion here is that specification of a fragmentation model affords a description of the volume-fraction exchange process. Shattering and evaporation are just two examples of fragmentation models. Condensation of soot aside, evaporation is the only fragmentation mode considered to date in

modeling detonated energetic and shocked polymeric materials. The results of Raz et al. [5H, 5K, 5U] argue for consideration of shattering behavior behind the shock front.

III. Topical Summaries

1. Equations of State (EOSs)

Many different EOSs are used to model both high-explosives (HE) and polymeric materials. They run the gamut from very general to very specific, from low to high temperatures and pressures, and from weak to strong shocks. Different EOSs are used for gases and solids. Detonation products are frequently modeled as being completely gaseous. If the HE is known to produce little in the way of solid byproducts, this approach may be appropriate. The HEs fitting this criterion usually contain a smaller atomic fraction of carbon or have a very good balance of carbon to oxidizer in the molecular formula.

Among the general-purpose gas-phase EOSs are the Mie-Grüneisen [1A, 1C-1D, 1T, 1V, 1BB, 1X], Tait and modified Tait [1A, 1H, 1FF], Becker-Kistiakowsky-Wilson (BKW) [1S, 1JJ, 4A], Jones-Wilkins-Lee (JWL) [3E, 4A, 6E, 6AA, 6DD, 8L], Birch-Murnaghan [1FF], JCZ3 [3E, 8L], and the quotidian EOS (QEOS) [1F-G, 1K, 1Q, 1U, 1LL]. See Mader for even more EOSs [1S], plus discussions about hot spots and numerical methods.

For concreteness, consider two of the most prominent EOSs: the BKW and the JWL. The BKW EOS pressure functional form is

$$P\,V/(R\,T) = 1 + x\,e^{\beta x}\,, \tag{III.1-1}$$

where P is the pressure, V is the molar volume, R is the gas constant, and T is the temperature. The parameter β is a constant of the order of 0.2 for most condensed explosives. The variable x is the ratio

$$x = \kappa\,k/(V_g\,(T + \theta)^{\alpha})\,, \tag{III.1-2}$$

where parameter κ is constant with an optimized value close to the universal value of 11.85 and the parameter θ improves the behavior of x at lower temperatures and has a value of about 400 K [1S]. The exponent α has values between 1/3 and 1/2 and is optimized to standard HEs. The variable V_g is the volume of the explosive system occupied by gas. Finally, the variable k is the mole-fraction weighted covolume of the gas-phase detonation products:

$$k = \sum_{i=1}^{N} x_i k_i\,, \tag{III.1-3}$$

where N is the number of gas-phase species and, for each species i, x_i is the mole fraction and k_i is the covolume associated with its rotational motion. Further analysis of the functional form shows that it is dominated by repulsive interactions between the atoms of the molecule. Note also the difference between this form and the polynomial expansions of the exponent in Eq. (III.1.2) which appear in, for instance, early versions of the CAVEAT code [4A, 4C]. Greater flexibility is achieved through these expansions.

The sensitivity of explosives behavior to the EOS is captured in the BKW form in the covolume, k, and the gaseous molar volume, V_g. Accurate partitioning between gas and condensed phases is necessary to model even the planar, steady, equilibrium detonation waves accurately [1S, especially pp. 3, 21, 57, and 389].

The JWL EOS is motivated by the unwieldy nature of the polynomial expansions that the BKW EOS evolved into [4A, 4C]. In some sense, the JWL EOS sums the expansions into a more compact form while maintaining accuracy. The basic form is [6DD]

$$P = A\,e^{-R_1 V} + B\,e^{-R_2 V} + \omega\,E/V\,, \tag{III.1-4}$$

where A, B, R_1, and R_2 are constants fit to experiment, V is the relative volume, E is the internal energy, and ω is the Grüneisen parameter. Tarver et al. [6DD] vary this basic form depending on whether they are modeling reaction products between the vN point and the CJ point, after the CJ point (i. e., isentropic release), or from superdetonation arising from ignition.

A representative solid-detonation-products EOS is the Cowan form. It expresses the pressure, P, as a polynomial in the temperature, T:

$$P = P_1 + a\,T + b\,T\,. \qquad \text{(III.1-5)}$$

In turn, the coefficients P_1, a, and b are expanded as polynomials in the compression, $\eta = \rho/\rho_0$, where ρ and ρ_0 are the density of the solid in the detonation and the density at ambient conditions, respectively.

Among the specialized EOSs are those developed by Baonza et al. [1A], Sanchez and Cho [1FF], Gujrati [1P], Berry et al. [1B], and Saeki et al.[1EE]. The CHEQ EOS [8L] is an exception in that it directly calculates a minimized free energy, whereas the others in the list use an analytical form for the necessary number of thermodynamic variables. Most are geared toward modest temperatures and pressures and are more appropriate for aging and damage studies. Numerical simulation methods based on Monte Carlo averaging, molecular dynamics, and/or statistical mechanical perturbation expansions [1P, 1CC, 1GG, 8L] are capable of generating EOS tables when the requisite atomistic potential energy surfaces are available.

If we ignore for the moment matrix effects in composites, polymers, in spite of their complexity, show remarkable consistency with respect to their Hugoniot behavior. Virtually all exhibit phase-change-like features at both low and high pressures at 1-2 [1X-1Y, 1HH] and 20-30 GPa [1E, 1V], respectively. These values correspond to particle velocities of 0.1-0.2 and 3-4 km/s. There are several explanations for each transition: The lower pressure/velocity transition is explained by anomalous disequilibrium in both the sound velocity and the Grüneisen parameter; and the higher one may be caused by the onset of additional dissipation mechanisms [1E, 3M].

The QEOS [1G, 1K, 1U, 1LL] is a very versatile EOS designed specifically for covering a very broad range of solid material conditions from ambient temperatures and pressures to plasma production and strong shocks (up to 4 TPa). Almost by necessity, the model does not treat any one material especially well. However, it seems to capture the essential shock behavior of most materials. It does so by starting with a cold Helmholtz free-energy term, adding vibrational and solid-solid phase-change contributions up to the melting point, and then including an electronic energy contribution modeled after Thomas-Fermi theory which deals with plasma behavior. Lawrence Livermore National Laboratory (LLNL) has added another feature recently to describe better the bond-breaking processes for chemically reactive species. This feature greatly improved the agreement with absolute-EOS experiments performed with the Nova laser source for materials such as polystyrene and deuterium.

Besides these traditional EOSs, there is a class of free-energy functions intended for very complex systems such as polymer conformations which are described by statistical distributions of local minima and transition states [1L, 1KK]. These are more commonly used to describe aging processes. Because our focus is on the shock regime, no further comments other than those made in the bibliographic notes in Sec. V.1 will be offered.

As a related topic, nonequilibrium effects deserve mention here. The most discussed sources of these effects arise from two-phase or multiphase flow, reaction dynamics, and reactive-nonreactive material mixing. In multiphase flows [9O], the phases may not be in equilibrium with each other in terms of flow fields, thermalization, and pressure distribution. Differences in velocity fields lead to additional viscous heating that does not occur in a comparable single-phase model.

Additionally, one solid phase may prevent complete mixing of a reactive second phase. There are measurable observations of this effect. If a model over-homogenizes the system, any of these behaviors may be misrepresented, leading to incorrect steady-state shock speeds.

Typically, however, each phase is considered as being locally in equilibrium with itself. For this reason, it seems likely that a defensible first approximation would be to consider the EOS for each phase to be independent of the presence of other phases. Note though that the potential for compositional

changes of a particular phase due to exchange processes, such as solution of decomposition products from HMX in unshocked binder or changes in gas phase composition as the detonation reaction progresses in a given region, should be regarded as separate. The EOS needs to be flexible enough to account for such changes and any attendant phase transformations.

2. Stress-Strain Constitutive Modeling

Stress-strain constitutive models for shock simulations present numerous challenges, particularly in needing to represent a variety of transport mechanisms; in calibration and testing over wide ranges of temperature, pressure, phase transformation and mixing conditions; and because of the presence of multicomponent materials. Most constitutive relations are meant for specific ranges of application and so, at best, represent only that range of physical phenomena. Moreover, the range of phenomena of existing models tends to be decidedly in the small-shock regime. Very few constitutive models, especially for polymers, deal with the phase transformation, failure, damage, and decomposition ranges inherent under strong-shock conditions. The range of behaviors induced by varying the strain rate is exceptionally large, including, at least, shear thinning, ductile-brittle transitions, shear-induced ionization, and nonequilibrium responses at lower-shock speeds.

The best-established models for polymers of interest here are the viscoelastic dashpot-spring models, also known as Maxwell models [2B, 2C, 2L]. The polymer is thought of as responding to stresses and strains through a set of characteristic frequencies that are dampened by viscous interactions with other components, such as plasticizers, solvents, or reaction products, as well as with itself. Note also that the model referred to here is able to capture the crucial behavior of shear thinning through the addition of strain-rate dependence to the original model [2B, 2P].

There is considerable controversy over the efficacy of these models because their harmonic-spring origin is not intended to describe extensive deformations that elastomeric polymers can undergo before failing. The bonding in these materials is often hydrogenic (quantum mechanical), and much mechanical behavior is determined by steric and entanglement interactions [2F] among various segments of the polymer chains.

Nevertheless, the model is very flexible because it is so easy to add mode frequencies to extend the range of validity of a material-specific model [2A]. Indeed Johnson et al. [2P] cite thermodynamic properties, especially heat capacity and Grüneisen parameters, as being the least adequately known with respect to shocked elastomers. Again though, these models have rarely been pushed into the explosive-shock regime [2C, 2L, 2P]. Specifically, little is known about the mechanical response of a plasticized volume of Estane confined between crystallites of HE, one of which is undergoing explosive-shock transformation.

Among the more general constitutive models under recent investigation is a class referred to as “differential constitutive equations” [2D, 2M, 2W]. Here, this means that one cannot express the stress-strain relationship in closed form, and the differential relationships are propagated numerically with the conservation equations. This class is particularly appropriate to polymeric materials and especially elastomers, which are often described mechanically in terms of the Doi-Edwards model, which, in turn, is based on the de Gennes reptation model. A related class of models originates from transient network models in which bonds in a sheared polymer break and reattach at another point in the same polymer chain or to another polymer chain [2S]. The details of the linkages are usually unspecified, allowing both scission-repolymerization and hydrogen-bonding events to be modeled. The physical reasoning behind this model has strong appeal because of its attention to bond breakage and reformation. Finally, there are constitutive laws developed from free-energy expressions. The generalized or nonequilibrium [2V] variety contains generalized thermodynamic forces. The equilibrium models are mostly of the free-volume type [2N]. Again, the physical reasoning behind these models appears to be quite sound. The nonequilibrium models, especially, are computationally intensive yet still not completely physically reliable. Moreover, there is no experience with them under strong-shock conditions.

A physically less sophisticated, but computationally more tractable and behaviorally more versatile model, the Johnson-Holmquist approach [2O], runs the gamut from elastic to plastic strains, damage, and failure. Each submodel is less sophisticated than the state of the art for the phenomenon modeled, but has all of the essential features. This approach also suffers from a lack of testing under strong-shock conditions and is a solids-only model. However, issues such as numerical stability and frame-of-reference compatibility (Lagrangian, Eulerian) have been addressed with some success. This approach may well be an adequate scoping model for testing various submodels both physically and numerically.

3. Shock Dynamics and Hugoniot Behavior

This section focuses on a small collection of narrower topics concerning the structure of the shock front and general characteristics of polymer Hugoniots. The latter topic has been covered to a certain extent in the section on EOSs (Sec. III.1). Two modes of turnover behavior in the shock Hugoniot are discussed, one at 0.1-0.2 km/s, and another at 3-4 km/s, for many polymers [1E]. The former is attributed to nonequilibrium behavior arising from the broad range of time scales associated with polymer mechanics at weak-shock strengths [1X-1Y, 3O]. The latter is attributed to the onset of new energy dissipation mechanisms for sufficiently strong shocks [1E, 1HH, 3M] and is likely to be a general feature in many materials. To some extent, these explanations are consistent in that, in a spectral representation of polymeric response, the lower-frequency responses cease to contribute, while higher-frequency responses become active as the shock strength is increased.

With the basic macroscopic behavior of shock dynamics now well established, microscopic structure of shock fronts, multiple shocks, and release waves has been getting greater attention. Predictive models of initiation, sensitization [3E], and damage effects require this level of resolution, as well as high-fidelity EOS and constitutive relations. Here, we are mainly concerned with packed, granular explosives. As discussed in Asay et al. [3B], the structure of the front decomposes into the three zones indicated in Fig. I-2: permeation, burn-front, and combustion. In this section, we focus primarily on the first two.

In the permeation zone, detonation products and heat advance somewhat ahead of the front. Since this zone is still a point of controversy, we are limited to being vague about its quantitative thickness. Immediately before the front, the oncoming shock begins compacting the HMX bed. The earlier thinking was that the permeation zone is on the order of millimeters. The recent arguments of Asay et al. [3B] suggest that the permeation zone is more likely on the order of microns (i.e., several grain diameters) because of large drag forces and nozzling effects caused by the compaction process. Instead of extensive permeation, plastic formation of crystals, viscoplastic heating, and fracture are given much more prominence. The fact that any of the common HEs or binders will have melted above approximately 500-600 K is not mentioned.

The emphasis on compaction has been extended by Gonthier et al. [3K] to model the effects of compaction in producing hot spots through dissipation of plastic work. Dissipation is captured through a volume fraction change in the solid HMX component. Since many shear deformations largely preserve volume, it seems more appropriate to think of the volume change as a proxy for the plastic work. This submodel has been incorporated into the two-phase DDT model of Baer and Nunziato [9A], about which much more will be said in Sec. III.9.

Moreover, emphasis on compaction is consistent with the importance that Gilman places on shear, uniaxial compression, and defect-shock interactions in both initiation and detonation reactions [3I-3J, 6R]. He argues convincingly that nonmetal-metal transitions and ionization processes [3L] must figure prominently in both. Both entail delocalization of electrons over a molecule, which is the intended sense of metallization. Simple, yet representative models of such processes are difficult to find. This difficulty, combined with incomplete characterization of internal shock front conditions and the general complexity of the reaction mechanisms, makes it difficult to assess these arguments quantitatively.

Also consistent with these notions is the analysis of Vineyard [3T] on the role of defects in generating ions, local hot spots, and transient instabilities, and the analyses of organic reaction products by Dremin and Babare [6J] and Enikolopyan et al. [6L]. These "deformation-induced" processes will be discussed further in Sec. III.6.

At the burn front, the pressure peak is followed at some distance by a temperature peak from the reaction, which coincides, more or less, depending on the extent of nonequilibrium effects present in a specific system [6G, 6K, 6BB], with what is referred to as the CJ state. This burn-front zone approximately corresponds to Tarver's shock front and transition-state stages shown in the lower panel of Fig. I-3. The combustion zone encompasses the release of chemical energy, turbulence, and some level of vibrational equilibration, again depending on system specifics and confinement. It corresponds to the bond-dissociation and CJ states in Fig. I-3 and to the vN spike. Other sections of this report, particularly III.6 and III.9, focus on this zone.

Returning to the theme of stability, Kopotev and Kuznetsov [3N] note the critical importance of whether the flow field at the CJ point is one- or two-phase. Two-phase flow possesses a spectrum of sound speeds which can cause disturbances at the CJ plane to propagate upstream to the shock front. This finding is part of a long history of investigations into shock stability. Other highlighted papers include [3F, 3P, 3U], chosen out of a huge literature on the subject.

Characterizing the substructure of detonation waves has been exceedingly difficult. Several sensing and measuring techniques have been developed to probe this structure: x-ray [3H], velocity interferometry system for any reflector (VISAR), laser fluorescence, and laser interferometry, which are all relatively well known. Among the newer techniques for studying initiation and transition to steady-shock conditions so crucial to corroborating models of detonation are emission spectra and atomic force microscopy (AFM). Yoo et al. [3V] use time-resolved emission spectra and thermal gray-body emission modeling to estimate CJ temperatures. Superdetonation, detonation, and steady-state signals show distinctive differences. Agreement with semiempirical models of CJ conditions is qualitatively good. The spectra are averages over the full depth of the sample, and so there is some mixing of the different zones at later times.

Similarly, Sharma and Coffey [3S] use AFM to examine plastic deformations resulting from drop-hammer tests on RDX. In subcritical impacts, the two primary features are shear bands and dislocations. Sharma and Coffey also report two types of reaction sites—hillocks, perhaps from a combination of melting and gas entrainment, and hemispherical craters 20-100 nm in diameter. In addition, direct evidence of a phenomenon called Munroe jets is seen [3R]. Coffey goes on to use these observations to modify ZND theory to permit a finite shock-zone thickness [3D] deemed necessary for support energy localization and dissipation and plastic deformation. Furthermore, arguments are advanced that high-velocity dislocations are a facile means of promoting intramolecular vibrations, a clear reference to Tarver's model. Critical shear stresses are estimated for the onset of detonation. For unexplained reasons, the figures in Coffey [3D] have the reaction zone before the detonation zone, contrary to most depictions of ZND theory.

Some of the most basic features of chemically sustained shock waves can be captured in MD simulations of prototypical models [3C]. Successes have been achieved in propagation stability, as demonstrated by Brenner et al. [3C, 3Q]. Other examples will be mentioned in discussing fragmentation (Sec. III.4) and initiation (Sec. III.6).

4. Fracture, Spall, and Strength

Fracture and strength appear as topics in this overview because intimate contact between polymeric materials and crystalline explosives is so closely tied to concepts of detonation initiation and propagation, because some materials of interest are composites, and because elastomers are strong and tough. As will

become apparent from the discussions in Secs. III.5 and III.6, models of material failure may be relevant to shock chemical kinetics as well.

The topic of material fracture is inseparable from multiphase-flow modeling. However, in this section, the focus is solely on the fragment nucleation, initiation, growth, and distribution models themselves and how they impact EOSs, constitutive relations, and turbulence. Fracture models fall naturally into two categories, brittle and ductile. Brittle fracture is characterized by shattering with more or less even distribution of energy over the entire body. Consequently, the entire body fractures in unison, and the strain-rate dependencies are absent. The mass distributions which characterize shattering have been discussed in Sec. II.

Two prevailing fracture models have emerged, one from Shockey, Curran, and Seaman [4Z], and another from Johnson and Addessio [4P].

Shockey et al. [4Z] have constructed a model and simulation code from a microstatistical fracture-mechanics point of view that is applicable to the study of failure in shocked materials. By taking such a broad point of view, Curran and Seaman are able to address both ductile and brittle materials with one model. It is worth noting that this point of view and the failure model derived from it have been applied to damage assessment of impacted high-energy propellants [4U]. The statistical approach is more detailed than a continuum approach, yet avoids the complications and uncertainties accompanying a microscopic dynamic model.

With this caveat, we examine the Curran-Seaman ductile fracture model in more detail. Two equations form the basis of the nucleation and growth of voids, the type of defect most closely associated with this mode of failure. The first governs the number of voids, N, as a function of instantaneous tensile stress, σ,

$$\dot{N} = \dot{N}_0 \exp((\sigma - \sigma_{n0})/\sigma_1) , \qquad \text{(III.4-1)}$$

where σ_{n0} is the stress controlling the nucleation threshold, σ_1 controls the nucleation sensitivity, and $\dot{N}_0$ defines the initial or threshold nucleation. The second equation governs the size distribution, R, as a function of σ, the growth threshold shear stress, σ_{g0}, and material viscosity, η:

$$\dot{R} = (\sigma - \sigma_{g0})/(4\eta)\, R . \qquad \text{(III.4-2)}$$

All of these parameters are determined through data generated from model experiments. Details of their determination are available in [4J] and [4Z] among others.

Ductile fracture takes on the appearance of void nucleation and growth with fracture occurring when the voids become large enough to coalesce. As a result, strain-rate dependencies are essential to the success of the model. So, for instance, Johnson [4Q] formulated a model of ductile fracture based largely on running the CH model in reverse [4W]. Curran and Seaman's code also models ductile fracture. Their review article is still definitive [4J].

Most ductile fracture models have been developed for metals and with an expanding-ring simulation as the litmus test for a model [4Q]. However, this simulation is not the norm in polymeric fracture modeling, in which flat-plate impact tests play the dominant role.

An important concern in ductile-fracture studies is the lack of model differentiability [4Y]: that is, many different models can be made to represent the same experimental data. These models may not even be based on the same physical phenomena. Differentiation must then be founded in correct physical reasoning. Fragmentation models suffer the same ambiguity and require resolution. The discussion of Sec. III.5 is relevant to this point in two ways. One way is that, though the main concept of shattering fragmentation may be applicable to release behavior in an unconfined shock, it may be difficult to verify or disprove because of a lack of model sensitivity to the void-growth model used to describe failure. A second way is that one could adopt the point of view that shattering is applicable in certain regimes of

temperature and pressure gradients and that one can remove the ambiguity in the fragmentation model for that regime by adhering to the model derived from shattering mode fragmentation.

A comment touching on chemical kinetics is in order. In Sec. III.6, there is a great deal of discussion about shear modes of material deformation being responsible for damage to heterogeneous HEs, detonation initiation kinetics, and steady-state detonation kinetics. The role of shear modes in shock kinetics is far from being definitely known. To the extent that shear modes are involved and that testing of the concept is desirable, the constitutive and failure models become intimately connected with the chemical kinetics.

5. Fragmentation

Shattering-mode fragmentation was treated above as a separate section. Here, we mention some models of polymer degradation based on fragmentation processes [5W]. A polymer chain may undergo scission with a probability distribution determined by the chain length (molecular weight) and position on the chain. The rate equation associated with the change in chain-length concentration, c(x,t) of length x at time t, takes the form

$$\partial c(x,t)/\partial t = -a(x)\, c(x,t) + \int_x^\infty dy\, a(y)\, b(x\,|\,y)\, c(y,t), \qquad \text{(III.5-1)}$$

where a(x) is the overall fragmentation rate, and b(x|y) is the conditional probability of producing a fragment of length x from a fragment of length y. The first term represents the fragmentation of chains of length x to smaller lengths, while the second term represents production of chains of length x from larger ones. Fragmentation rate functions, a, need to be developed for each process, but they typically assume a simple power-law form. Mass conservation and fragmentation termination conditions are imposed through separate expressions. The probability function b(x|y) can be normalized to achieve mass conservation,

$$\int_0^y dy\; x\, b(x\,|\,y) = y. \qquad \text{(III.5-2)}$$

The absence of a fragmentation-termination condition allows production of zero-length chains, but such chains violate mass conservation. For our purposes, this is physically nonsensical, and the resolution to avoiding this situation, as given by Maslov [5Q], is to use a discrete representation of Eq. (III.5-1). Molecular dynamics has yielded insights into the fragmentation process in two dimensions and for the adiabatic-expansion case [5L], a particularly difficult one to model in a continuum mode [4Q]. Finally, Boyer et al. [5E] show that power-law mass fragmentation distributions, Eq. (2.2), can be obtained from multivariate forms of the rate function. Bivariance, with a power-law dependence on the two chain-length variables,

$$a(x,y) = x^\alpha\, y^\beta, \qquad \text{(III.5-3)}$$

is sufficient to achieve this behavior in the mass distribution. It is necessary for $\alpha = \beta < 0$. Moreover, it is not possible to reduce the bivariant model to a univariant one and preserve the power-law mass distribution.

Specific to polymers, Singh and Rogers [5W] find that kinetics models of the fragmentation rate function yield the bivariant forms,

$$f(x,y) = (x+y)^\alpha\, \delta(x-y), \qquad \text{(III.5-4)}$$

for a binary scission process. The form is based on depolymerization kinetics through shearing, stretching, and irradiation. They reduce this model to a univariant form by integrating out one of the variables to yield

$$a(x) = x^{\alpha+1}. \qquad \text{(III.5-5)}$$

As is evident from the discussion in the preceding paragraph, it is necessary to introduce the modifications suggested by both Maslov [5L] and Boyer [5E] in order to model polymer shattering kinetics with a sensible termination of the fragmentation process and a power-law mass distribution. Models of this form have been successfully developed using moment methods. (See references in [5E].) It is probably desirable to generalize the results for a non-delta function dependence in Eq. (III.5-3) to a realistic form yet to be identified. Exploring appropriate multivariate-rate functions can be approached with MD simulations of shocked hydrocarbon polymers using the Brenner potential for the atomic interactions [7EE]. Overall, a sound, fundamental basis for studying polymeric shattering kinetics is readily available and relatively straightforward.

Equation (III.5-1) is a very general expression for the linear evolution of a species undergoing formation and disintegration. Because of this generality, Kun and Herrmann [5N] use exactly the same equation to model a shocked, elastic-plastic, random medium. The species of interest here are the fragments of the shocked material. The random medium is represented by a distribution of cell centers or "atoms." In turn, the atoms are surrounded by Voronoi polyhedra. The atoms are joined by elastic-plastic beams. A von Mises plasticity criterion determines when the beams break. Breakage can be regulated so as to result from tensile stresses, compressive stresses, or both. A pseudo-MD technique propagates the "atoms" when they are impacted by the shock front. The technique also is capable of simulating multiple shocks.

6. Reaction Dynamics

Chemical kinetics at shock fronts are athermal. A 3-km/s shock front takes just 25 fs to traverse half of a typical bond length in HMX, a fraction of a vibrational period. Such a driven atom has enough kinetic energy to cross any barrier lower than 1 eV. How these rapid events set the stage for eventual energy release to produce and sustain the shock front is a hotly contested issue.

Chemical kinetics in detonations have given rise to three basic schools of thought: the Arrhenius form with or without activation volume modification, starvation kinetics, and shear-driven reactivity. Formulations of any of these concepts do not require that they be exothermic. For this reason, I assume that they are also applicable to strongly-shocked polymers as well.

The most prevalent viewpoint is the traditional Arrhenius form of chemical rates,

$$r_{Arr} = A \exp(-\Delta E_{Arr}/RT) , \qquad \text{(III.6-1)}$$

where r is a rate; A is a constant which embodies concentration dependence(s), attempt frequency and unit conversion; ΔE_{Arr} is the thermal activation energy barrier; R is the gas constant; and T is the absolute temperature. More theoretically rigorous forms of A would include a power-law dependence on temperature. Most detonation models use rates of this form, partly out of habit, partly out of consistency, and partly out of insufficient evidence to support other concepts decisively—no matter how well-reasoned they may be. Within this school also falls the activation volume form [6E]

$$r_{av} = r_{therm} \, (r_{vol}/r_{vol}(0)) , \qquad \text{(III.6-2)}$$

where, for most organics,

$$r_{vol}/r_{vol}(0) = \exp(-\Delta V \, \Delta P/RT) , \qquad \text{(III.6-3)}$$

where ΔV is the activation volume, ΔP is the pressure change, and $r_{vol}(0)$ is the reaction rate at the reference pressure. With this modification, large amounts of high-temperature, high-pressure organic reactivity can be explained [6E].

The second school is a variant developed by Eyring [6N] which takes into account the bath-like character of the vibrational modes in a detonation environment. When an atom is attempting to dissociate from its parent molecule, not only are collisions from multiple atoms thought to contribute to the excitation process, but, in addition, the average vibrational energy corresponds to several vibrational

excitation levels (n ~ 4-5). To account for this environment, the above Arrhenius form, without volume activation, is also modified [6N, 6BB-6DD]. The normal activated process is thought of as being in series, with a dissociating bond interacting with the vibrational bath to give an overall rate constant of

$$r = r^*(\Delta E^*)\, r_{Arr}(\Delta E_{Arr})/(r^*(\Delta E^*) + r_{Arr}(\Delta E_{Arr}))\ , \qquad \text{(III.6-4)}$$

where

$$r^* = r_{Arr}(\Delta E^*)\exp(-s)\sum_{i=0}^{s-1}\ (\Delta E^*/RT)^i/i!\ , \qquad \text{(III.6-5)}$$

and ΔE^* is the bond energy which may or may not be close in value to ΔE_{Arr}, and s is the average number of bath modes in contact with the dissociating atom. Typical values for s range from 10 to 20. The main virtue of this form is the ability to track the turnover in increasing reaction rate with increasing temperature. Increasing thermal energy increases the chances of a deactivating collision while an atom traverses the effective barrier [6N]. The concept depends on local equilibration at two stages of the detonation, vibrationally after passage of the shock but before the atom traverses the barrier, and again after traversal in the release of the cold compression energy of the shock. Note that the preponderance of rearrangements involve nuclei.

The third school of thought holds that explosive reactions behave more like a phase transformation than a thermally activated process [6K-6L]. Shear strains induce potential energy surface crossings that would not occur under comparable thermal and hydrostatic-pressure conditions, allowing electronic rearrangements to produce new bonding patterns. The appropriate rate expressions would reflect the driven nature of the shock-induced reactions which we write in the very general form

$$r_{shear} = \dot{\sigma}\ P(\Delta E_{shear}, D)\ , \qquad \text{(III.6-6)}$$

where $\dot{\sigma}$ is a shear strain rate, and ΔE_{shear} is a barrier to that motion which could be due to gap closure, bond compression, bending forces, and/or diffusional rearrangement. The unspecified function P represents a population of atoms that are available to be driven to this barrier or beyond for detonation velocity D.

Gilman in particular [6R-6S] has shown that reaction paths involving bond-angle deformations rather than bond-length changes may permit extensive delocalization of electrons akin to insulator-metal transitions. Explosives and polymers, being molecular in nature, do not become metallic in the usual sense, but rather in a bond-resonance and orbital-hybridization sense. In short, the difference between the highest occupied orbitals and the lowest unoccupied ones can be closed. When closure occurs, valence electrons can rearrange to form a new bonding pattern with relatively little atomic motion. The example given in the bibliography notes on the diamond-to-beta-tin phase transformation illustrates the point. The diamond phase can be deformed through uniaxial compression and shear into the beta phase with almost no change of nearest neighbors. At the critical point, the electrons rearrange into a metallic phase—the extreme limit of delocalization. Another example would be graphitization of or production of benzene from some organic solid under shear. The delocalization of the electrons takes on the form of resonances in graphite in-plane bonding or a benzene ring.

An approach that seems to span some features of all of the above approaches is promoted by Frankel [6P]. Apparently, however, the approach has not matured fully since its introduction and is quite complex, relying on first-principles calculations for several parameters.

Electronic rearrangements can occur far more rapidly than the activated reactions; they can more readily account for phenomena such as ionization, defect sensitization, and current concepts of initiation; and they have strong experimental foundations, as do the other concepts. Note that the type of potential energy surface required here would be multiple-valued and would rely extensively on nonadiabatic transitions. Whether an anisotropic version of the activation volume concept can bring it into philosophical agreement with the shear-driven reactivity concept is completely unknown at this time.

Finally, note that the shearing concept fits most naturally with nonequilibrium free-energy functions of the type mentioned in Sec. III.2 in which mechanical contributions appear in the formalism [2E].

A related topic is the production of ionic species in detonation waves. It is quite clear that polar molecules, such as HMX and polymethylmethacrylate (PMMA), undergo much greater ionization for a given shock strength than do nonpolar species such as a pure hydrocarbon. There is some disagreement over the mechanism of ionization (cf. [6T, 7I] versus [6J, 6L, 7TT]), but the most plausible explanation requires dipole elongation (through shearing or tension) followed by bond dissociation [7TT]. For a permanent dipole with charges ±q, the probability for dissociation into ions would be on the order of q since these partial charges are also time-averaged occupation numbers. For a nonpolar molecule, the appropriate probability is the instantaneous polarizability. This phenomenon also appears in many porous and defect-structure situations, in which, again, shearing processes are operational. More discussion on this topic will appear in Sec. III.7.

Polymeric and other slowly reacting, inert, or endothermic materials present numerous issues. They alter the chemical mixes of both reactants and products; they hold the potential for destabilizing the shock front; they introduce nonequilibrium effects by interfering with complete reaction of explosive compounds, with heat transfer, and with energy production rates; and they influence the transfer of sustaining energy to the shock front. Only recently has there been much effort to deal in some comprehensive way with all these issues.

Although the bibliography in Sec. V.6 is incomplete, among the most notable efforts listed are those of Howard et al. [6V], Nichols [6Y], Dionne and Lee [6G], Demol et al. [6F], Cook and Haskins [6D], and Kennedy and Nunziato [6X]. Recently, the Kennedy-Nunziato work has evolved to become the dominant focus in the form of the Baer-Nunziato DDT model [9A] which will be discussed much more extensively in Sec. III.9. Here we note the salient features of the other works.

Howard et al. [6V] modified the CHEETAH code to allow separate treatments of explosive and binder. Binder is modeled as an Einstein oscillator to prevent it from reacting. The Einstein temperature which calibrates the model to a real system can be artificially raised to prevent heat adsorption.

Nichols [6Y] modified the CHEQ code to allow nonequilibrium analogs to the CJ conditions. The shock front progresses through four stages as described by Tarver; levels of equilibration characterize each stage. Generally, nonreactive components increase the detonation velocity.

Dionne and Lee [6G] model a mixture of nitromethane and glass beads to demonstrate how an inert material can interfere with thermal equilibration and alter reaction rates compared to a purely homogeneous explosive. The dominant parameter in the model is the heat-transfer coefficient between the liquid explosive and the inert beads. So only thermal equilibration, one of four modes considered by Nichols, is modeled in [6G]. The two-phase system is still approximated as a homogeneous system.

Demol et al. [6F] simplify the Saurel et al. pore-collapse model and implement it in an Ouranos hydrocode. The Saurel model is a generalization of the CH model [7F]. The combination of simplified model and code is referred to as CHARME. Through this combination, they capture some pore- and grain-size effects, especially sensitivity. Below a certain pore size, the pores are not allowed to become hot spots. The model predicts at first increasing sensitivity with decreasing grain size because of a corresponding increase in porosity, and then decreasing sensitivity because too many pores fail to heat. This prediction agrees qualitatively with MD simulation results [7DD-7EE, 7RR]. Interestingly, in agreement with Davis and Brower [6E], Gilman [6R], and Dremin and Barbare [6J], these authors find strong-shock pressure/shear stress sensitivity to the ionic reaction rates. To capture this sensitivity in the model, they had to revise the incumbent reaction-rate expressions. Stewart and coworkers [7OO, 7SS] see this sensitivity as most pronounced in single-phase models of DDT.

Similarly, Cook and Haskins [6D] extend three-step Arrhenius kinetics models for homogeneous explosives (TOPAZ2D kinetics model) by introducing porosity. As the shock passes a pore, it collapses

adiabatically, and, subsequently, locally heats the nearby explosive (i. e., forms a local hot spot). The temperature and heat transport in a region around a typical pore is tracked as a separate subprocess. In essence then, this is a two-temperature model. Murnaghan and JWL EOSs are used for the reactants and products respectively. The system as a whole is treated homogeneously with the pores given as a size and number distribution. The pore-collapse model is not specified. The outcome is a plot of threshold velocity for flat-nosed projectile impact ignition of the explosive for both the homogeneous and the heterogeneous cases. For some cases, the differences are dramatic.

The favored form of kinetics laws is still Arrhenius [6D, 6O]. Radical formation is undoubtedly important [6H-6I] even if it is not the main contributor to ionic processes, as discussed above. Most concepts of polymer kinetics are takeoffs from analogous organic species reactions. The rarefied nature of the shock state has made definitive distinctions between highly compressed organic liquids and solids on the one hand and highly compressed polymers of similar chemical composition on the other difficult to identify. More study in this area is needed.

Burn models themselves deserve mention. The original CAVEAT code write-up [4A] discusses three that are still in common use: Programmed, Forest Fire, and Chapman-Jouget Volume Burn. See also Mader [1S].

7. Shocked Porous Media

Virtually all solid, real-world materials contain some porosity because of the accumulation of defects. When shocked, pores often act as stress concentration regions. The cracks leading to failure, yielding, or ignition, in the case of energetic solids, have pores as their growth nuclei. For highly porous materials, the mechanical response is much more profound. They can dissipate the mechanical energy of shock, causing it to slow. They also play a critical role in shock-wave analysis. Foams are used as impedance mismatch materials [7FF] in Hugoniot mapping experiments. Just as significantly, they can be used to explore off-Hugoniot conditions [7M-7N] that are so vital for constructing robust EOSs.

As was evident in the end of the last section, the topics of chemical kinetics and mechanical response are intimately coupled. As a combination, sometimes called mechanochemistry, the connection between these two subjects occurs through a myriad of local phenomena such as shear thinning, turbulence, interfacial instability in both the RT and RM modes, and Kelvin-Helmholtz instabilities. The upshot however is three effects: (1) local mixing, (2) local heating, and (3) changes in reaction pathways. Here, we focus on the RM instability and chemical kinetics as they relate to porosity. Other types of instabilities will not be considered in detail here. The RM instability will be treated in an analytical way in order to illustrate the potential magnitude, length scale, and time scale of the process. Also, we will make particular note of how material strength appears in the analytical model.

For instance, consider the analysis of Bolkhovitinov and Khvostov [7D-7E]. The usual Hugoniot relationship for the energy jump across a shock front is modified to include a dissipation term for the collapse of a foam and for the ionization processes they observe in polymeric foams. Their approach takes the form:

$$h_s - h_0 + h_{dis} = 1/2\ (p_s + p_0)\ (V_0 - V_s) \qquad \text{(III.7-1)}$$

where the h's are enthalpies behind the shock, in front of the shock, and dissipation within the shock, for subscripts s, 0, and dis, respectively. The notation for the pressures (the p's) and the specific volumes (the V's) is analogous to the enthalpies. The enthalpy behind the shock front, h_s, can be related to the EOS of the material at that location. If a sufficiently simple EOS is used for the shock reaction products, such as a van der Waals EOS, one can actually solve analytically for the shock pressure. The shock pressure is proportional to the new term enthalpy, h_{dis}:

$$p_s = -h_{dis}/([(\gamma V_s^2)/(\gamma-1)(V_s+b)] - 1/2\ (V_0 - V_s)) \qquad \text{(III.7-2)}$$

where γ is the heat capacity ratio for the shocked material, and b is the second van der Waals coefficient. Given the convention that enthalpies of dissipative processes are positive, a positive p_s requires that the denominator in Eq. (III-7.2) be negative. A schematic representation of the effect on the shape of the Hugoniot is shown in Fig. III-1.

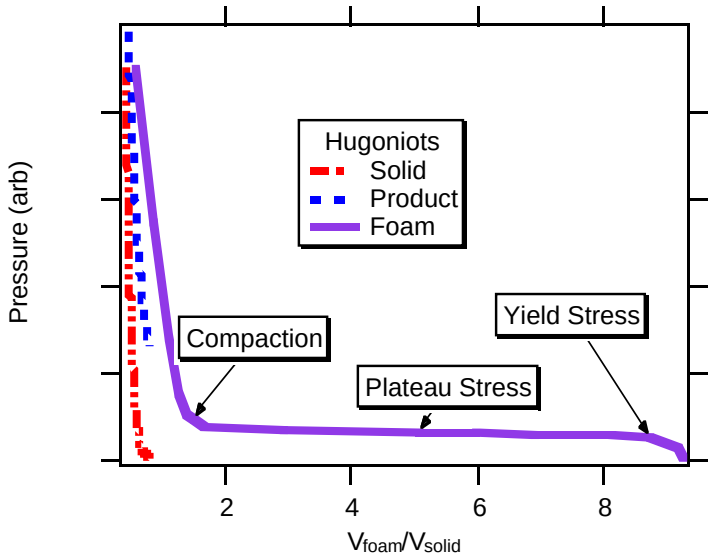

Figure III-1. This graph shows a schematic representation of a shock Hugoniot for a foam in the P-V plane. The specific volume of the foam is in units of the specific volume of the solid constituent.

Other more realistic examples appear in, for example, Zaretsky and Ben-Dor [7VV-7WW]. While this gives a simple, analytical model to use as guidance, all of the complex issues concerning chemical kinetics, mechanical strength, pore collapse, and hydrodynamic instabilities are buried in the enthalpy, h_{dis}. In addition, the effects of this list of phenomena are intimately coupled to the phase behavior inherent in the EOS. The point is that, given shock pressure and specific volume data, one must have an accurate EOS to model h_{dis} correctly from a variant of Eq. (III-7.2) which employs the accurate EOS.

It is worth noting that this discussion will not always make a strong distinction about which material is under discussion. Remarkably, the dominant features of pore response to shocks, local shear, shear-induced local heating, local-heating-induced ionization, shock-induced conduction and polarization, and the various interfacial instabilities often cut across material type. The material properties most often appearing in models of shocked porous media are pore size, shape, possibly orientation of the shock front to the pore shape, and polarity or polarizability of the material, density difference across an interface, shock strengths, and material strengths.

The basic scenario as supported both empirically [7HH] and through simulations [7NN, 7RR] is that a sufficiently strong shock impacting a pore will cause a microscale instability at the first pore surface encountered. In general, the instability will be a combination of RM and RT instability modes. Drag-induced shearing results in jetting into the pore cavity, an example of which can be seen in the hydrodynamic model of Holmes et al. [7O]. As a result, this material heats more than surrounding material not undergoing the same degree of deformation and shear rate [3T]. If the pore is large enough, a full jet will form until it impacts an opposing wall of unreacted material. If the shear-induced heating is high enough, the material in the jet will partially ionize when it impacts the opposing wall. Ionization introduces the possibility of a Kelvin-Helmholtz instability, a phenomenon most often associated with

plasmas. For instance, Peyser et al. [7KK] observe this kind of instability within 0.5 ns of the passage of a 70 km/s shock over the interface between brominated polystyrene at 1.22 g/cc and carbon resorcinol foam at 0.1 g/cc. Thus a foamed form of a polymer will show higher shock temperatures and greater luminosity because of electron-ion recombination than its bulk counterpart under similar shock conditions.

Shape and orientation enter in because of the requirement that the pore surface have high enough curvature to meet the instability criterion. Size also enters in in both ways modeled by Demol et al. [6D]—as influencing the internal surface area, and as allowing the instability to develop enough for heating and ionization to take place. Moreover, passage of a shock wave causes permanent dipoles to align perpendicular to the shock front. Alignment acts as a secondary orientational effect that can enhance ionization.

Porosity dictates acknowledgment of the intrinsic, two-phase nature of the system. Some discussion of this topic appears in Sec. III.5 in relation to fragmentation processes, but further discussion is delayed until Sec. III.9 in which the Baer-Nunziato model [9A] is discussed in more detail. Void or pore collapse also pertains to the topic of compaction in DDT theories which will also be discussed in Sec. III.9.
The most frequently cited model for shocked porous media is the CH model [7F], a single-phase model with an effective single-phase EOS. The CH model has been widely tested and used with considerable success for closed pores. Its applicability to open-cell foams is much less certain. In the CH model, the effective EOS is approached by modifying the EOS of the nonporous material. First, the pressure of the nonporous material is expressed as a function of specific volume, V_{np}, and specific internal energy, E_{np},

$$P_{np} = P(V_{np}, E_{np}) \qquad \text{(III.7-3)}$$

Then, the pressure of the porous material is obtained from the pressure of the nonporous material by scaling the specific volume and the whole pressure function by the volume ratio, $\alpha = V/V_{np}$,

$$P = P(V/\alpha, E)/\alpha \; . \qquad \text{(III.7-4)}$$

The internal energy of the porous material is modified by a potential that describes compaction [7AA]. This form for the effective pressure is closely related to the more general expression which results from taking the effective EOS as a linear combination of the EOSs of the gas and solid phases in which the volume fractions of each phase serve as the linear coefficients [7NN].

To connect the pore structure with a constitutive model which will tell how the shape of a pore will change when it is shocked, the volume ratio, α, is related to the radii of a hollow sphere which represents a pore. Infinitesimal changes in the pore radii are related to bulk and yield-strength moduli. With these constitutive relations established, a second-order differential equation in time for the evolution of α is constructed which must be solved in concert with the usual shock dynamics equations. The time evolution of the porosity is required to calculate the work required to collapse the pore, the energy for which comes from the shock wave. Finally, critical pressures are defined corresponding to catastrophic collapse of the pore. (The interested reader is referred to [7F] for the complete details.)

The substance of the CH model is the addition of compaction and reaction progress thermodynamic variables to single-phase equations of motion. There are physically more complete models [6F, 7R-7S, 7W], but generally these do not conform to the highly viscoplastic scenario described above. These move to the more sophisticated two-phase flow formalism and achieve closure through application of mixture theories [7S, 9A and references therein]. On the other hand, at least two earlier but less well known models [7K, 7U] achieve the desired direct connection between viscoplastic work and heating while maintaining a reasonable level of tractability.

Most of the work on the CH model is derived from energetic materials. Structurally, the formalism for nonenergetic porous materials is the same: mass density and velocity are scaled by the volume fraction that the mass actually occupies. (See [7RR] for one particularly clear exposition.) So, for instance,

Trucano and Grady [7PP] use, for copper impacting polyurethane foam, the same basic code that Baer and Nunziato [9A] use for DDT simulations in granular HMX.

Strongly shocked foams also behave much like a material of the equivalent bulk density. For sufficiently low density foams, Yakushev [7TT] and Bolkhovitinov and Khvostov [7E] found behavior akin to gas-phase detonation even though the foam was nonenergetic. These conclusions are supported by a host of other observations [7D-7E, 7K, 7U].

However, shock strength and degree of porosity do matter as demonstrated by Zaretsky and Ben-Dor [7VV-7WW] and Skews et al. [7MM]. They found that the plastic deformation work of collapsing pores at moderate shocks and higher-density and/or more rigid foams accounts for most of the difference in shock behavior between these foams and their bulk counterparts. The model, another takeoff from the P-α model and its extensions, is fairly detailed. Likewise, in one of the rare references to foam structure [7D, 7UU], the authors found that open foams admit greater gas permeation ahead of the front which again drives the modeling toward the two-phase regime.

One limitation of the CH model is the form of energy dissipation embedded in the model. Given its origins in solid, energetic materials, it is understandable that the yield strength is used as a measure of the energy-adsorbing capacity of the material. In short, it is a model for elastic-plastic materials, for example, the crystalline phase of PBX-9501 (Fig. III-2a). For one strongly dissenting view on using an elastic-plastic constitutive model for a viscoelastic material (Fig. II-2b), see Wallace [7QQ].

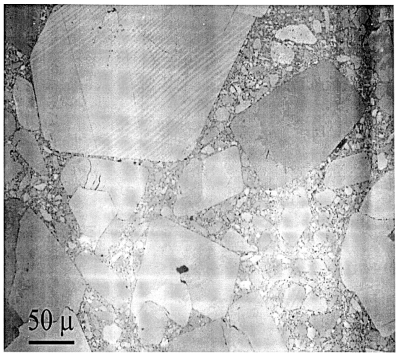

Figure 7a. This illustration shows an optical micrograph image of PBX-9501, courtesy of Cary Skidmore, LANL, DX-2.

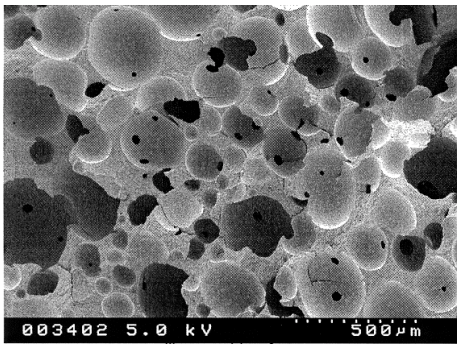

Figure 7b. This is a scanning electron microscopy image of S5370 estane, courtesy of Warren Steckle, LANL, MST-7.

Another limitation of the CH model is that it is only considers phenomena on a single-pore scale. For sufficiently strong shocks, larger length and time-scale phenomena must be taken into account. Prominent among these are the interfacial instabilities that arise 1) when a fluid of one density is accelerated through a fluid of lower density (an RT instability), and 2) when a shock wave crosses an interface between fluids of differing density (an RM instability). The density difference is a ubiquitous feature of models of these instabilities. It is expressed as the Atwood number, which is the ratio of the density difference to the total density of the two materials,

$$A = (\rho_1 - \rho_2)/(\rho_1 + \rho_2) \, . \qquad \text{(III.7-5)}$$

A tremendous amount of effort has been expended recently in understanding the nature of these instabilities. The difficulty with the early treatments of Richtmyer in 1960 [7KK] is that, in general, the linearized stability analysis gives too high a growth rate at later times, even for fluids which fulfill the assumptions of the model. The central assumptions of the analysis are that both fluids are structureless,

incompressible, and inviscid, and that the shock wave accelerates the second fluid impulsively. The need to account for materials properties seems to be exacerbated in polymeric materials of all kinds. While for very strong shocks in the 10 Mbar shock-pressure regime, these assumptions are fair [7KK], in the 0.1 Mbar regime, these assumptions are inappropriate [7VV-7WW]. The material properties of polymers become even more important below this pressure regime [7MM]. Foamed materials add yet another complication because they themselves are two-phase materials. If they are shocked by a third fluid differing in density from either of the two constituting the foam, strictly speaking, there is a three-density problem.

Orler discusses some cases of interest to the Laboratory involving silica-filled polymers [7JJ]. In some of these cases, the sign of the Atwood number may be reversed. The silica particles used in these filler applications can be at fairly low densities themselves. Fortunately, Chen et al. [8C] from the geological community present a very thorough, up-to-date analysis of shocked silica.

It is very instructive to present the analytical analyses of Koenig et al. [7V] and Alon et al. [7A, 7L], in spite of their shortcomings. These analyses will qualitatively illustrate the time scales, length scales, and material-properties dependence of the idealized models applied to PBX-9501 driving low-density polyurethane foam. Koenig et al. measure the particle velocity of a foam strongly shocked by a laser-driven aluminum plate. They are able to fit their results to a model assuming that both materials become ideal gases after the passage of the shock front. Their model estimates the initial particle velocity of polyurethane driven by PBX-9501. This value gives the initial velocity jump at the fluid interface. (Note that these experiments occur on a 10 ps time scale, whereas the instability phenomena occur on a 10 ns time scale). Peyser et al. measure the mixing zone width as a function of time. Again they are in a very strongly shocked regime for which the idealized RM model applies. They use a model developed by Alon et al. The viscous drag between the fluid of the detonated PBX-9501 and the foam enters the model analytically.

In this idealized model, we will appeal to two models. The first gives the change in the foam-particle velocity relative to the particle velocity of the driving fluid, and the second gives the mixing zone width due to the RM instability. As a driving fluid, we use PBX-9501 at its CJ pressure, density, and velocity. Its EOS is approximated as an ideal gas. For the foam, we examine postshock densities of 0.1 and 1.0 g/cm^3. The relative particle velocity between the explosive and the foam is given by the expression

$$g = 1 - \sqrt{\varepsilon}\,[(\alpha\, g^2)^{1/\varepsilon} - 1]\,, \qquad \text{(III-7.6)}$$

where $g = U_{foam}/U_{PBX}$, $\varepsilon = (2\,\gamma_{PBX})/(\gamma_{PBX}-1)$, $\alpha = [\rho_{foam}(\gamma_{foam}+1)]/[\rho_{PBX}(\gamma_{PBX}+1)]$, the ρ's are the densities, the γ's are the heat capacity ratios, and the U's are the particle velocities. As an approximation, we take $\gamma = 5/3$ which makes $\varepsilon = 5$.

The second model, for the RM instability, consists of two parts—the early time, which is linearized in the inverse wavelength of the perturbation, and the late time, which behaves nonlinearly, reflecting the fact that the interpenetrating fluids take on a universal shape near their tips, defined by the drag forces between the fluids. In the impulsive approximation, the linearized regime growth rate, v, is given by

$$v(t)/v_0 = 1 \pm A\,\Delta U\,k\,t\,. \qquad \text{(III-7.7)}$$

The growth rate v is scaled by initial perturbation in the velocity profile, v_0. The variable k is the inverse wavelength of the perturbation, and ΔU is the velocity jump at the fluid interface imparted by the shock. The linearized regime is assumed to last $1.1\lambda/t$. Richtmyer estimates that $v_0 \sim A\,\Delta U\,k\,a_0$, where a_0 is the initial perturbation amplitude at the interface [7A]. The $\pm$ is associated with bubble (lower density fluid) and spike (higher density fluid) velocity perturbation growth, respectively. This approach is the original analysis of Richtmyer as reproduced by Alon et al. [7A, 7L and references therein], Peyser et al. [7KK], and Mikaelian [7BB], among others.

The growth rate v(t) slows at later times relative to the rate in the linearized regime. At later times, the mixing zone width takes the form [7A]

$$a(t) = a(t_0) + b \ln(1 + \Delta U\,(t - t_0)/b)\,, \qquad \text{(III-7.8)}$$

where a(t) is the mixing zone width at time t; t_0 is the time constant for the linearized regime; and b is a constant depending on the coefficient of drag, the densities of the materials, and the wavelength of the perturbation. The late-time behavior is determined from the Bernoulli equation [7L].

As an estimate of the velocity jump as the shock crosses the material interface, we use g from Eq. (III-7.6). (Note that the experiments determining g take place on a 10-ps time scale, whereas the RM instability develops over a 10-ns time scale.) In terms of g, the jump velocity $\Delta U = U_{PBX}$ (g -1). The constant $a(t_0)$ from the linearized growth regime is given by Eq. (III-7.7) [7L]. The characteristic time t_0 is determined by the point at which the linear growth rate crosses the asymptotic bubble velocity, $\lambda/(3\pi v_0)$. Another equally valid value for the asymptotic bubble velocity is λ/C_s, where C_s is a sound speed in the material. The velocity jumps and mixing-zone widths implied by Eqs. (III-7.6) and (III-7.8) for foam densities of 0.02 and 0.40 g/cm^3 are shown in Fig. III-3. The perturbation wavelengths are taken as the average, spherical pore size as implied by the ratio of the foam density to the density of polyurethane. The corresponding wavelengths are estimated by the average center-to-center separation between spherical voids. The results are $\lambda(0.02) \sim 146$ μm and $\lambda(0.40) \sim 86$ μm. The initial amplitudes are approximated by a pore diameter of 100 μm, so that $a_0 \sim 50$ μm regardless of the foam density. Note, though, that the grains of HMX shown in Fig. III-2a are of comparable size to the foam pore sizes. One could equally well base amplitudes and wavelengths on the HMX.

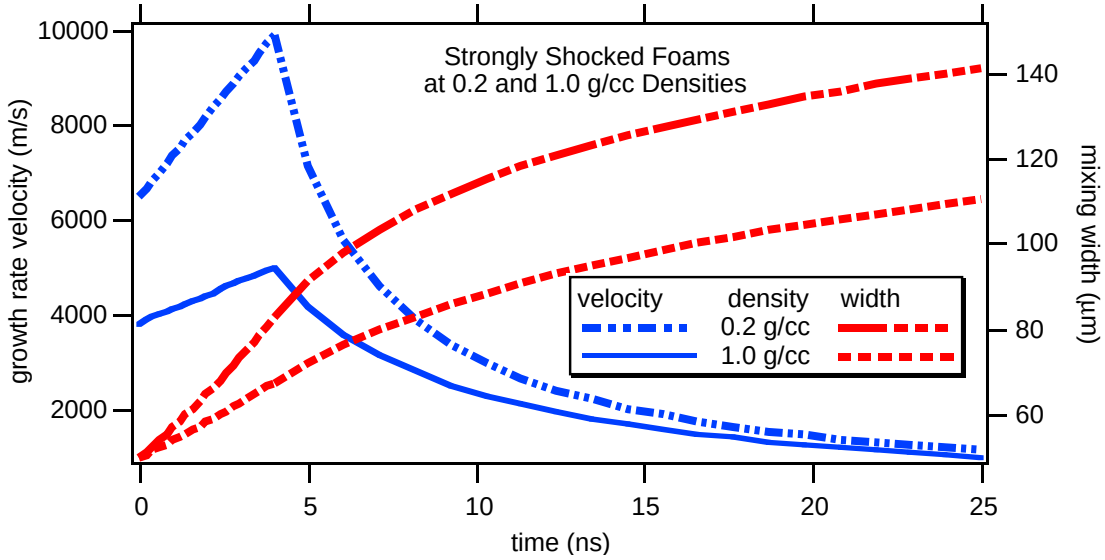

Figure III-3. This figure shows examples of predictions of mixing zone front velocities and mixing zone widths for PBX-shocked foams. The foams are at different densities leading to differences in the transmitted shock strength, particle velocity, and decay rates. These examples are meant only as order-of-magnitude estimates of the mixing lengths and decay times. They also serve to illustrate the use of the Eqs. III-7.7 and III-7.8, representing the different time regimes of the RM instability.

Even the analysis of the linearized growth regime itself is controversial. Which physical effects must be included for a given process is not always agreed upon by the experts in the field. For example, if viscous effects are included, Mikaelian [7BB] modifies Eq. (III-7.7) to

$$v(t)/v_0 = 1 \pm A\,\Delta U/(2k\nu)\,(1 - \exp(-2\,k^2\,\nu\,t))\,, \qquad \text{(III-7.9)}$$

where the effective kinematic viscosity, $\nu = (\mu_{PBX}+\mu_{foam})/(\rho_{PBX}+\rho_{foam})$, with the μ's being viscosities. At short times, this expression agrees with Eq. (III-7.7). Including compressibility—as do Holmes et al. [7O]—imparts an oscillatory dependence to the time-dependent term of Eq. (III-7.7). Surface tension imparts yet another oscillatory dependence. How great an effect compressibility and viscosity have on any given final analysis about shocked-foam behavior is still an open question.

Clearly though, the impulsive analysis is too simple. The impulsive approximation assumes that the velocity jump ΔU takes place instantaneously. Yet the width of the shock zone in PBX-9501, 100 μm, is on the order of the mixing zone width itself. In addition, material strength, decomposition, and transformation rates all play a significant role at the strong shocks of typical weapons explosives. For these reasons, it seems likely that the more complete analysis of Holmes et al. [7O] will be necessary for quantitative work. While the key expressions are more complex than those presented here, they appear tractable as submodels within other hydrodynamic codes. In addition, earlier work by Mintmire et al. [7DD-7EE] and Wang and Zhang [7RR] suggests that molecular dynamics can be a useful tool for furthering our understanding of the short-time behavior of these systems.

8. Phase Transitions in Shocked Materials

The importance of phase transitions in shock propagation lies in the energy dissipation associated with the transition process. This dissipation can act to destabilize the propagation, leading to oscillatory behavior or splitting of the shock front, or, in extreme cases, the propagation can be arrested. As noted in the discussion about EOSs (Sec. III.1), modeling the shock states of a material is sensitive to partitioning energy among unreacted solid material, gaseous reaction products, and solid reaction products. The more phases present in the reacted and unreacted solids, the more difficult it is to achieve the required accuracy [1S]. Bates and Montgomery [8A] and Chen et al. [8B] analyze the impact of the proximity of the Hugoniot state to the phase transition critical constants to the destabilizing propensity of the transition. Chen et al. demonstrate by analytical modeling and simulation that the pressure in a spherical release wave is sensitive to the presence of irreversible phase changes. The pressure, P, follows a power-law dependence on the radius, R, of the sphere, $P \sim R^{\alpha}$. The power, α, changes from –1.1 to –2.7 when the phase transformation is included in the material under study. Ree [8L] demonstrates the sensitivity of EOS models on the number of fluid phases assumed to be present in the combustion zone in predicting the CJ state of PBX-9404.

The hallmark of phase transitions under shock conditions is that the slope changes in the u_s–u_p Hugoniots for that material [1E, 1S, 3M, 8C]. The slope reflects the dissipation added by the phase transition. The slope changes in the Hugoniots in most materials are readily observable, and this includes polymeric materials as well. The shock equations of state discussed in Sec. III.1 can be consulted for examples of these behaviors. As far as modeling goes, tabular EOSs, such as the SEAME and QEOS forms, can more readily represent phase changes. Analytical forms tend to have much more difficulty with phase transitions. In either case, the difficulty is finding or generating sufficient data to quantify the thermodynamic state and properties of the transition. Even though u_s-u_p data is not particularly sensitive to material properties, piecewise linear fits of the data do provide a reasonable approach to capturing phase-change behavior.

A second difficulty is in identifying the mechanism of the transition. MD simulations have demonstrated some success in modeling shock-wave stability in simple molecular solids [8M, 8P]. Mechanistic assessments become possible when a match can be found between simulation and experiment for a particular material. More realistic atomic-potential energy surfaces are needed to

produce these matches, but possibilities do exist. More advanced experimental techniques discussed in Sec. IV will also play a pivotal role in determining phase-transition mechanisms. Mechanistic determination is particularly important with regard to materials substitution issues.

Polymeric materials exhibit a number of phase transitions, but most seem to be washed out by the high propagation rate of the shock or detonation front compared to the rate characterizing the phase transition. Consequently, the observed behavior in the u_s–u_p Hugoniots is largely restricted to at most two changes in slope [1E, 1V, 1X-1AA]. A third transition of significance is the onset of ionization. The energy dissipation [7F, 7X, 7Z], phase separation [8H, 8L] changes in reaction pathways, and pressure sensitivity of ionic reaction rates [6E] make ionization a singularly important transition [3M, 5V, 8H].

A final qualification of the previous paragraph is that slower-phase transitions make their presence felt in the permeation-compaction zone discussed in Sec. I. This sensitivity will certainly apply to polymeric foams and composites.

9. Multiphase Flow

Multiphase-flow simulations constitute a discipline in themselves. Nevertheless, some account of the current thinking with respect to explosively driven shocks is required here. For present purposes, three major themes deserve mention: exchange of energy, mass, and momentum between phases; reduction of multiphase models to single-phase ones; and vapor-explosion models. The first topic is pertinent because porous media are inherently two-phase materials, because phase separation can occur within the product gases or fluids [8L], because of the sensitivity induced by product-phase separation or by solid products (i. e., carbon soot) [1GG, 7N], and because of the propensity of supercritical fluids to shatter upon release [5U]. The second topic is pertinent because single-phase flow models are so much simpler and numerically more robust. If it is possible to avoid explicit consideration of multiphase flow through suitable averaging, introducing new state variables, and/or physical reasoning, one should take advantage of the situation. The third topic is important for the development of multiphase flow simulation techniques, which the thermal- and vapor-driven-explosions community has had to develop out of necessity.

Fortunately, some simplification of the discussion is possible because a prevailing two-phase model has emerged, the Baer-Nunziato (BN) DDT model [9A]. If it is indeed necessary to model a detonation as a multiphase system, the BN model provides a comprehensive, well-tested framework from which to start. The comparative value of the BN model can be deduced by observing just how many efforts have been made to improve and correct it and how many research groups have been involved. The essence of the model with respect to exchange processes is based on a theory of mixing by Passman, Nunziato, and Walsh [9M]. They exploit a principle promoted by Truesdell (see references in [9M]) in which the entropy of the whole system is required to increase continuously through its dynamical evolution. This increasing-entropy principle is only an inequality and does not uniquely decide the issues of exchange, but it does seem to be a sufficiently strong constraint to keep the evolution process behaving in a physically sensible manner.

The debate between single-phase and two-phase flow models is as active as ever. There seems to be little doubt that two-phase flow models are superior in their physical fidelity. The main issue of contention is whether the improvement in fidelity warrants the higher computational cost. One possible resolution: Given the need to calibrate single-phase follow models to construct effective EOSs and constitutive models, it seems possible to use two-phase flow models to aid in the calibration.

In thermal and vapor-driven detonations [9D-9F], it is customary to treat the fluid fragmentation. Even though the fragmentation process is due to RT instabilities which evolve on a different time scale and have different physical origins, becoming familiar with the state of the art in this field is beneficial just for the numerical methodology. In addition, the description by Bolkhovitinov and Khvostov [7D] of

shocked foams as behaving like vapor explosions enhances the importance of work in the vapor-detonation community to Laboratory programs.

IV. Recommendations

Suggestions for topics of near-term focus appear below, sometimes accompanied by a recommendation on the most promising models deserving deeper exploration. In this section, the numbers in parentheses at the beginning of paragraphs refer to the numbered topics in Sec. III.

At a more general level, the strategy of this overview has been to explore concepts used to understand shocked energetic materials that might be applied to understanding the less-well-studied shocked, nonenergetic materials. The most promising of these concepts involve applying pore-collapse models used in explosive initiation [7F, 7OO] to shocked porous, nonenergetic materials, viewing shocked, low-density foams as behaving like a vapor detonation [7E, 9F], and adopting one of the major schools of explosives kinetics models to the shock decomposition of the polymeric materials. The adaption of pore collapse to open foams is less certain and requires additional study as to feasiblity and required modifications. Constitutive models by Zaretsky and Ben-Dor [7VV-7WW], Krysanov and Novikov [7X], and Nesterenko [7GG] are especially important as starting points, since these types of submodels are even more scarce than EOS submodels. Most of what has been done in modeling especially low-density and open-cell foams is at low-shock speeds compared to Laboratory needs. It seems that a good number of these topics converge on the topic of hydrodynamic instabilities.

Recommendations on specific topics are as follows.

(III.1) It seems that the QEOS is the most versatile of the EOSs in that it spans wide ranges of temperature, pressure, and materials types and includes straightforward treatment of phase transitions of several types, as well as coping with both neutral and ionic species in a continuous manner. If one systemwide EOS form is desired, this has to be the leading candidate.

At least in the near term, specialized models of kinetics and EOSs for polymeric materials seem too restrictive. Moreover, they have usually been tested only in environments that are much more benign than a strong, explosively driven shock. It is not yet clear whether additional effort would result in a comparable improvement in simulation fidelity.

(III.2, III.4, III.5, III.6) If shear modes of material deformation are important for shock chemistry in all of the materials of a heterogeneous explosive, then the constitutive models, failure models, and chemical kinetics models need to be connected with an unprecedented degree of consistency.

(III.2, III.4, III.9) Johnson and Holmquist [2O], Curran and Seaman [4U], Johnson and Addessio [4P], and Bürger, Unger, and coworkers [9D] propose general-purpose shock models that might act as frameworks for testing submodels of kinetics, pore collapse, ionization, fragmentation, shattering, and EOSs. Ultimately, more comprehensive models such as the Baer-Nunziato DDT model [9A] will be more desirable, but in the near term, simplicity is preferable.

(III.5) An effective, single-phase model [7OO, 7SS] may be a reasonable starting point for assessing the relative importance of shattering processes. Implementing this study requires translating into a numerically compatible form the model free-energy function that Raz et al. [5U] developed for shattering transitions.

Models of fragmentation have been successfully developed for shearing, stretching, and irradiating modes of polymer fragmentation and depolymerization. Overall, a sound, fundamental basis for studying polymeric shattering kinetics is readily available and relatively straightforward to understand and implement. It may be desirable to generalize the results for a non-delta function dependence in Eq. (III.5-3) to a realistic form yet to be identified. Exploring appropriate multivariate-rate functions can be approached through MD simulations of shocked hydrocarbon polymers using the Brenner potential for the atomic interactions [7EE].

(III.6) It is noteworthy that the first two concepts for chemical kinetics can be tested fairly rigorously through MD simulations on selected organic molecules. Three particularly attractive candidates are cyclopropane [6N], cyclobutane [6N], and norbene [6CC]. Since all three are pure hydrocarbons, the Brenner potential [6S] should behave very well for these molecules. As for metallization processes, the Brenner hydrocarbon potential makes some provision for resonance bond structures. Thus it can stabilize benzene relative to other hydrocarbons. While certainly not completely accurate, this potential can at least give some sense of the metallization processes that Gilman [3I-3J, 6R], Dremin [6J], Enikolopyan [6K-6L], and Coffey [3D] emphasize.

Those working on shear-driven kinetics concepts need to develop working equations that can be tested in a numerical simulation. I believe that the lack of such equations has hampered investigation of shear-driven chemical kinetics.

The CH model [7F] is among the most widely accepted submodels in the field. It may be used with reasonable expectation of success in modeling HE porosity, foams, damage-induced gaps and voids, and porous ceramics at high-shock strength. I am almost certain that Demol and Saurel would disagree with my assessment, but here, the issue of complexity also must be considered. However, the model of Nesterenko [7HH] would seem to be a preferable alternative to the CH model.

(III.7) Constitutive models for polymeric materials are another matter. Because of the tremendous toughness of many polymers over huge ranges of strain, specialization in the model seems warranted. In particular, toughness may be a preferable measure of energy dissipation in pore collapse for viscoelastic materials rather than yield strength as in the CH model. At this time, it simply is not clear how polymer toughness, strong shocks, explosive products, and high temperatures and pressures interact. This question needs to be resolved, and additional study to identify a starting point is necessary.

All of the above considerations have an impact on modeling the hydrodynamic stability of shocked porous materials. The best model available at the moment appears to be the Zhang-Son model cited by Holmes et al. [7O]. There have been many successes with several instability models, including the Zhang-Son model, in which materials actually become fluids after they are strongly shocked. However, these models are still somewhat deficient in modeling foam. The issues surrounding filled polymers and loaded foams are essentially unexplored at this time.

(Experimental) Experimentally, optical and electronic plasma diagnostic techniques, indirect-laser-driven shocks, more elaborate nanoscale flyer-plate studies, and "model" experiments of polymer kinetics and transport behavior deserve as much attention as can be financed. Mass spectrometry holds great promise for highly controlled product collection, a recurring obstacle to model development.

Finally, I want to mention two topics not covered in this overview—numerical methods and highly energetic reactions. During the development of this report, it appeared that the performance of various numerical methodologies involved sufficient model dependence to warrant a delay in discussion. It seems more profitable to examine several physical submodels for a given phenomenon and then to discuss simultaneously their computational tractability, numerical stability, and physical fidelity merits. In addition, highly exothermic but non-explosive reactions have not been discussed in this overview but may be of some importance at a later date.

V. Annotated Bibliography

References appear alphabetically within each subsection. Each subsection here corresponds to a subsection in Sec. III. The references containing *SHOCKXY* refer to the AIP series, *Shock Compression in Condensed Matter,* for the year 19XY. The associated conference proceedings would have been published the succeeding year.

1. **Equations of State**

A. V. G. Baonza, M. Cáceres and J. Núñez, "Universal compressibility behavior of dense phases," *Phys. Rev. B: Condens. Matter* **51**, 28 (1995-I).

Generalizations of the Tait and the Murnaghan EOSs, applicable to solids under compressions up to several GPa's and below 500 K. Some reasonable evidence for breadth of materials as claimed.

B. J. M. Berry, W. Brostow, and M. Hess, "P-V-T relations in a series of longitudinal polymer liquid crystals with varying mesogen concentration," *Polymer* **39**, 4081 (1998).

Pressure-volume-temperature relations for polymer liquid crystals up to 400°C and 0.24 GPa. Effects of mesogen concentration. Corresponding states formulation, Hartmann EOS. Essentially, normal conditions appropriate to damage and insult.

C. G. H. Bloom, "Grüneisen parameter measurements for high explosives," *SHOCK81*, 588 (1982).

Determines Grüneisen parameters for PBX9404 and RX-03-BB at full density and a reduced density. Aluminum used as a calibration material. Electron-beam material heating and laser interferometry front tracking. LLNL.

D. A. V. Bushman, I. V. Lomonosov, V. E. Fortov, K. V. Khishchenko, M. V. Zhernokletov, and Yu. N. Sutulov, "Experimental investigation of phenylene and polystyrene under conditions of shock loading and isentropic expansion. Equations of state of plastics at high energy densities," *Sov. Phys. JETP* **82**, 895 (1996).

Shock adiabat and isentropic release data on polystyrene and on phenylene used to construct a high-temperature/-pressure EOS that looks to be of the Mie-Grüneisen form. Caloric form.

E. W. J. Carter and S. P. Marsh, "Hugoniot equations of state of polymers," J. N. Fritz and S. Sheffield, Eds., LANL report LA-13006-MS (1995).

Still the most cited work on polymer Hugoniot EOSs. Work actually is from 1977 and before.

F. R. Cauble, L. B. Da Silva, T. S. Perry, D. R. Bach, K. S. Budil, P. Celliers, G. W. Collins, A. Ng, T. W. Barbee, Jr., B. A. Hammel, N. C. Holmes, J. D. Kilkenny, R. J. Wallace, G. Chiu, and N. C. Woolsey, "Absolute measurements of the equations of state of low-Z materials in the multi-Mbar regime using laser-driven shocks," *Phys. Plasmas* **4**, 1857 (1997).

Laser-driven shock experiments on polystyrene for ICF program (LLNL, University of British Columbia-Vancouver, and Queens University-Belfast) up to 4 GPa. Claim absolute Hugoniot measurements. Compare SESAME model and their QEOS model for polystyrene and their dissociative model for D_2. Massive differences. Clearly need to check things out with folks at TFF. Companion articles are (1) More, Warren, Young, and Zimmerman, *Phys. Fluids* **31**, 3059 (1988) and (2) Holmes, Ross, and Nellis, "Temperature measurements and dissociation of shock-compressed liquid deuterium and hydrogen," *Phys. Rev. B: Condens. Matter* **52,** 15835 (1995-II). (1) contains a generalized EOS for materials at high pressure with electronic properties estimated from Thomas-Fermi theory. Temperature treatment appears to be ad hoc though.

G. R. Cauble, T. S. Perry, D. R. Bach, K. S. Budil, B. A. Hammel, G. W. Collins, D. M. Gold, J. Dunn, P. Celliers, L. B. Da Silva, M. E. Foord, R. J. Wallace, R. E. Stewart, and N. C. Woolsey,

"Absolute equations-of-state data in the 10–40 Mbar (1–4 TPa) regime," *Phys. Rev. Lett.* **80**, 1248 (1998).

Absolute Hugoniot EOS data for polystyrene and beryllium metal in the terapascal regime with indirect-drive laser-irradiated hohlraum-mounted targets. Indirect drive enables absolute rather than relative EOS data, meaning no standard is required. X-ray transmission radiography measurements give both the particle speed and the shock speed. Give references for absolute data on aluminum, tungsten, molybdenum, and LiD to confirm earlier data based on relative EOSs. Only the polystyrene EOS was found to be in error.

H. R. Y. Chang, C. H. Chen, and K. S. Su, "Modifying the Tait equation with cooling-rate effects to predict the pressure-volume-temperature behaviors of amorphous polymers: Modeling and experiments," *Polym. Eng. Sci.* **36**, 1789 (1996).

Formulate a time-dependent version of the widely used Tait EOS in order to capture cooling-rate effects. Argue that this is important because of the dependence of the glass transition temperature on cooling rate.

The basic EOS relationship is

$$V(P,T) = V(0,T)\ \{1 - C \ln[1 + P/B(T)]\},$$

where V is the specific volume, P the pressure, T the temperature, and B an exponential function of temperature. Here, C is a universal constant given by Simha as 0.0894. This relationship is modified to represent crystallization/melting transitions. The functional forms of $V(0,T)$ and $B(T)$ are allowed to change depending on whether one is above or below the glass transition temperature. Other researchers have found an empirical relationship between glass transition temperature T_g and cooling rate q of the form

$$\theta = \mathrm{d}\ T_g/\mathrm{d} \log(|q|).$$

The material parameter θ appears in the functional forms for $V(0,T)$ and $B(T)$ below the glass transition. More appropriate to damage and insult.

I. F. Charlet, M.-L. Turkel, J.-F. Daniel, and L. Kazandijan, "Evaluation of various theoretical equations of state used in calculation of detonation properties," *Int. J. Impact Engng.* **20**, 533 (1997).

Description of theoretical EOSs such as those originating from the Lennard-Jones-Devonshire theory and as implemented in their thermochemistry code called CARTE.

J. R D. Cowan, and W. Fickett, "Calculation of the detonation products of solids explosives with the Kistiakowsky-Wilson equation of state," *J. Chem. Phys.* **24**, 932 (1956).

Use of Cowan EOS for solids.

K. C. W. Cranfill and R. M. More, "IONEOS: A fast, analytic, ion equation-of-state routine," LANL report LA-7313-MS (1978).

Early computer code and explanation of the basic QEOS concepts.

L. A. Fernández and E. I. Shakhnovich, "Activation-energy landscape for metastable RNA folding," *Phys. Rev. A* **42**, 3657 (1990).

The landscape for the activation energies, as opposed to the metastable equilibrium energy landscape, for ribonucleic acid folding. Might be a useful strategy for modeling irreversibility and locally nonequilibrium effects.

M. J. N. Fritz, R. S. Hixson, C. E. Morris, and R. G. McQueen, "Overdriven-detonation and sound-speed measurements in PBX-9501 and the 'thermodynamic' Chapman-Jouguet pressure," *J. Appl. Phys.* **80**, 6129 (1996).

Constant, adiabatic Grüneisen EOS. Technique decouples the CJ/detonation pressure measurement from reaction zone effects. As a consequence of this model and associated experimental conditions, the pressure measurements are considered very accurate, but the detonation velocities and ordinary Grüneisen parameter determinations are in error, as expected.

N. S. Gabbanelli and S. Roux, “Energy landscape for directed polymers,” *J. Phys. A: Math. Gen.* **27**, 5079 (1994).

Energy landscape concept, probability distribution of free energies, applied to polymers. Orientational effects (from, e.g., hard segments) included.

O. V. K. Gryaznov, V. E. Fortov, M. V. Zhernokletov, G. V. Simakov, R. F. Trunin, and L. I. Trusov, "Shock compression and thermodynamics of highly nonideal metallic plasma," *Sov. Phys. JETP* **87**, 678 (1998).

Model of strongly shocked metallic foams as dense plasmas rather than a hot, dense, but neutral gas.

P. P. D. Gujrati, “Universal equation of state for an interacting multicomponent mixture of polymers,” *J. Chem. Phys.* **108**, 6952 (1998).

Universal EOS for polymer mixtures up to 400°C and 2 GPa, based on a Bethe lattice. Random-mixture theory related to lattice gas models of mean-field theories, of which Flory-Higgins theory is a special case. Reduces to Flory-Higgins theory in certain limits. Treats free volumes, voids, or holes as a separate species.

Q. K. V. Khishchenko, V. E. Fortov, and I. V. Lomonosov, “High-temperature, high-pressure equation of state for polymer materials,” *SHOCK97*, 103 (1998).

Semiempirical EOS for polymers. Internal energy function divided into the usual additive contributions: 0 K elastic, anharmonic, and electronic excitation. This division is extremely prevalent, especially in the quotidian type. Model is, in fact, very reminiscent of that model.

R. D. L. Littlefield, "ANEOS extensions for modeling hypervelocity impact," *Int. J. Impact Engng.* **20**, 533 (1997).

Claims that ANEOS needs modification to deal with hypervelocity impact because the position and shape of the EOS near the liquid-vapor critical point influences the behavior of the release isentrope. Critical constants for Zn become (3.040 kbar, 1.55 g/cc, 3130 K) compared to (2.904 kbar, 2.01 g/cc, 3170 K) experimentally. Both the cold curve and the nuclear contribution needed to be adjusted to achieve this agreement. See also [5F] for another reference on ANEOS and [1F-1G, 1U, 1LL] for strikingly similar adjustments made to the QEOS.

S. C. L. Mader, *Numerical modeling of detonations* (University of California Press, Berkeley, 1979) and *Numerical modeling of explosives and propellants* (CRC Press, Boca Raton, FL, 1998).

Primer, also on video. See also numerous LANL LA-series reports and manuscripts detailing work on EOSs, hot spots, and numerical methods. Later addition contains a "top-to-bottom" discussion of the history of and problems inherent in explosives modeling.

T. J. R. Maw and N. J. Whitworth, “Shock compression and the equation of state of fully dense and porous polyurethane,” *SHOCK97,* 111 (1998).

Polymer EOS of polyurethane. I am sketical of their conclusion, which is summarized by Fig. 5.

U. R. M. More, K. H. Warren, D. A. Young, and G. B. Zimmerman, “A new quotidian equation of state (QEOS) for hot dense matter,” *Phys. Fluids* **31**, 3059 (1988).

Meant as a general-purpose, nonideal EOS; forms the foundation for the EOS used to interpret NOVA: indirect-drive EOS experiments performed in the last couple of years. Consists of three additive terms:

ionic, electronic, and chemical bond effects. The ionic (atomic motion and configuration) term combines Debye (lattice vibration), Grüneisen (pressure–internal energy relation in a solid), and Lindemann melting (relationship of melting temperature and Debye temperature to the fluid density). Original formulation is from Cowan (see [1K]). The electronic term models ionization processes to produce free electrons as in plasmas. This step is done through Thomas-Fermi theory, which treats the classical behavior of the electrons, and, specifically, in a form developed by Feynman, Metropolis, and Teller. Considered adequate above 10 eV. Below that energy, chemical bonding effects become noticeable. The last term plays the role of correcting this low-temperature/-energy deficiency.

The ionic and electronic contributions are considered additive and are allowed to operate at different temperatures. Thomas-Fermi theory is the most primitive form of density functional theory but is retained for reasons of numerical stability and simplicity. For this reason, the chemical bond correction accounts for exchange and correlation effects, as well as chemistry itself.

This approach is especially appropriate for foamed and polarizable materials because of the increased ionization produced when they are shocked. Corrections to this basic theory are noted in the work of Cauble et al. [1F-1G] when applied to the NOVA shots.

V. C. E. Morris, J. N. Fritz, and R. G. McQueen, "The equation of state of polytetrafluoroethylene to 80 GPa," *J. Chem. Phys.* **80,** 5203 (1984).

High-pressure polytetrafluoroethylene EOS. One of the seminal works. Describes dissociation products and phase transitions. Mie-Grüneisen EOS.

W. N. Mousseau and G. T. Barkema, "Traveling through energy landscapes of disordered materials: The activation-relaxation technique," *Phys. Rev. E* **57**, 2419 (1998).

Energy landscape where each local minimum is surrounded by several activation barriers as well. Similar to Fernández and Shakhnovich [1L] and with a strong transition-state theory flavor as well.

X. K. Nagayama and Y. Mori, "Anomaly in the temperature calculations of shocked polymers," *SHOCK97*, 107 (1998).

Low-pressure polymer EOS. Anomaly shows up in the Grüneisen parameter at 0.14-km/s particle speed and 0.50-km/s shock speed in PMMA. Interpreted as a "nonequilibrium" effect.

Y. K. Nagayama and Y. Mori, "Thermal nonequilibrium of the shock compressed state of polymers realized by 1 GPa shock waves," *J. Appl. Phys.* **84**, 6592 (1998).

Low-pressure polymer EOS with emphasis on nonequilibrium aspects. Mie-Grüneisen EOS with three models of the Grüneisen parameter and sound velocity. Both are thought to change at the kink in the u_s-u_p Hugoniot curves.

Z. B. Olinger, J. N. Fritz, and C. E. Morris, "Candidate materials for EOS," LANL internal memo 23 March, (1993).

Composite EOSs for select materials.

AA. B. Olinger, B. McQueen, J. Fritz, and C. Morris, "Candidate materials for EOS," LANL internal memo, 11 September, (1992).

Composite EOSs for select materials.

BB. F. H. Ree, "Systematics of high-pressure and high-temperature behavior of hydrocarbons," *J. Chem. Phys.* **70**, 974 (1979).

Behavior of hydrocarbons associated with high temperature and high pressure. Hugoniot behavior seems to be dominated by carbon-to-hydrogen ratio. Mie-Grüneisen EOS used in analysis of existing data.

CC. F. H. Ree and M. van Thiel, "Effective like- and unlike-pair interactions at high pressure and

high temperature," *SHOCK91*, 225 (1992).

General treatment of high-temperature, high-pressure behavior of carbon, nitrogen, and oxygen mixtures. Use a code called CHEQ, which contains multiphase, multicomponent phase equilibria, "accurate" interatomic potentials (pairwise, between centers of mass of different molecules), high-accuracy mixture model, and EOSs containing all condensed phases of carbon: graphite, diamond, and liquid Supercritical fluid phase separation is found to be very sensitive to the rule of mixture used. EOS numerically defined through free-energy function of composition with specific free energies computed through statistical mechanical models.

DD. V. K. Sachdeva, P. C. Jain, and V. S. Nanda, "Equation of state of poly-di-methyl siloxane fluids," *Mater. Res. Soc. Symp. Proc.* **22**, 243 (1984).

Model of strongly shocked metallic foams as dense plasmas rather than a hot, dense, but neutral gas.

EE. S. Saeki, S. Takei, Y. Ookubo, M. Tsubokawa, T. Yagaguchi, and T. Kikegawa, "Pressure dependence of melting temperatures in branched polyethylene up to 2 GPa," *Polymers* **39**, 4267 (1998).

Pressure dependence of melting temperature on branching in polyethylene.

FF. I. C. Sanchez and J. Cho, "A universal equation of state for polymer liquids," *Polymer* **36**, 2929 (1995).

Universal EOS for polymer liquids up to 400 C and 1 GPa developed from a corresponding states relation. Scaling temperature, pressure, and density are needed. Concise summary of existing EOSs, including Tait, modified Tait, and Murnaghan, with some comments on each. Emphasizes negative curvature in bulk modulus at higher pressure.

GG. M. S. Shaw, "An equation of state for detonation products incorporating small carbon clusters," *SHOCK97*, 69 (1998).

HE EOS from combination of atomistics and perturbative methods. Note that the polymer binder is just blended in with the HE. This method influences the mole fractions of mostly carbon and hydrogen, which are known to influence product distribution and shock stability. (See articles by Erpenbeck [6M] and by Ree [1BB-1CC, 8L]). LANL.

HH. S. A. Sheffield and D. D. Bloomquist, "Low pressure Hugoniot cusp in polymeric materials," *SHOCK81*, 57 (1982).

Make a case for low-pressure Hugoniot cusp in polymers being due to the onset of shock-induced polarization. This represents a new dissipation mechanism. This cusp is at higher shock pressures, speeds, etc., than the cusp discussed by Nagayama and coworkers [1X-1Y].

II. P. Sibani and K. H. Hoffman, "Aging and relaxation dynamics in free-energy landscapes with multiple minima," *Physica A* **234**, 751 (1997).

Rigorous, highly orthodox, thermodynamic, master-equation, phase-space evolution view of aging from a coarse-grain averaging perspective.

JJ. M. E. van Leeuwen, "Deviation from corresponding-states behaviour for polar fluids," *Mol. Phys.* **82**, 383 (1994).

Uses the Stockmayer potential to describe fluids with permanent dipole moments. The critical constants are expressed as a function of the magnitude of the dipole moment as derived from the Clayperon equation. Results from analytical forms are compared to the results from Gibbs Ensemble Monte Carlo simulations. The agreement is not very satisfactory, but the trends are preserved, and the analytical forms provide a more direct means for understanding those trends. The Stockmayer potential is the Lennard-Jones, 6-12 potential plus a dipole term. The LJ pieces strictly adhere to the corresponding-states form. According to this formulation, the polar fluid will become more

corresponding-states-like in its behavior as the dipoles are compressed, but less so when stretched. In a shocked environment, these two processes, compression and extension, compete. The degree of ionization for the particular material under shock becomes crucial. See references and discussion on porous materials, Secs. V.7 and III.7, respectively.

KK. E. D. Weinberger, "Local properties of Kauffman's *N-k* model: A tunably rugged energy landscape," *Phys. Rev. A* **44**, 6399 (1991).

Kauffman model of rugged energy landscape: each Potts or spin-glass-like model in which site is influenced by *k* neighbors. More appropriate for aging properties.

LL. D. A. Young and E. M. Corey, "A new global equation of state model for hot, dense matter," *J. Appl. Phys.* **78**, 3748 (1995).

Updated version of original cited in [1U]. Concentrate on improving agreement with other EOS determination methods (diamond-anvil, laser-generated shocks, sonoluminescence, and laser ablation), liquid-vapor critical points, more-detailed molecular motion models, and better bond dissociation models. Other situations requiring more-accurate EOS data include isobaric expansion of liquid metals, shocked porous materials, solid-solid phase transitions, and shock propagation in rocks. Grüneisen function still used as an adjustable parameter. Cite full electronic structure calculations as the next logical steps in the development of the technique.

Note that the formulation here is a bit different than in the earlier work. The three terms are a cold reference state, nuclear motion and configuration, and electron energy (Thomas-Fermi model). Phase transformations resulting in jump discontinuities in the Helmholtz energy are permitted here. Bond dissociation in, for instance, highly compressed H_2 or polystyrene is treated more extensively as a new contribution to the nuclear motion term.

MM. See http://www.questconsult.com/~jrm/thermot.html .

NN. See http://www.aist.go.jp/RIODB/db030/hy/estimate.html .

2. **Stress-Strain Constitutive Modeling**

A. M. R. Baer, Sandia National Laboratories, Albuquerque, private communication, 1999.

B. S. G. Bardenhagen, M. G. Stout, and G. T. Gray, "Three-dimensional, finite deformation, viscoplastic constitutive models for polymer materials," *Mech. Mater.* **25**, 235 (1997).

Shear-thinning model of polymer viscoplasticity with provision for additional generalization. The typical dashpot-linear spring model lacks shear-thinning behavior. A modification by Bird (of Bird, Stewart, and Lightfoot; Hirschfelder, Curtis, and Bird) capturing this effect (decreasing viscosity with increasing strain rate) has the form

$$\eta = \eta_\infty + (\eta_0 - \eta_\infty)/(1 + (\lambda\varepsilon')^2)^{(1-n)/2} ,$$

where η_0 and η_∞ are the zero and infinite strain-rate limit viscosities, respectively, λ and n are adjustable parameters, and ε' is the strain rate. A formula is given for converting a fraction of the inelastic response into heat. The model is compared for an epoxy resin over the strain-rate range, 10^{-4} through 3×10^3. The resin is not decomposing to any extent at these rates and total strains of 0.4. Qualitatively correct behavior observed.

C. S. G. Bardenhagen, E. N. Harstad, P. J. Maudlin, G. T. Gray, and J. C. Foster, Jr., "Viscoelastic models for explosive binder materials," *SHOCK97*, 281 (1998).

Adiprene-100 binder viscoelasticity Maxwell model compared with experimental deformation profile. The experiment is a slug of binder shot at 303 m/s and photographed. Mention that aged binder is stiffer, but no quantification is given. Deformation profiles qualitatively the same.

D. T. J. Burns, D. E. Grady, and L. S. Costin, "On a criterion for thermo-plastic shear instability,"

SHOCK81, 372 (1982).

Constitutive model with shear instability. Predicts critical strain rate at which shear bands, a bifurcation, appear. Shear stress given the form

$$\tau = c[1 - a(\theta - \theta_0)]\,(1 + b\gamma')^m\,\gamma'^n\,,$$

where γ and γ' are the strain and the strain rate, respectively, and θ is the temperature. Temperature controls thermal softening. Model from Litonski, *Bull. Acad. Pol. Sci. Ser. Sci. Tech.* **25**, 7 (1977). Model predicts critical strain rates of 500/s and 1000/s for cold- and hot-rolled steels, respectively.

E. X. Chen, P. Tong, and R. Wang, "Nonequilibrium statistical thermodynamic theory for viscoelasticity of polymers," *J. Mech. Phys. Solids* **46**, 139 (1998).

Nonequilibrium statistical thermodynamic model of viscoelasticity in polymers focusing on molecular relaxation. Generalizes concepts of thermally activated relaxation mechanisms developed by Eyring, Robertson, and others. The generalization makes use of constraining conditions placed on the deformation/relaxation at some location in a polymer caused by its local environment. That is, how far a polymer unit can move depends on the movement of other units around it and on whether it is attached to those units. Nonequilibrium effects are included through generalized force and displacement contributions to the free energy.

F. S. M. Chitanvis, "Mesoscopic theory of the viscoelasticity of polymers," Los Alamos National Laboratory document LA-UR-98-4805 (1998).

Polymer entanglement model in the linear viscoelastic regime.

G. P. A. Conley, "An estimate of the linear strain rate dependence of octahydro-1,3,5,7-tetranitro-1,3,5,7-tetrazocine," *J. Appl. Phys.* **86**, 6717 (1999).

Comparison of pore collapse models in hot-spot initiation mechanisms. Argue that the singularity of spherical pore collapse in P-α and CH pore collapse is unphysical in a shock context. Very convincing. Wondering if we may be able to apply RM instability concepts as well.

H. O. Coussy, "A thermodynamical approach to nonlinear poroelasticity for unsaturated porous materials," Z. Ange. Math. Mech. **77**, S393 (1997).

Mixture theory for unsaturated porous materials applying Truesdell theory among others. Truesdell's work is also the foundation for the Baer-Nunziato model.

I. O. Coussy, L. Dormieux, and E. Detournay, "From mixture theory to Biot's approach for porous media," *Int. J. Solids Structures* **35**, 4619 (1998).

A strategy for connecting mixture models to single-phase models in porous media.

J. A. D. Drozdov, "Modelling an anomalous stress relaxation in glassy polymers (The Kitagawa effect)," *Math. Comput. Modell.* **27**, 45 (1998).

Constitutive relations for nonlinear viscoelastic response based on a transient network model. These relations are ordinarily considered more physically realistic than dashpot-spring models for elastomeric polymers. They are, however, relatively recent and have not been tested nearly as much as the latter. The anomaly referred to in the title is the stress relaxation that occurs after the strain has been reversed from tensile to compressive. This phenomenon pertains to nonmonotonic strains such as may occur in vibrations or repeated insults.

K. A. D. Drozdov, "Kinetics of volume recovery in amorphous polymers," *Physica D* **124**, 299 (1998).

Constitutive relations for amorphous polymers derived from free-volume concepts. Significant conceptual similarity to void-growth models of damage and failure in ductile materials developed by Murri and coworkers [4U]. Focus is on diffusional behavior of voids, or "holes," constituting the free volume.

L. K. S. Haberman, J. G. Bennett, B. W. Asay, B. F. Henson, and D. J. Funk, "Modeling, simulation and experimental verification of constitutive models for energetic materials," *SHOCK97*, 273 (1998).

PBX constitutive relations accuracy crucial to modeling ignition behavior. Comparison of DYNA3D with laser-induced fluorescence map of impact-ignited PBX9501. DYNA3D utilizes the "Generalized Cell Method" micromechanical model of Aboudi, *Compos. Eng.* **5**, 839 (1995) and Visco-SCRAM constitutive model, Addessio and Johnson, *J. Appl. Phys.* **67**, 3275 (1990). Visco-SCRAM combines the Maxwell dashpot-spring model with a statistical fracture model. HE and binder represented as separate cells in the Lagrangian code. Experiments show far less symmetry and much greater particle/fragment dispersion (spatially) than the simulations.

M. P. Halin, G. Lielens, R. Keunings, and V. Legat, "The Lagrangian particle method for macroscopic and micro-macro viscoelastic flow computations," *J. Non-Newtonian Fluid Mech.* **79**, 387 (1998).

Kinetic theory model approach to simulating constitutive law for a viscoelastic fluid. The evolution of the constitutive relation is tracked through a stochastic differential equation. This paper implements the "dumbbell model" for polymer solutions, but the technique is general. This paper is complementary to Yao, McKinley, and Debbaut [2V] in that the kinetic modeling approach here is offered as an alternative to the purely continuum approach of [2V] and most studies to date. A major advantage is that the constitutive law need not be related to the momentum fluxes of the general conservation equations as a closed form, as for example in a Newtonian fluid. The kinetic equations are solved in a Lagrangian fashion (as is appropriate to most methods of solving a Fokker-Planck equation), while the conservation equations are solved in an Euler form. Polynomial interpolation is used to relate the two meshes.

N. H. Higuchi, Z. Yu, A. M. Jamieson, R. Simha, and J. D. McGervey, "Thermal history and temperature dependence of viscoelastic properties of polymer glasses: Relation to free volume quantities," *J. Polym. Sci. B: Polym. Phys.* **33**, 2295 (1995).

Temperature and thermal history effects on glass polymer properties through free-volume models. Volume measured through positron annihilation lifetime spectroscopy. Free-volume models based on classic Flory-Higgins theory.

O. G. R. Johnson and T. J. Holmquist, "An improved computational constitutive model for brittle materials," *SHOCK93*, 981 (1994).

General constitutive model containing both intact and fracture strength models, touted as suitable for large strains, high strain rates, and high pressures. Most recent model (as of publication date) adds features to account for materials softening during impact. Also touted as suitable for both Lagrangian and Eulerian codes.

Intact strength is given by

$$\sigma_i = A\,(P^* + T^*)^N\,(1 + C\,\ln(\dot{\varepsilon}^*))$$

and the fracture strength is given by

$$\sigma_f = B\,(P^*)^M\,(1 + C\,\ln(\dot{\varepsilon}^*)),$$

where P^* and T^* are normalized external and tensile pressures, and $\dot{\varepsilon}^*$ is a scaled strain rate. Other parameters are empirical material constants. The total normalized stress is the difference

$$\sigma = \sigma_i - D\,(\sigma_i - \sigma_f).$$

The total and individual stresses are normalized to the stress at the Hugoniot elastic limit. The plastic strain-to-fracture is modeled similarly as a function of the two reduced pressures.

The parameter D is the "damage state" variable, which ranges from 0 to 1. A fragmentation model would determine this parameter, whether the model is a void nucleation failure model, one of a variety of statistical crack models, or a shattering model.

P. J. N. Johnson, J. J. Dick, and R. S. Hixson, “Transient impact response of three polymers,” *J. Appl. Phys.* **84**, 2520 (1998).

Impact response for Estane, Estane with nitroplasticizer, and Adiprene. Generalized Maxwell model of polymer response. CHARADE simulation, Johnson and Tonks, Los Alamos Report LA-11993-MS (January 1991). Relatively low pressure regime, <1 GPa. Strain-rate-dependent viscosity, same as in [2B].

Q. N. Katsube and Y. Wu, “A constitutive theory for porous composite materials,” *Int. J. Solids Structures* **35**, 4587 (1998).

Phenomenological poroelastic constitutive model for layered porous materials also including thermochemical decomposition as a result of high temperatures and high heating rates. Strength parameters include Young's and the bulk moduli.

R. V. N. Pokrovskii, Yu. A. Altukhov, and G. V. Pyshnograti, “The mesoscopic approach to the dynamics of polymer melts: Consequences for the constitutive equations,” *J. Non-Newtonian Fluid Mech.* **76**, 153 (1998).

Use of one representative macromolecule to track the complex dynamics of an entire polymer melt. Highly detailed, complex dynamics. Brownian motion again assumed for components of macromolecule.

S. J. Remmelgas, G. Harrison, and L. G. Leal, “A differential constitutive equation for entangled polymer solutions,” *J. Non-Newtonian Fluid Mech.* **80**, 115 (1999).

Attempts a simplified Doi-Edwards-Marrucci-Grizzuti model of extension flow in highly entangled polymers. The simplification is to represent extension of a polymer under shear by a single polymer length vector. This eliminates a multiplicity of length and time scales that appear in the original. The original model is considered physically correct at a qualitative level, whereas most models proposed to date are neither qualitative nor computationally tractable, even at the date of publication, 2000. The simplified model sometimes gives better results than the full model, and is more tractable computationally. The constitutive law is solved using stochastic differential equations for the length and orientation.

T. S. K. Schiferl, R. F. Davidson, and P. J. Maudlin, “Effects of anisotropy on dynamic tensile behavior,” *SHOCK91*, 273 (1992).

Stability analysis of behavior of long rod under tensile conditions. Rapid stretching conditions. Exploring effects of anisotropy on necking behavior. Comparison with classical theory appears unfavorable.

U. J. W. Shaner, R. S. Hixson, M. A. Winkler, D. A. Boness, and J. M. Brown, “Birch’s law for fluid metals,” *SHOCK87*, 135 (1988).

Application of Birch’s law to the acoustic velocity of a liquid metal. Birch’s law says that both the bulk and elastic wave velocities should scale linearly with the density and inversely with the atomic mass. Excellent agreement with experiment. LANL.

V. M. Yao, G. H. McKinley, and B. Debbaut, “Extensional deformation, stress relaxation and necking failure of viscoelastic filaments,” *J. Non-Newtonian Fluid Mech.* **79,** 469 (1998).

Simulations of necking behavior in non-Newtonian polymer solutions. Oldryd-B model does not exhibit necking and never fails. Both Newtonian and Giesekus models, *J. Non-Newtonian Fluid Mech.* **11**, 69 (1982), exhibit necking leading to failure in a stretching filament. Uses POLYFLOW code of Crochet, Debbaut, Keunings, and Marchal, in *Applications of CAE in Extrusion and Other Continuous Processes*, O’Brien, Ed., (Carl Hanser, München, 1992), Chap. 2.

W. J. Zhang, N. Kikuchi, V. Li, A. Yee, and G. Nusholtz, "Constitutive modeling of polymeric foam material subjected to dynamic crash loading," *Int. J. Impact Engng.* **21**, 369 (1998).

Constitutive modeling of the elastic-plastic genre focuses on the low end of foam densities. Study polyurethane, polyethylene, and polystyrene. Both open- and closed-cell structures modeled with LS-DYNA3D. Impact velocities low.

X. M. Zhou, R. J. Clifton, and A. Needleman, "The role of material inhomogeneities in the localization of strains," *SHOCK93*, 1185 (1994).

Flow behavior of tungsten particulates suspended in a soft alloy. Shear bands form because of strain localization. Strain rates from 10^5 to 10^6 and pressures on the order of 10 GPa.

3. **Shock Dynamics and Hugoniot Behavior**

A. T. A. Andreeva, S. N. Kolgatin, and K. V. Khishchenko, "Choosing an adequate mathematical model in problems with high pulsed energy deposition," *Tech. Phys.* **43**, 518 (1998).

Dimensional and similarity analysis of shock dynamics in choosing EOS models.

B. B. W. Asay, S. F. Son, and J. B. Bdzil, "The role of gas permeation in convective burning," *Int. J. Multiphase Flow* **22**, 923 (1996).

Gas permeation in DDT; Darcy flow not important ahead of burn front; still lots to consider about behavior of polymer and HE interactions. Mention shattering of HE in compression wave. Two-phase flow model. Building case for compaction model that is developed in [9B]. Referring back to Fig. 2 of this report (from this reference), note the two-phase flow ahead of the burn front and the indication of a multiphase flow region immediately behind it. The point of their investigation is that the permeation zone is not large, as is generally assumed, even in high-density preforms as shown in Fig. 2. The sense of large is in terms of average grain size.

C. D. W. Brenner, D. H. Robertson, M. L. Elert, and C. T. White, "Detonation at nanometer resolution using molecular dynamics," *Phys. Rev. Lett.* **70**, 2174 (1993).

MD simulations establishing shock front width, transient-to-steady flow time constants, and consistency with ZND theory.

D. C. S. Coffey, "Energy dissipation and the initiation of explosives during plastic flow," *SHOCK95*, 807 (1996).

Discussion of shear localization in HMX crystals in the context of ZND theory. Shock front given a nonzero width in order to accommodate initiation processes within this theory. Naval Surface Warfare Center.

E. M. D. Cook and P. J. Haskins, "Projectile impact initiation of a homogeneous explosive," *SHOCK95*, 823 (1996).

One-reaction Arrhenius kinetics for nitromethane in pure and sensitized forms. Addition of nonenergetic material adds much more complication to the rate law. Need separate parameterization to do sensitization correctly. DYNA2D calculation of aluminum barriers impacted by steel rod. Projectile diameter dependence is clearly observable and lessens modeling agreement at smaller diameters.

F. M. Cowperthwaite and G. K. Adams, "Explicit solutions for steady- and unsteady-state propagation of reactive shocks at constant velocity," in *Eleventh Symposium (International) on Combustion* (The Combustion Institute, Pittsburgh, PA, 1967), p. 703.

MD simulations establishing shock front width, transient-to-steady flow time constants and consistency with ZND theory.

G. V. M. Fomin, "Mathematical modelling of problems of high-speed collision of bodies," *Mater. Res. Soc. Symp. Proc.* **22**, 175 (1984).

Thin- and thick-flyer-plate failure patterns.

H. E. Fugelso, J. D. Jacobson, R. R. Karpp, and R. Jensen, "Radiographic study of impact in polymer-bonded explosives," *SHOCK81*, 607 (1982).
PBX fragmentation measured radiographically from impact of mockup on steel plates. Impact velocity is 0.667 m/s. LANL and Hercules Corp.

I. J. J. Gilman, "Shear-induced metallization," *Philos. Mag. B* **67**, 207 (1993).
Examines the role of shear strains in semiconductor-metal transitions. Uses the case of transformation from a diamond crystal structure (a nonconducting state) to a β-tin structure (a conducting state) as an illustration. Volume change is modest, ~30 %, compared with approximately 50 % volume changes needed in hydrostatic compression to induce the same change.

J. J. J. Gilman, "Plasmons at shock fronts," *Philos. Mag. B* **79**, 643 (1999).
Describes a shock in a metal as an interface between two plasmas of differing densities. The plasmon frequency at the shock front is related to root mean square of the plasmon frequencies on either side of the shock front. The suggestion is to use electron spectroscopies to probe these frequencies.

K. K. A. Gonthier, R. Menikoff, S. F. Son, and B. W. Asay, "Modeling energy dissipation induced by quasi-static compaction of granular HMX," *SHOCK97*, 289 (1998).
HMX DDT experiments and modeling. Emphasis on role of compaction in producing volume changes that are a source of shock energy dissipation. An extension of the Baer-Nunziato model [9A]. LANL.

L. B. Hayes, "The detonation electric effect," *J. Appl. Phys.* **38**, 3135072 (1967).
Early observation of shock-induced conduction and polarization, which Graham and others [7I, 7S, 7V] pick up on later.

M. J. D. Johnson, "The features of the principle Hugoniot," *SHOCK97*, 27 (1998).
General characteristics of shock Hugoniot behavior—the turnover feature that is attributed to activation of more dissipation channels as the shock velocity is increased. LANL.

N. V. A. Kopotev and N. M. Kuznetsov, "Structure of the stationary zone and relaxation instability of a detonation wave in heterogeneous media," *Fiz. Goreniya Vzryva* (English) **22**, 219 (1986).
Detailed discussion of problems in determining the Jouguet point in a heterogeneous detonation wave. Relaxation of temperature and phase velocity between phases and phase transitions lead to a multiplicity of operative sound speeds, i.e., a dispersion. Compares single- and two-velocity models.

O. K. Nagayama, Y. Mori, and K. Hidaka, "Shock compression experiments on several polymers in the 1 GPa stress region," *J. Mater. Process. Tech.* **85**, 20 (1999).
Combine total internal reflectance and gauge (PVDF—polyvinyledine difluoride) measurements to evaluate the Hugoniot EOS for PMMA and polyethylene.

P. R. L. Panton, "Effects of structure on average properties of two-dimensional detonations," *Combust. Flame* **16**, 75 (1971).
Advances the notion that the appropriate sense in which to understand the properties of material behind a detonation front is a spatially and temporally averaged one similar to those used in turbulence modeling.

Q. D. H. Robertson, D. W. Brenner, and C. T. White, "Split shock waves from molecular dynamics," *Phys. Rev. Lett.* **67**, 3132 (1991).
MD simulation of a phase-transition-induced split in the shock wave.

R. J. Roth, "Hot spots," in *Encyclopedia of Explosives*, B. T. Fedroff and O. E. Sheffield, Eds. (Dover, N.J., Picatinny Arsenal, 1975), Vol. 7, p. H170.

Basic explanation of Hugoniot EOSs and pressure-induced chemistry.

S. J. Sharma and C. S. Coffey, "Nature of ignition sites and hot spots, studied by using an atomic force microscope," *SHOCK95*, 811 (1996).

AFM micrographs of RDX crystals subjected to drop-hammer tests. Authors conclude that hot-spot areas range from 1 to 10,000 nm and that molecules can show undular patterns due to residual stress from hammer impact or from partial reaction or due to cracking of crystallites. However, there are some features indicative of melting, Munroe jetting, and gaseous byproduct formation. Naval Surface Warfare Center.

T. G. H. Vineyard, "Simple model to explain inhomogeneous structures in shocked solids," *J. Appl. Phys.* **54**, 7198 (1983).

Starts from the point of view of the amplification of existing inhomogeneities in a material under shock loading as a source of stress focusing. Amplification of small differences in viscosity to produce localized heating used as an example. The point is to suggest the possibility that localized shear banding, a hydrodynamic instability, is not necessarily the only source of such behavior.

U. W. W. Wood and Z. W. Salsburg, "Analysis of steady-state supported one-dimensional detonations and shocks," *Phys. Fluids* **3**, 549 (1960).

Early resolution of the question about the stability of the "frozen" CJ point, corresponding to a high-frequency sound velocity. Conclusion is that this point is unstable and will decay to the "equilibrium" CJ point of the products under the conditions presupposed.

V. C. S. Yoo, N. C. Holmes, and P. C. Souers, "Time-resolved temperatures of shocked and detonating energetic materials," *SHOCK95*, 913 (1996).

Measurement of temperatures at the CJ points of three explosives from emission spectra. Gray-body assumption allows a correlation between emission intensity and temperature. The temperatures are estimated to be 3800 K for nitromethane, 2950 K for tetranitromethane, and 4100 K for pentaerythritol tetranitrate. Looks very promising.

4. **Fracture, Spall, and Strength**

A. F. L. Addessio et al., "CAVEAT: A computer code for fluid dynamics problems with large distortion and internal slip," LANL report LA-10613-MS (1986).

CAVEAT code original write-up. Has the virtues of discussing several EOSs and several burn models.

B. F. L. Addessio and J. N. Johnson, "A constitutive model for the dynamic response of brittle materials," *J. Appl. Phys.* **67**, 3275 (1990).

Micromechanical model of crack development with a constitutive relation that maintains some level of compatibility with earlier ductile failure models [2B, 2P]. LANL.

C. F. L. Addessio et al., "CAVEAT: A computer code for fluid dynamics problems with large distortion and internal slip," LANL report LA-10613-MS, Rev. 1 (1992).

CAVEAT code final write-up.

D. F. L. Addessio and J. N. Johnson, "Rate-dependent ductile fracture," *J. Appl. Phys.* **74**, 1640 (1993).

Micromechanical ductile failure model with greater stability with respect to changes in mesh size. Earlier models ignored rate dependence in the plastic response, leading to poor numerical behavior. LANL.

E. S. T. S. Al-Hassani, D. Chen, and M. Sarumi, “A simple non-local spallation failure model,” *Int. J. Impact Engng.* **19**, 493 (1997).
CAVEAT code original write-up. Has the virtues of discussing several EOSs and several burn models.

F. B. W. Asay, G. W. Laabs, B. F. Henson, and D. J. Funk, “Speckle photography during impact of an energetic material using laser-induced fluorescence,” *J. Appl. Phys.* **82**, 1093 (1997).
Use laser fluorescence signals to record speckle pattern. Impact speeds of 0.185 km/s. Nonshock regime. Simulated PBX specimens. Use MESA hydrocode to simulate results, but complain about the lack of an adequate strength model for the material.

G. E. Bar-on and D. Z. Yankelevsky, “Using Maxwell-Boltzmann’s statistics for microcrack distribution function in a failure model,” *SHOCK93*, 1165 (1994).
On the use of microcrack distributions having a Boltzmann form, as opposed to a Weibull or exponential form (as used in the flaw growth models of Grady and Kipp [4L] and Murri, Curran, and Seaman [4U]). Give a single example where it applies.

H. B. M. Belgaumkar, “Shock-induced instability due to crack-like defects in a solid propellant,” *SHOCK81*, 598 (1982).
Mechanical crack failure concepts applied to destabilization of detonation wave propagation. Mostly analytical criteria.

I. R. V. Browning and R. J. Scammon, “Mechanical strength model for plastic bonded granular materials at high strain rates and large strains,” *SHOCK97*, 277 (1998).
Mechanical strength of PBX. LANL.

J. D. R. Curran and L. Seaman, “Dynamic fracture of solids,” *Phys. Rep.* **147**, 253 (1987).
Full article deals with the general topic of fracture, both brittle and ductile. Models presented for the various phenomena associated with each. Statistical distributions of cracks or voids, coalescence of each type of flaw, etc., are used throughout. Sample micrographs showing different types of voids and cracks photocopied separately.

K. P. M. Duxbury and Y. Li, “Scaling theory of the strength of percolation networks,” in *Disorder and Fracture*, J. C. Charmet et al., Eds. (Plenum Press, New York, 1990), Chap. 8, pp. 141–147.
Gauge of material strength through percolation models.

L. D. E. Grady and M. E. Kipp, “Geometric statistics and dynamic fragmentation,” *J. Appl. Phys.* **58**, 1210 (1985).
Excellent summary of various fragmentation models and their histories. Preshattering.

M. M. R. Gurvich, E. Vaccaro, and A. T. Dibenedetto, “Macromechanical evaluation of random strength of heterogeneous materials,” *J. Mater. Sci.* **32**, 1509 (1997).
Purely statistical treatments of mechanical strength in heterogeneous materials. Very general. Seemingly lacking in physical reasoning.

N. H. J. Herrmann and L. de Arcangelis, “Scaling in fracture,” in *Disorder and Fracture*, J. C. Charmet et al., Eds. (Plenum Press, New York, 1990), Chap. 9, pp. 149–163.
Review of scaling properties in fracture.

O. J. N. Johnson, “Dynamic fracture and spallation in ductile solids,” *J. Appl. Phys.* **52**, 2812 (1981).
Dynamic fracture model of expanding copper ring. LANL.

P. J. N. Johnson and F. L. Addessio, "Tensile plasticity and ductile fracture," *J. Appl. Phys.* **64**, 6699 (1988).
Failure model with sufficient generality to account for both tensile response and spall behavior. CAVEAT code application. LANL.

Q. J. N. Johnson, "Spallation by ductile void growth," *SHOCK81*, 438 (1982).
Application of CH model [7F] to void growth rather than void collapse. Model is essentially run in reverse with a pressure inside a void greater than that of the surrounding material. Applied to copper-plate impact experiments. LANL.

R. V. K. Kinra, N. A. Day, K. Maslov, B. K. Henderson, and G. Diderich, "The transmission of a longitudinal wave through a layer of spherical inclusions with a random or periodic arrangement," *J. Mech. Phys. Solids* **46**, 153 (1998).
Longitudinal wave transmission in polymers containing spherical inclusions.

S. M. E. Kipp and L. Davison, "Analysis of ductile flow and fracture in two dimensions," *SHOCK81*, 442 (1982).
Void growth in ductile material fracture modeling and experiments.

T. P. Meakin, G. Li, L. M. Sander, H. Yan, F. Guinea, O. Pla, and E. Louis, "Simple stochastic models for material failures," in *Disorder and Fracture*, J. C. Charmet et al., Eds. (Plenum Press, New York, 1990), Chap. 7, pp. 119–140.
Review of stochastic models of failure. Meakin is famous for diffusion-limited aggregation (DLA) modeling. Not surprisingly, the emphasis is on fracture as the reverse of aggregation, particularly DLA.

U. W. J. Murri, D. R. Curran, and L. Seaman, "Fracture model for high energy propellant," *SHOCK81*, 460 (1982).
Statistical model fragmentation applied to energetic propellants.

V. A. Needleman, "Damage, evolution, instability and fracture in ductile solids," in *Disorder and Fracture*, J. C. Charmet et al., Eds. (Plenum Press, New York, 1990), Chap. 12, pp. 219–238.
Review of damage in ductile solids. Perhaps relevant to release wave behavior.

W. L. Seaman, M. Boustie, and T. de Resseguier, "Use of the Steinberg and Carroll-Holt model concepts in ductile fracture," *SHOCK97*, 219 (1998).
Recent use of DFRACT code, an SRI product. See, as an example of using this code, D. R. Curran, "Computer models of dynamic fracture and fragmentation," *SHOCK93*, 1149 (1994).

X. L. Seaman, D. R. Curran, J. B. Aidun, and T. Cooper, "A microstructural model for ductile fracture with rate effects," *Nucl. Eng. Des.* **105**, 35 (1987).
Smaller version of Physics Report article [4J] focusing on ductile fracture (void nucleation).

Y. L. Seaman, "Development of computational models for microstructural features," *SHOCK81*, 118 (1982).
Summary of microstructural ductile and brittle fracture models. Nonuniqueness a big concern here, as in fragmentation behavior.

Z. D. A. Shockey, L. Seaman, and D. R. Curran, "The micro-statistical fracture mechanics approach to dynamic fracture problems," *Int. J. Fract.* **27**, 145 (1984).

Comparison of continuum and microstatistical models of various void growth and nucleation events and failure events. Presence of and interactions among a multiplicity of voids favor the latter approach.

AA. D. Sornette, A. Johansen, A. Arneodo, J. F. Muzy, and H. Saeur, "Complex fractal dimensions describe the hierarchical structure of diffusion-limited-aggregation," *Phys. Rev. Lett.* **76**, 251 (1996).
Fractal dimensionality of diffusion-limited aggregation.

BB. S. Tamura and Y. Horie, "Discrete meso-dynamic simulation of thermal explosion in shear bands," *J. Appl. Phys.* **84**, 3574 (1998).
Shear banding plays a role in shock synthesis of intermetallics from powders. This simulation may be useful for understanding some heterogeneous materials interactions.

CC. D. L. Tonks, R. Hixson, R. L. Gustavsen, J. E. Vorthman, A. Kelly, A. K. Zurek, and W. R. Thissell, "Spallation studies on shock loaded uranium, Los Alamos National Laboratory document LA-UR-97-3169," *SHOCK97*, 239 (1998).
Spall modeling with CHARADE.

DD. M. Vujosevic and D. Krajcinovic, "Creep rupture of polymers—A statistical model," *Int. J. Solids Struct.* **34**, 1105 (1997).
Creep rupture in epoxy resins modeled statistically on a two-dimensional lattice.

EE. T. Vu-Khanh, "Time-temperature dependence in fracture behavior of high impact polystyrene," *Theor. Appl. Fract. Mech.* **29**, 75 (1998).
Fracture in polystyrene as it depends on temperature and load rate. Even toughened polystyrene will fracture in a brittle mode when loaded fast enough.

5. **Fragmentation**

A. B. W. Asay, G. W. Laabs, B. F. Henson, and D. J. Funk, "Speckle photography during impact of an energetic material using laser-induced fluorescence," *J. Appl. Phys.* **82**, 1093 (1997).
Experiments and modeling on PBX fragmentation. Speckle photography of surface displacements during high-strain-rate impacts. LANL.

B. P. Bak, C. Tang, and K. Wiesenfeld, "Self-organized criticality," *Phys. Rev. A* **38**, 364 (1988).
One of the founding articles on self-organized criticality. Helps establish the vast generality of criticality concepts and their scaling behavior. Not specific to fragmentation.

C. E. Ben-Naim and P. L. Krapivsky, "Multiscaling in fragmentation," *Physica D* **107**, 156 (1997).
Multiscaling fragmentation processes, general concept. Generalized random scission model (multidimensional instead of the more usual one-dimensional form), shows more complex behavior—multiscaling behavior in which each subdimension obeys a different scaling law. Scaling appears at long times. Method suffers a deficiency also found in earlier references: a loss of mass/volume to zero-mass/-volume entities, which of course should be monomeric units. Maslov [5Q] takes issue with this approach for precisely this reason. Zero-mass entities make fine sense mathematically, but are nonsense physically. Dissipation stops at the monomeric unit. Placing a lower bound on the mass/volume makes analytical results more difficult to achieve, but the essential scaling behavior survives. See also preprint at Ben-Naim's LANL website.

D. R. Botet and M. Ploszajczak, "Universal features of the off-equilibrium fragmentation with gaussian dissipation," *Phys. Rev. E* **57**, 7305 (1998).
At least gaussian dissipation processes (white noise) preserve the essence of fragmentation scaling.

E. D. Boyer, G. Tarjus, and P. Viot, “Shattering transition in a multivariable fragmentation model,” *Phys. Rev. E* **51**, 1043 (1995).

Example of power-law decay of mass distribution, instead of exponential. Differs from McGrady and Ziff [5R], for instance, in the assumed form of the breakup law. Applicable to polymer decomposition.

F. R. M. Brannon and L. C. Chhabildas, "Experimental and numerical investigation of shock-induced full vaporization of zinc," *Int. J. Impact Engng.* **17**, 109 (1995).

Shock-induced fragmentation of zinc. Fragmentation modes progress from spall to mixed spall and vapor to full vaporization depending on the impact velocity. Results interpreted in terms of proximity to critical point of zinc (ANEOS values), 3175 K, 408.5 MPa, and 2.751 g/cm3. ANEOS EOS, CTH code [1R].

G. W. Christen, U. Even, T. Raz, and R. D. Levine, “The transition from recoil to shattering in cluster-surface impact: An experimental and computational study,” *Int. J. Mass Spectrom. Ion Processes* **174**, 35 (1998).

Ammonia clusters impacting silicon wafer surfaces coated with diamond film. Clusters show a shattering-fragmentation (as opposed to normal fragmentation analogous to evaporation) transition at supersonic velocities for each cluster size. Very small clusters, here leading to a broad transition from one regime to the other.

H. W. Christen, U. Even, T. Raz, and R. D. Levine, “Collisional energy loss in cluster surface impact: Experimental, model, and simulation studies of some relevant factors,” *J. Chem. Phys.* **108**, 10262 (1998).

Similar to [5G]. Small clusters.

I. D. E. Grady, “Fragment size prediction in dynamic fragmentation,” *SHOCK81*, 456 (1982).

Explains the basic energy balance governing fragmentation in impact loading, shock-compression-induced shear banding, and plastic deformation. For this purpose, it is sufficient to consider the simple expression for a nonenergetic material,

$$E(A) = \gamma A + (3\dot{\rho}^2)/(10\rho A^2) ,$$

where E is the energy; A is the area of the fragments; γ is the surface tension or, more generally, the shear-band localization energy; ρ is the material density; and $\dot{\rho}$ is the rate of change of the density. So the total energy is partitioned between surface or interfacial energies and kinetic energy of the fragments. By identifying the strain rate as

$$\dot{\varepsilon} = \dot{\rho}/(3\rho) ,$$

the energy can be expressed in those terms if desired. If local equilibrium is assumed, then the area of the fragments would be governed by the condition

$$dE/dA = 0 ,$$

which leads to the distribution $A = [(3\dot{\rho}^2)/(5\rho\gamma)]^{1/3}$. Other fracture models, especially of the shattering type, would require somewhat different relationships to establish the areal distribution. This is because shattering often implies a supercritical initial state. Nevertheless, the general features of the discussion form essential elements of a required model which may be coupled to strength, fragmentation, and energy production elements.

J. M. K. Hassan, “Multifractality and the shattering transition in fragmentation processes,” *Phys. Rev. E* **54**, 1126 (1996).

Difference between random and uniform initial crack distributions in two systems.

K. E. Hendell, U. Evens, T. Raz, and R. D. Levine, “Shattering of clusters upon surface impact: An experimental and theoretical study,” *Phys. Rev. Lett.* **75**, 2670 (1995).

Shattering behavior of 4 to 40 ammonia molecular clusters impacting a graphite surface. For sufficiently fast initial velocities, the cluster will superheat over virtually the whole cluster in unison before it can dissociate. The cluster, as a whole, shatters. For clusters of 10 or more molecular units, the transition sharpens to a velocity of 7.0 or 7.5 km/s. This type of behavior is typical of a phase transition (e.g., large length scale, abrupt phenomena). As such, the transition can be characterized by a free-energy function. The balance occurs between the internal energy of the different-size fragments and the entropy embodied by the isomeric conformations of those fragments. Specifically, Raz et al. [5U] argue for the application of a maximum entropy formalism that operationally would replace the inequality constraints commonly used in two-phase flow models to bound the behavior of the exchange processes between phases.

L. B. L. Holian and D. E. Grady, "Fragmentation by molecular dynamics: The microscopic 'big bang'," *Phys. Rev. Lett.* **60**, 1355 (1988).

MD simulation of fragmentation process under homogeneous expansion. Results argue for polynomial distribution rather than other models of the fragment mass distribution.

M. N. L. Kafengaus, "Behavior of liquids at supercritical pressures and high temperature gradients," *Fluid Mech. Sov. Res.* **16**, 79 (1988).

Basically describes shattering transition in supercritical fluids. Does not use that language, but the basic elements are present. Uses release behavior of supercritical CO_2 as an example. Cites a power-law relationship, between surface tension and density gradient in the condensed fluid and surrounding vapor. (Developed by van der Waals).

N. F. Kun and H. J. Herrmann, "A study of fragmentation processes using a discrete element method," *Comput. Methods Appl. Mech. Eng.* **138**, 3 (1996).

Simulations of fragmentation including multishock case. Already considered by some to be a seminal calculation in the field. Early numerical evidence for the general theories cited in this fragmentation listing, especially Oddershede et al. [5T]. Uses a pseudo-MD technique to propagate the shock in a macroscopic body. The "atoms" are cell centers. Voronoi polyhedra are constructed around each atom or cell center. The atoms are joined by beams. The material being modeled here is elastic-plastic. So the beams are elastic up to a breaking point, which is determined by a von Mises plasticity criterion. The fragment concentration equation being modeled with the pseudo-MD is exactly the one that Singh and Rodgers use [5W].

O. R. B. Larson, "A simple probabilistic theory of fragmentation," *Mon. Not. R. Astron. Soc.* **161**, 133 (1973).

One of the earliest discussions about fragmentation from a statistical point of view. Masses of interest are galaxies.

P. M. Marsili and Y.-C. Zhang, "Probabilistic fragmentation and effective power law," *Phys. Rev. Lett.* **77**, 3577 (1996).

Derive power-law fragmentation distributions under very general assumptions. Treatment recognizes when fragments are too small to break further. Cite Kun and Herrmann [5H] as crucial numerical evidence for fragmentation theories with power-law behavior. Both initial conditions and fragmentation mechanism are found to influence the full range of physically accessible exponents.

Dimensionality is argued to be of importance in the correlation of energy density throughout a body, with one-dimensional objects having low correlation and three-dimensional ones having high correlation. Even though polymers may be thought of as quasi-one-dimensional under normal conditions, it seems likely that under high compression, they will act more like three-dimensional objects. If this is indeed the case, the analysis of this work applies. If not, the shattering behavior of thin glass rods (also quasi-one-dimensional) may be a better analogy.

Q. D. L. Maslov, "Absence of self-averaging in shattering fragmentation processes," *Phys. Rev.*

Lett. **71**, 1268 (1993).

Discusses self-averaging in shattering processes compared with normal fragmentation. Shattering processes have very large root-mean-square fluctuations in their distributions. Normal processes have small root-mean-square fluctuations. Another characterization of shattering is increasing breakup times with increasing fragment size. Emphasizes the preference for discrete model over continuum model in order to terminate the fragmentation process.

R. E. D. McGrady and R. M. Ziff, "'Shattering' transition in fragmentation," *Phys. Rev. Lett.* **58**, 892 (1987).

Shattering transitions, general concept. Seminal work, but creates fractal dust due to the assumption of a never-ending fragmentation process. Leads to violation of mass conservation. The concept of shattering here refers to generation of the dust, not to the fragmentation of an entire body in unison.

S. A. Meibom and I. Balslev, "Composite power law in shock fragmentation," *Phys. Rev. Lett.* **76**, 2492 (1996).

Compares different mass-law distributions to measured distributions. Both laws give qualitative agreement with these measured distributions. Compare with Grady and Kipp [4L] and Holian and Grady [5L], in which high differentiability is seen. Here, both laws are power laws. The fragmentation mechanisms differ.

T. L. Oddershede, P. Dimon, and J. Bohr, "Self-organized criticality in fragmenting," *Phys. Rev. Lett.* **71**, 3107 (1993).

Among the original experiments on self-organizational behavior, in the sense of Bak et al. [5B, 5Z], on critical fragmentation. Sounds like these guys started breaking things and ended up with a published letter.

Among the most-cited works in the field, it provides some of the most suggestive evidence at the time of its publication for the vast generality of power-law forms, with respect to dimensionality, for the mass distributions of fragmentation. The general form is discussed in Eqs. (II-1 - II-3). Objects of different dimensionality are fragmented (broken), and the transitions to three-dimensional fragmentation from initially quasi-one- and -two-dimensional ones can be observed.

This work is pivotal in stimulating many others to look for more evidence in more diverse settings. In the present context, the next big leap is by Raz et al. [5G-5H, 5U], in which they argue that supercritical fluids shatter as well and therefore follow these same forms.

U. T. Raz, U. Evens, and R. D. Levine, "Fragment size distribution in cluster impact: Shattering versus evaporation by a statistical approach," *J. Chem. Phys.* **103**, 5394 (1995).

Use maximum entropy approach to calculate fragment distributions. Graph-theoretical approach used to calculate entropic contribution for small clusters. Find discontinuous behavior of heat capacity at the evaporation-shattering transition. The use of maximal entropy would replace the entropy constraints as discussed by Passman, Nunziato, and Walsh [9M]; Powers, Stewart, and Krier [9N]; Baer and Nunziato [9A]; and Bdzil et al. [9B] in the release zone if applied to detonation wave behavior. In a macroscopic application, the large-number asymptotic form of the entropy distribution function is all that would be needed. Presumably, this asymptotic form connects to the universal scaling forms of Oddershede et al. [5T].

V. W. A. Saunders, "Metal-cluster fission and the liquid drop model," *Phys. Rev. A* **46**, 7028 (1992).

Shattering of metallic clusters due to a fluid instability caused by Coulombic interactions on a single cluster. Instability only observed in multiply charged clusters. Smaller clusters are the ones susceptible to fissioning, i.e., shattering. The higher the charge, the higher the mass needs to be to maintain stability. Relevant to mass fragments in two-phase flow with velocity differences between the phases large enough to induce ionization.

W. P. Singh and G. J. Rodgers, “Kinetics of depolymerization,” *Phys. Rev. E* **51**, 3731 (1995).
Binary fragmentation processes in depolymerization including a shattering transition in the time-asymptotic regime. Depends on initial conditions, such as object size, initial fragment distribution, and amount of energy introduced. Very general model in which shattering comes about for certain parameter values.

X. O. Sotolongo-Costa, Y. Moreno-Vega, J. J. Lloveras-González, and J. C. Antoranz, “Criticality in droplet formation,” *Phys. Rev. Lett.* **76**, 42 (1996).
Critical transition in mercury droplets to shattering. Use a Bethe lattice model to illustrate the transition. Normal size distribution is log-normal, while the shattered size distribution shows scaling behavior.

Y. C. Tang and P. Bak, “Critical exponents and scaling relations for self-organized critical phenomena,” *Phys. Rev. Lett.* **60**, 2347 (1988).
Companion article to [5B]. Studies critical exponents with discrete simulations.

Z. C. Tang and P. Bak, “Self-organized criticality: An explanation of 1/f noise,” *Phys. Rev. Lett.* **59**, 381 (1987).
Companion article to [5B, 5Y]. Relationship of 1/f, flicker, noise to self-organized criticality, specifically examining self-organized criticality as a source of flicker noise and, more generally, fractal objects.

AA. P. P. Whalen, "Algebraic limitations on two-dimensional hydrodynamics simulations," *J. Comp. Phys.* **124**, 46 (1996).
Simulate isentropic expansion of cylindrically symmetric gas. Show that finite difference methods favor preservation of circularity and entropy while finite element methods favor preservation of circularity and energy. Neither these two methods nor finite volume methods can preserve all three quantities simultaneously.

BB. L. Zhang and X. Jin, “Predicting of fragment number and size distribution,” *SHOCK97*, 227 (1998).
Statistical fragmentation distribution model coupled to dynamic fracture process.

6. **Reaction Dynamics**

A. R. D. Bardo, “Theoretical prediction of novel molecular solids formed at high pressure,” *SHOCK91*, 209 (1992).
Solid byproducts at high pressures. Could also be classed with phase transformation behavior. Argues for superconducting behavior at high dynamic pressures as a general phenomenon for quasi-one-dimensional polymeric systems. Naval Surface Warfare Center.

B. N. C. Blais and J. R. Stine, “A model of reactive dynamics in a detonation,” *J. Chem. Phys.* **93**, 7914 (1990).
Analysis of symmetry restrictions on detonation pressures for different atomic cell sizes in detonation. Symmetry restrictions abate with just a few atoms (six or more) per cell. LANL.

C. D. W. Brenner, C. T. White, M. L. Elert, and F. E. Walker, “Chemical model for intrinsic detonation velocities,” *Int. J. Quantum Chem. Symp.* **23**, 333 (1989).
Early MD simulations on shocks in solids. Simple model of shock velocity self-regulation.

D. M. D. Cook and P. J. Haskins, “The development of a new Arrhenius-based burn model for both homogeneous and heterogeneous explosives,” *SHOCK97*, 337 (1998).

Arrhenius kinetics for both homogeneous and heterogeneous explosives. DYNA2D hydrodynamics simulations.

E. L. L. Davis and K. R. Brower, "Reactions of organic compounds in explosive-driven shock waves," *J. Phys. Chem.* **100**, 18775 (1996).

Pressure-dependent chemical kinetics. I find this argument very persuasive, but the role of shear processes is unaccounted for. Ionic reactions are strongly pressure-dependent. See also *SHOCK95*, p. 775. New Mexico Tech. (Davis is now at LANL).

F. G. Demol, J. C. Goutelle, and P. Mazel, "CHARME: A reactive model for pressed explosives using pore and grain size distributions as parameters," *SHOCK97*, 353 (1998).

Use of CHARME code for explosives with either pore structure or granularity or both. Compare with experiment and with Tang, Johnson, and Forest ["Shock-wave initiation of heterogeneous reactive solids," *J. Appl. Phys.* **57**, 4323 (1985)]. Pore-collapse model from Saurel et al., *Phys. Fluids* **11**, 710 (1999), an enhanced version of the CH model [7F], the standard pore-collapse model.

G. J. P. Dionne and J. H. S. Lee, "Modeling the detonation structure of heterogeneous explosives," *SHOCK97*, 317 (1998).

Nonequilibrium and heterogeneity interplay. Clear discussion of roles played by nonenergetic materials in promoting nonequilibrium behaviors. ZND theory in one dimension for heterogeneous explosives. Cite evidence of non-CJ, nonequilibrium behavior in composite explosives. Use nitromethane and glass beads as an example. The glass beads prevent thermal equilibrium and hence CJ deviations. Naturally, need to use different thermal transport properties in the glass to see the effect in the simulation. Basically, the shock wave has passed, and the HE reacted before the beads heated up. This leaves more heat for the HE, so the detonation front travels faster than predicted by the equilibrium codes.

H. B. W. Dodson, "An exploration study of reactivity in organic compounds subjected to shock loading," *SHOCK81*, 62 (1982).

Analysis of some shock reaction byproducts after complete relaxation (i.e., not at the shock front), starting from organic solids. Cites several compounds that are remarkably stable to shock. Polar materials more reactive.

I. B. W. Dodson and R. A. Graham, "Shock-induced organic chemistry," *SHOCK81*, 62 (1982).

General review of reaction products in select organic compounds.

J. A. N. Dremin and L. V. Babare, "The shock wave chemistry of organic substances," *SHOCK81*, 27 (1982).

General discussion of mostly polymerization reactions under shock loading. Point out the differences in reactions under static compression (hydrostatic loading) and shear compression, uniaxial strain and other asymmetric loadings, the small time scales of the shock passage relative to reaction, and vibrational relaxation rates. These are nonthermal and nonhydrodynamic equilibrium effects. The thinking here bears more resemblance to that of Gilman than of Graham.

K. N. S. Enikolopyan, V. N. Vol'eva, A. A. Khzardzhyan, and V. V. Ershov, "Explosive chemical reactions in solids," *Dokl. Akad. Nauk SSSR* **292**, 1165 (1986).

Experimental demonstration of shear effects in organic solid explosive reactions. Compare yields of simple peroxide reactions as they depend on the relative shock and crystallographic orientations. Foundational work for Dremin et al. [6J] and for Gilman [6R-6S].

L. N. S. Enikolopyan, "Detonation, solid-phase chemical reactions," *Dokl. Akad. Nauk SSSR* **302**, 630 (1988).

Experimental demonstration of solid-solid conversion in a thermite mixture (e.g., Al + Fe_2O_3) shocked within a Bridgman anvil. The products do not have to pass through a gas phase as an intermediate; the temperature stays far below that of the thermal analog; and the reaction rate is at least an order of magnitude higher.

M. J. J. Erpenbeck, "Two-reaction steady detonations," *Phys. Fluids* **4**, 481 (1961).
Although more oriented toward stability analysis, article is included here as an example of how reaction kinetics, particularly endothermic branches, can lead to instability, non-CJ behavior, and nonequilibrium states.

N. H. Eyring, "Starvation kinetics," *Science* **199**, 740 (1978).
Argument for starvation kinetics in gaseous and solid detonations. The basic idea is that a shock atom has a translational energy that is out of equilibrium with some nearby atoms that are at some cold vibrational level. Simultaneous with surmounting reaction barriers, the translationally hot atom is equilibrating with its surroundings.

O. J. C. Foster, Jr., F. R. Christopher, L. L. Wilson, and J. Osborn, "Mechanical ignition of combustion in condensed phase high explosives," *SHOCK97*, 389 (1998).
Low shock environments studied with Frank-Kamenetski thermal explosion model ["Calculation of thermal explosion limits," *Acta Physicochimica U.S.S.R.* **10**, 365 (1939) and the discussion in Mader [1S].] Several mechanical models included as sources of ignition in HE. Most models come from LANL. Authors from or closely associated with the U.S. Air Force.

P. M. J. Frankel, "Pressure dependent vibronic relaxation in shocked explosives," *SHOCK81*, 593 (1982).
Influence of pressure on molecular vibrational relaxation processes under shock conditions. Begins with an equipartition of shock energy into intermolecular vibrational modes. Relaxation consists of energy transfer from these modes into intramolecular modes, which cause bond breaking. At some point in this process, any fragmentation model requires that the energy deposition become very unequal. Naval Surface Warfare Center.

Q. J. Franken, S. A. Hambir, D. E. Hare, and D. D. Dlott, "Shock waves in molecular solids: Ultrafast vibrational spectroscopy of the first nanosecond," *Shock Waves* **7**, 135 (1997).
Companion paper to [6U]. Claim 50 ps time resolution of 675 K temperature, 4 km/s, 25 ps risetime, 5 GPa peak pressure shock in anthracene and NTO high explosive.

R. J. J. Gilman, "Chemical reactions at detonation fronts in solids," *Philos. Mag. B* **71**, 1057 (1995).
Discussion of compression-induced metallization, [N. F. Mott, bond-bending metallization, and the piezoelectric effect (compression-induced polarization). Makes terrific sense physically and chemically, perhaps even compelling, but is unorthodox compared with the norm for this field. Series of articles over 20 years developing the basic themes discussed here. A drastically different view of reaction dynamics at a shock front, at least compared with, for instance, Tarver [6BB-6CC] and Davis [6E]. In a nutshell, Gilman thinks that nonadiabatic pathways dominate at the kinetics just after the vN pressure spike. Might be an example of the physical phenomena being insensitive to details of the model being applied, or perhaps is part of the picture needed to explain initiation, damage-accumulation sensitivity, and DDT behavior.

S. J. J. Gilman, "Mechanochemistry," *Science* **274**, 65 (1996).
Illustration of basic concepts discussed in [6R].

T. R. A. Graham, "The electrical-to-chemical connection," *SHOCK81*, 52 (1982).

General discussion about polarization of molecules under shock loading. As discussed in other references [7I-7J] for Graham's bond-scission model, the basic concept and observation are at odds with each other. Bond scission, leading to two radical species, does not lead to charge separation as the data require.

U. D. E. Hare, J. Franken, D. D. Dlott, E. L. Chronister, and J. J. Flores, "Dynamics of a polymer shock optical microgauge studied by picosecond coherent Raman spectroscopy," *Appl. Phys. Lett.* **65**, 3051 (1994).

Chemical dynamics of shocked PMMA monitored through vibrational shifts observed through coherent Raman spectroscopy. Embedded optical gauges have ns response times. I think that they, and some other "CARS" references, mean coherent anti-Stokes Raman spectroscopy. Companion article is *Chem. Phys. Lett.* **244**, 224 (1995).

V. W. M. Howard, P. C. Souers, and L. E. Fried, "Kinetic calculations of explosives with slow-burning constituents," *SHOCK97*, 349 (1998).

Polymers as "bad HE" notion. More typically referred to as nonideal HE or nonenergetic materials in the context of explosively driven shocks. Modified equilibrium code CHEETAH v. 1.40 so that some detonation behavior is captured. Treat explosive and binder as separate entities. Binder is modeled as an Einstein oscillator to prevent it from reacting. The Einstein temperature, which calibrates the model to a real system, can be artificially raised to prevent heat adsorption. LLNL.

W. C. Hübner, E. Geissler, P. Elsner, and P. Eyerer, "The importance of micromechanical phenomena in energetic materials," *Propell. Explos. Pyrotech.* **24**, 119 (1999).

The interplay between mechanical insult and accidental explosions and fires.

X. J. E. Kennedy and J. W. Nunziato, "Shock-wave evolution in a chemically reacting solid," *J. Mech. Phys. Solids* **24**, 107 (1976).

Laser interferometry used to deduce a value of energy release rate at a shock front in PBX. Some of the early measurements, showing that reaction takes place largely after passage of the shock front. This is a basic assumption of ZND theory. See articles by Tarver [6BB–6DD] for more discussion. SNLA.

Y. A. L. Nichols, "Nonequilibrium detonation of composite explosives," *SHOCK97*, 345 (1998).

Nonequilibrium detonation in composite explosives. Tracks various transit and equilibration times to determine reaction completeness. Can assess changes in shock speed depending on chemical reaction completeness. Uses Ree's CHEQ code with modifications. LLNL.

Z. D. A. Rose and C. C. Martens, "Coherent ultrafast vibrational excitation of molecules in localized shock wave fronts," *J. Phys. Chem.* **101**, 4613 (1997).

Theory of coherent shock-induced vibrational excitation of molecules in solids. Treat a diatom solid.

AA. L. I. Stiel and E. L. Baker, "Detonation energies of explosives by optimized JCZ3 procedures," *SHOCK97*, 357 (1998).

JCZ3 EOS detonation dynamics in PBX. Consider this EOS, with sufficient generalization, a successor to JWL. Use a free-energy minimization along an adiabatic expansion to establish EOS parameters. The JCZ3 EOS relies on effective exponential-six pair interactions for calculating thermodynamic quantities. Methodology mainly reported in internal and program reports. Make comparisons among JCZ3, JWL, BKW, and Peng-Robinson EOSs.

BB. C. M. Tarver, "Chemical energy release in one-dimensional detonation waves in gaseous explosions," "Chemical energy release in the cellular structures of gaseous detonation waves," and "Chemical energy release in self-sustaining detonation waves in condensed explosives," *Combust. Flame* **46**, 111, 134, and 156 (1982).

NEZND theory of gas-phase and solid-phase detonations. Companion papers supporting concepts expounded in [6CC]. LLNL.

CC. C. M. Tarver, "Multiple roles of highly vibrationally excited molecules in the reaction zones of detonation waves," *J. Phys. Chem.* **101**, 4845 (1997).

Non-equilibrium ZND theory with starvation kinetics originated by Eyring [6N] for solid explosives. Detonation kinetics broken out into four steps, analogous to gas-phase detonations. Zone thicknesses differ considerably from the gas-phase case, though. LLNL.

DD. C. M. Tarver, R. D. Breithaupt, and J. W. Kury, "Detonation waves in pentaerythritol tetranitrate," *J. Appl. Phys.* **81**, 7193 (1997).

Discussion of detonation waves, specifically in pentaerythritol tetranitrate. CJ detonation model, JWL EOS in a DYNA2D hydrodynamics simulation. ZND model of ignition and growth needed to explain superdetonation in highly densified preforms.

EE. D. K. Zerkle, "Phase segregation effects on the calculation of ODTX in HMX spheres," *Comb. Flame* **117**, 657 (1999) and "LA-UR-98-1238, Multiphase treatment of ODTX in HMX spheres," memo CST-6-U-97:93 to Phil Howe, (1997).

Quantifies the temperature deviation from the single-phase model of one-dimensional time-to-explosion from heat-transfer effects originating in multiphase systems. FLUENT code. LANL.

7. **Shocked Porous Media**

A. U. Alon, J. Hecht, D. Ofer, and D. Shvarts, "Power laws and similarity of Rayleigh-Taylor and Richtmyer-Meshkov fronts at all density ratios," *Phys. Rev. Lett.* **74**, 534 (1995).

Extension of original Richtmyer-Meshkov analyses dealing with the linear regime of front development. Bubble and spike fronts are analyzed. Key physical property is the Atwood number, $(\rho_1-\rho_2)/(\rho_1+\rho_2)$ where ρ_1 and ρ_2 are the mass densities of the two materials in the shocked interface. Find that the bubble and the spike velocities behave inversely with time in the asymptotic limit.

B. M. R. Baer, "A numerical study of shock wave reflections on low density foam," *Shock Waves* **2**, 212 (1992).

Simulation of Skews' experiments on weakly shocked, low density open-cell polyurethane foam. Uses mixture theory of Baer and Nunziato [9A]. Foam density is 0.0148 g/cc, and initial shock pressure from an air-gun driver is 1 MPa. Finds good agreement with details of the experiment such as interactions with rigid cylinder walls, peak pressures at the back wall, and interactions of the compressed foam with secondary (reflected) shock waves.

C. M. R. Baer, R. A. Graham, M. U. Anderson, S. A. Sheffield, and R. L. Gustavsen, "Experimental and theoretical investigations of shock-induced flow of reactive porous media," SNLA report SAND-96-1378C (1996).

Recent example of a complete DDT simulation with Kel-F binder and HMX crystals. CTH code, Baer-Nunziato mixture theory, Maxwell model of viscoelastic response of Kel-F, elastic–perfectly plastic strength models for both binder and HMX crystals, and Mie-Grüneisen EOS for HMX. Modest shock speeds (1–3 km/s) in a square-cylindrical geometry.

Emphasize the need for multistep chemistry, thermal conduction, binder-HMX interface model, material strength, shear localization, and nonjump structure of the front. Bdzil and coworkers uncomfortable with amount of gaseous diffusion allowed in the CTH code.

D. L. C. Bolkhovitinov and Yu. B. Khvostov, "Polystyrene and copper isentropes obtained on the data of shock compressed materials of high porosity," *Lett. Appl. Eng. Sci.* **22**, 491 (1984).

Closed-cell polystyrene and copper show remarkable similarity in the structure of their shock behavior. Large amounts of gasification and extensive damping of the shock wave and speed in both cases for sufficiently low initial density. See gas-shock dynamics in those cases.

E. L. G. Bolkhovitinov and Yu. B. Khvostov, “The Rankine-Hugoniot relation for shock waves in very porous media,” *Nature* **274**, 882 (1978).

The most comprehensible of the Russian papers on the topic. Rankine-Hugoniot relations are adjusted for heat of vaporization due to shear heating. For the case in which the density is sufficiently low to make the shock behavior appear to be in the gaseous regime. Argue that shocked, low-density foams can be modeled as detonations.

F. M. M. Carroll and A. C. Holt, “Static and dynamic pore-collapse relations for ductile porous materials,” *J. Appl. Phys.* **43**, 1627 (1972).

Single-phase model of changes in EOS, internal energy, and local heating, accounting for presence of porosity in a shocked material. The absence of separate phases is compensated for by treating compaction and reaction-progress variables as additional thermodynamic variables. Ubiquitous.

G. M. M. Carroll, K. T. Kim, and V. F. Nesterenko, “The effect of temperature on viscoplastic pore collapse,” *J. Appl. Phys.* **59**, 1962 (1986).

Include temperature dependence in viscosity and yield-strength properties of the CH dynamic pore-collapse model [7F]. Importance of temperature effects depends on whether viscoplastic properties or inertia effects dominate the pore collapse mechanism. That is, materials properties are important for viscous and high-yield-strength materials and for low-shock pressures, while inertia effects, i. e. the amount of kinetic energy deposited in the pore-collapse process, dominate for the opposite sets of conditions of materials properties and shock pressures. Use compaction of solid copper powder as a test material. Concepts and results jibe well with Vineyard's arguments [3T].

Mark Smith (LANL) would argue that yield strength is an inappropriate measure of the energy dissipation for viscoelastic materials and open-cell polymeric foams. A more appropriate one would be toughness, i. e. the area under the stress-strain curve. So, whereas metals have a relatively high yield strength compared to viscoelastic polymers, they break, and hence stop dissipating energy, after small strains. Viscoelastic polymers, on the other hand, yield easily but can be strained much more extensively, leading to much greater energy dissipation than suggested by their yield strength. This would account for the shock-adsorption properties of open-cell foams and differentiate open- and closed-cell foams through the range of allowed strain in the pore-collapse process.

H. D. S. Drumheller, “A theory for the shock-loading response of an alumina-filled epoxy,” *SHOCK81*, 527 (1982).

Example of results for filled polymer composites from the armor programs.

I. R. A. Graham, “Shock-induced electrical activity in polymeric solids. A mechanically induced bond scission model,” *J. Phys. Chem.* **83**, 3048 (1979).

“The bond scission model” of electrical activity in shock-loaded polymers. Strong correlation between polarization and conduction. Associated with the broader field of mechanochemistry. Bond scission here follows the traditional polymeric notion of free-radical formation. However, these species possess only weak electrical activity. As noted in [7OO], elongation of dipoles makes much more sense physically, leading to charge separation with bond breakage according a probability proportional to the partial charges on the different atoms constituting the polymer. Even in Graham’s own work, the preponderance of evidence is that nonpolar systems like polyethylene exhibit little electrical activity, whereas PMMA shows much greater activity.

J. R. A. Graham, P. M. Richards, and R. D. Shrouf, “Direct evidence for formation of radicals in a shock-loaded polymer,” *J. Chem. Phys.* **72**, 3421 (1980).

Looked for radical formation in shock-loaded polymers. Didn't seem to find any, which contradicts Graham's own bond-scission model [7I] of these processes. Russian concept of dipole elongation described in [7OO] seems much more on the mark.

K. L. G. Gvozdeva and Yu. M. Faresov, "Approximate calculation of steady-state shock wave parameters in porous compressible materials," *J. Appl. Mech. Tech. Phys.* **83**, 107 (1986).

Model the shock behavior of open-cell polyurethane foam, assuming ideal gas behavior of the air and incompressibility of the polymeric material forming the skeleton of the foam. Infiltration of gases in an open-cell foam ahead of the front reported to be "insignificant" for strong shocks. Also neglect heat exchange between foam and air. Estimate 76 % porosity behind the front starting from 95 % porosity, based on a heat capacity ratio of 1.4.

This estimate implies that the greatest compression possible for an ideal gas with this heat capacity ratio is a factor of 6. However, Holmes et al. [7M] can compress silica aerogel by factors of 6-7 starting from the same 95 % porosity levels. One way to reconcil the difference is to change the value of the heat-capacity ratio. Holmes measurements substituted into the equations of this work imply a heat-capacity ratio of 1.28 instead of 1.4.

Also, Holmes et al. [7N] shocked carbon aerogels, achieving a compression factor of 3.7 starting from 74 % porosity, as determined from the density of diamond of 3.52 g/cc. The carbon aerogel may be a more appropriate material to compare to.

L. J. Hecht, U. Alon, and D. Shvarts, "Potential flow models of Rayleigh-Taylor and Richtmyer-Meshkov bubble fronts," *Phys. Fluids* **6**, 4019 (1994).

Detailed exposition of results given in [7A]. Here it is made clear that the initial front propagation rate is linear in time; that the spike velocity becomes constant after this for Atwood number identically equal to one; that the spike velocity decays for Atwood numbers less than one; that the universality of the asymptotic behavior comes from drag between the "bubble" fluid and the "spike" fluid; that the saturation time should be on the order of $\lambda/(3\pi v_0)$, where v_0 is the initial velocity of the front; and that bubbles slow exponentially as they approach a rigid wall. The asymptotic velocity goes as $\lambda/(3\pi t)$ or as λ/C_s, where C_s is a sound speed in the material.

The analysis is derived from the Bernoulli equations for the flow field. The RM case is regarded as the g = 0 case of the Rayleigh-Taylor instability analysis, where g is the acceleration constant.

M. N. C. Holmes, H. B. Radousky, M. J. Moss, W. J. Nellis, and S. Henning, "Silica at ultrahigh temperature and expanded volume," *Appl. Phys. Lett.* **45**, 626 (1984).

Demonstrate that densities of a material intermediate of the solid and gas densities can be achieved through strongly shocking porous samples. Silica aerogel at $1/20^{th}$ the density of crystalline silica is shocked to a density 6 times higher than the density of the aerogel, but that is still about three times lower than the density of the crystalline material. Very high temperatures, on the order of 1 eV or 11,500 K, are achieved. The shock velocity-particle velocity Hugoniot does not depend on initial density in the 0.06-to-0.128 g/cc range.

N. N. C. Holmes, "Shock compression of low density foams," *SHOCK93*, 153 (1994).

Reiterates silica results, but also adds results from carbon aerogels. The shock velocity-particle velocity Hugoniot does depend on initial density. At sufficiently high initial density, diamond reaction products begin to form. The example given here is initially 0.9 g/cc. Nonmonotonic Hugoniot behavior is seen in the P-ρ plane. The results of Gvozdeva and Yu. M. Faresov suggest that the boundary between diamond and no-diamond formation is around 85 % initial porosity. If the porosity exceeds 85%, it is unlikely that any diamond will form in these nearly pure carbon aerogels.

O. R. L. Holmes, G. Dimonte, B. Fryxell, M. L. Gittings, J. W. Grove, M. Schneider, D. H. Sharp, A. L. Velikovich, R. P. Weaver, and Q. Zhang, "Richtmyer-Meshkov instability growth: experiment, simulation, and theory," *J. Fluid Mech.* **389**, 55 (1999).

Simulations by three different hydrodynamics codes of NOVA laser experiments. Numerical simulations predict the formation of a mushroom head in the spike front which turns back on itself after sufficently long times. The analytical theories do not capture this feature, but do get the peak of the spike correct. Analytical models by Zhang are favored over the asymptotic models of Alon et al. [7A, 7L]. Zhang frames the problem in much the same way that Zaretsky and Ben-Dor do for weak-to-intermediate shocks [7VV-7WW]: Mixing front-growth rates are linear in the perturbation at early times during the compressible stage and nonlinear at the later times during the incompressible stage. Also avoid the impulsive approximation. Note the difference between early time dependence of the impulsive model versus the linearized compressible flow model.

P. L. Houas, E. E. Meshkov, and G. Jourdan, "Overview of diagnostic methods used in shock-tube investigations of mixing induced by Richtmyer-Meshkov instability," *Shock Waves* **9**, 249 (1999).
Overview or compilation of experimental methods used to diagnose shocked, layered materials.

Q. G. I. Kanel', Z. G. Tolstikova, and A. V. Utkin, "Effect of filler-particle size on the cleavage strength of elastomers," *J. Appl. Mech. Tech. Phys.* **34**, 399 (1993).
A rare study in shocked, filler materials. Filling matters.

R. J. Kang, P. B. Butler, and M. R. Baer, "A thermomechanical analysis of hot spot formation in condensed-phase, energetic materials," *Combust. Flame* **89**, 117 (1992).
Most complete of the pore-collapse models. Strong emphasis on viscoplastic properties, roles of surface kinetics, and exchange of material between solid and gas phases.

S. B. A. Khasainov, A. A. Borisov, B. S. Ermolaev, and A. I. Korotkov, "Two-phase visco-plastic model of shock initiation of detonation in high density pressed explosives," in *Proceedings of the Seventh Symposium (International) on Detonation*, (Annapolis, MD, 1981), pp. 435–447.
Viscoplastic pore-collapse model of SDT. Considered a simplification of Kang et al. [7R].

T. O. Ki-Hwan, "Graphical construction of P-U_p porous Hugoniots from solid Hugoniot curve," *SHOCK89*, 109 (1990).
Graphical extrapolation method from solid to porous material, based on an EOS in which the approximation $(\partial E/\partial V)_H \approx (\partial E/\partial V)_p$ is applied to construction of Hugoniots for porous materials.

U. K. Kim and S. I. Oh, /Dynamic compaction of elastic-visco-plastic porous materials under shock," *SHOCK81*, 376 (1982).
Early application of CH pore-collapse model [7F] to RDX under strong-shock conditions.

V. M. Koenig, A. Benuzzi-Mounaix, F. Philippe, B. Faral, D. Batani, T. A. Hall, N. Grandjouan, W. Nazarov, J. P. Chieze, and R. Teyssier, "Laser driven shock wave acceleration experiments using plastic foams," *Appl. Phys. Lett.* **75**, 3026 (1999).
Nova laser experiments driving an aluminum-plastic layered plate. The free aluminum was patterned with square-wave steps and then coated with trimethyl propane triacrylate foam, the same material as the plastic layer on the opposite side of the aluminum layer. Temporal resolution was on the order of 15 ps and the spatial resolution was on the order of 7 μm.

The laser drive creates particle and shock velocities up to 25 and 40 km/s, respectively. These are very strongly driven systems. The variation in acceleration factor, i. e. the ratio of the foam particle velocity to the aluminum particle velocity, is found to follow quite well an analytically-expressed transcendental equation which depends on the ratio of the foam density to the aluminum density, the heat-capacity ratio for aluminum, and the heat-capacity ratio for the foam. The transcendental equation is derived from basic relationships between particle velocity and gradients in thermodynamic properties across a shock front for materials which quickly become ideal gases behind the shock front. Claim good agreement between the analytical model and SESAME table model.

W. A. D. Krall, B. C. Glancy, and H. W. Sandusky, “Microwave interferometry of shock waves. I. Unreacting porous materials, and II. Reacting porous materials,” *J. Appl. Phys.* **74**, 6322 and 6328 (1993).

Monitor degree of ionization and other state variables in material between the shock front and a piston in porous materials. Reactive porous materials exhibit microwave reflectances similar to unreacting material loaded with metal particles.

X. Yu. A. Krysanov and S. A. Novikov, “Shock compression of porous materials,” *J. Appl. Mech. Tech. Phys.* **29**, 814 (1988).

Analytical treatment of porosity effects.

Y. Y. P. Lagutov, L. G. Gvozdeva, Y. L. Sharov, and N. B. Sherbak, “Experimental investigation of gas percolation through porous compressible material under the effect of shock wave,” *Physica A* **241**, 111 (1997).

Low-density (0.97 porosity), open-cell polyurethane foam shocked at 0.55-km/s initial impact speed and 1-bar initial, internal gas pressure. Streak camera record of shock front. For the case in which a mylar cap is placed over the free-surface end of the foam, the thickness of the compression zone increases continuously with time. For the case in which the free-surface end of the foam is left open, the foam is prevented from collapsing immediately because of buildup of high gas pressure. The trailing edge of the compression zone does not coincide with the free surface.

Z. J. Massoni, R. Saurel, G. Baudin, and G. Demol, “A mechanistic model for shock initiation of solid explosives,” *Phys. Fluids* **11**, 710 (1999).

Very complete, but complex, pore-collapse model of shock-to-detonation transition (SDT). This model is considered a simplification of an even more complex model developed by Kang et al. [7R]. Even so, model does not conform to basic concept of Rayleigh instability and to MD simulation results. Although this model is considered to be in the SDT category, the Baer-Nunziato DDT model [9A] is compared and discussed frequently.

AA. R. Menikoff and E. Kober, “Equation of state and Hugoniot locus for porous materials: P-α model revisited,” Los Alamos National Laboratory document LA-UR-99-2364 (1999).

P-α model in the weak compaction regime where decomposition, jetting, and other instabilities can be ignored. Here, the relevant materials properties are frozen and equilibrium sound speed, yield strength of the solid material, and the adiabatic exponent of the solid. Offer the quote, "Porosity is significant only at pressures below the pure solid yield-strength." Clearly, this statement is only true in certain shock-strength regimes. In other regimes, the shock-strength regime is important.

BB. K. O. Mikaelian, “Effect of viscosity on Rayleigh-Taylor and Richtmyer-Meshkov instabilities,” *Phys. Rev. E* **47**, 375 (1993).

Viscosity modifies the early-time perturbation amplitude of Richtmyer which is a constant plus a term linear in time. The viscosity replaces the time by one minus an exponential in time. The exponent is quadratic in the pertubation wave number and linear in the composite viscosity, $(\mu_1 + \mu_2)/(\rho_1 + \rho_2)$. Surface tension causes a oscillatory time dependence. A turbulence energy model is derived from the viscous results.

CC. K. O. Mikaelian, “Analytic approach to nonlinear Rayleigh-Taylor and Richtmyer-Meshkov instabilities,” *Phys. Rev. Lett.* **80**, 508 (1998).

Improved form of the early-time, inviscid results.

DD. J. W. Mintmire, D. H. Robertson, D. W. Brenner, and C. T. White, “Molecular dynamics simulations of pressure wave effects at voids in a model condensed-phase material,” *SHOCK91*,

147 (1992).

MD evidence supporting pore-collapse models.

EE. J. W. Mintmire, D. H. Robertson, M. L. Elert, D. W. Brenner, and C. T. White, "Molecular dynamics of void collapse mechanisms in shocked media," *SHOCK93*, 969 (1994).

MD simulation of pore collapse. Concept and results apply generally to both HE ignition and foam behavior. Brenner, now at North Carolina State University, is the author of a well-known hydrocarbon potential [*Phys. Rev. B* **42**, 9458 (1990)] and is working with Ree (LLNL) on a generalization to handle an arbitrary $C_xH_yO_zN_w$ mixture/composition. The standard pore-collapse model is from CH [7F]. Find generally good agreement. The MD results support the basic physical picture of the model.

FF. C. E. Morris, "Shock-wave equation-of-state studies at Los Alamos," *Shock Waves* **1**, 213 (1991).

Strongly shocked foam model. Finds shock-velocity (U) - particle-velocity (u) relationship of the form U = S u, where S is a constant. Zaretsky and Ben-Dor [7VV-7WW] show that $S = \rho_s/(\rho_s-\rho_c)$. The densities ρ_s and ρ_c are for the solid material and the foam material, respectively. Actually this paper has this same relationship in different form. Morris wants to verify the relationship empirically. There is the long-standing puzzle of why there is no zero-order (zero pressure) term. Uses polystyrene foams for impedance mismatch experiments.

These results seem to be at odds with the low shock-speed results discussed in other papers. Perhaps this is because the experiments performed here are in fact all in the strong-shock regime.

There is also, for foams, the useful relationship that the Mie-Grüneisen parameter has the value $\gamma = 2(S-1)$, independent of temperature.

GG. V. F. Nesterenko, "Thermodynamics of shock compression of porous materials," *Mater. Res. Soc. Symp. Proc.* **22**, 195 (1984).

Basic discussion of behavior of shocked porous materials. Formula for relating heat generated to plastic deformation.

HH. V. F. Nesterenko, M. P. Bondar, and I. V. Ershov, "Instability of plastic flow at dynamic pore collapse," *SHOCK93*, 1173 (1994).

Explore the transition of shear localization in metals to a fluid-like regime.

II. M. Olim, M. E. H. van Dongen, T. Kitamura, and K. Takayama, "Numerical simulation of the propagation of shock waves in compressible open-cell porous foams," *Int. J. Multiphase Flow* **20**, 557 (1994).

Present numerical evidence that, even for weak shocks, foam strength is negligible. At least for low-density polyurethane foams, a Mach number of 1.4 defines the boundary between very weak and weak shocks. Assume inviscid air, infinite thermal conduction between air and foam.

JJ. E. B. Orler, "The aging of silica filled polysiloxane composites," Los Alamos National Laboratory document LA-UR-99-0936 (1999).

Discusses basic physical properties and chemical reactivity of polysiloxane, silica, and filled polysiloxane.

KK. T. A. Peyser, P. L. Miller, P. E. Stry, K. S. Budil, E. W. Burker, D. A. Wojtowicz, D. L. Griswold, B. A. Hammel, and D. W. Phillion, "Measurement of radiation-driven shock-induced mixing from nonlinear initial perturbations," *Phys. Rev. Lett.* **75**, 2332 (1995).

Nova laser-driven shock studies of foams to explore the Richtmyer-Meshkov (RM) instability. The RM instability, in which a shock front crosses a material interface between two materials having different initial densities, is the shock analog of the RT instability for gravitational systems. The study

intends to measure mixing lengths and compare the results to the asymptotic solution to the single-mode problem found by Alon et al. [7A]. The asymptotic form depends logarithmically on time.

LL. B. W. Skews, "The reflected pressure field in the interaction of weak shock waves with a compressible foam," *Shock waves* **1**, 205 (1991).
Experiments on weakly shocked, low-density polyurethane foam modeled by Skews et al. [7LL-7MM] and Baer [7B].

MM. B. W. Skews, M. D. Atkins, and M. W. Seitz, "The impact of a shock wave on porous compressible foams," *J. Fluid Mech.* **253**, 245 (1993).
Model experiments on weakly shocked, low-density polyurethane foam first studied by Skews [7LL-7MM]. Reflective gridlines are painted onto the side of the foam layer to act as fiduciary marks for the shock dynamics.

NN. S. F. Son, J. B. Bdzil, R. Menikoff, A. K. Kapila, and D. S. Stewart, "Two-phase flow: Reduced models and numerical simulations" (paper in preparation), private communication, LANL, 1999.

OO. D. S. Stewart, B. Asay, and K. Prasad, "Simplified modeling of transition to detonation in porous energetic materials," *Phys. Fluids* **6**, 2515 (1994).
Single-phase DDT model based on CH pore-collapse model [7F]. Compaction variable added to model pore collapse and attendant decrease in internal energy. Thermally sensitive kinetics forces reaction zone to be in the wrong part of the shock front. This seems to be the main flaw in an otherwise very successful model. The study in [7SS] seeks, in part, to overcome this deficiency.

PP. T. G. Trucano and D. E. Grady, "Impact shock and penetration fragmentation in porous media," *Int. J. Impact Eng.* **17**, 861 (1995).
Discussion of a shock Hugoniot for foams, based on an assumption of no pore-collapse heating. The shocked-foam density is assumed to stop increasing (lock) at some specified value, which allows derivation of the Hugoniot relations. Specific treatment of polyurethane foam and saboted copper impactor. Cell structure not specified. Backing material not clear either, but above 4.3 km/s, copper impactors started to show shattering behavior.

QQ. D. C. Wallace, "Thermoelastic-plastic flow in solids," Los Alamos National Laboratory report LA-10119, UC-34 (June, 1985).
Differentiation of elastic-plastic solids and viscoelastic fluids as far as constitutive properties go. Condemns practice of modeling elastic-plastic solids as viscoelastic fluids.

RR. J. Wang and J. Zhang, "Molecular dynamics simulation of ejection induced by reflection of shock wave at free surface of metals," *SHOCK91*, 151 (1992).
MD simulation at free surface included here to illustrate similarity to pore-collapse case.

SS. S. Xu and D. S. Stewart, "Deflagration-to-detonation transition in porous energetic materials: A comparative model study," *J. Eng. Math.* **31**, 143 (1997).
Comparison of one-, two-, and three-phase models of DDT process. The single-phase model homogenizes gas, pore, and solid phases; the two-phase model treats the solid as one phase and the pore and gas phases together. Note that deflagration has more thermal sensitivity to reaction kinetics, whereas shock has greater pressure sensitivity. A reaction progress variable relates compaction, the solids EOS, and the gaseous EOS.

TT. V. V. Yakushev, "Shock-induced electrical polarization of organic materials," *Mater. Res. Soc. Symp. Proc.* **22**, 199 (1984).

Review of shock-induced polarization in organic materials. Presents examples that do not follow the Graham bond-scission model. Basically, shear in polar molecules leads to charge separation, which might then relax violently enough to accelerate shock propagation.

UU. M. Yasuhara, S. Watanabe, K Kitagawa, T. Yasue, and M. Mizutani, "Experiment on effects of porosity in the interaction of shock wave and foam," *JSME Int. J.* **39**, 287 (1996).

Modeling of and experiments on shocked, open-cell polyurethane foam. Examine the influence of different open-foam structures on shock propagation. Conclude that this foam is an intrinsically two-phase system. Open-cell structure necessitates accounting for gas-phase dynamics through the cells. References to shocked rubber materials. No mention of ionization, probably because of the low-shock speeds, 0.57-km/s initial and 0.09-km/s average.

VV. E. Zaretsky and G. Ben-Dor, "Compressive stress-strain relations and shock hugoniot curves of flexible foams," *Trans. ASME* **117**, 278 (1995).

Basic development of a model correcting Herrmann's P- α model, the precursor to the CH pore-collapse model, and the Gibson-Ashby model. The later model is based on numerical correlations. As in [7WW], the model is intended for moderate-shock strengths. Cites mechanical differences in the types of "flexible" foams depending on the mechanical origins of the pore collapse. Elastomers collapse by nonlinear elastic buckling of the cell walls; elastic-plastic foams by plastic yielding of the cell walls; and elastic-brittle by brittle fracture of the cell walls. Also cites Morris [7FF] as producing a model suitable for the strong-shock regime and suggests a simple, analytical relation between shock velocity and particle velocity in low-density foams.

WW. E. Zaretsky and G. Ben-Dor, "Thermodynamic law of corresponding shock states in flexible polymeric foams," *J. Eng. Mater. Tech.* **118**, 493 (1996).

Extension of *P-*α and CH pore-collapse models, which are also related, originated by Gibson and Ashby and formulated as a corresponding states law in stress-strain space:

$$\sigma = E_s\,(a-1)^2/(a)^3\,[x/(1-x) - 27/8x^2]\,,$$

where $x = a\varepsilon$, σ is the compressive stress under uniaxial strain ε, E_s the foam elastic modulus, and $a = \rho_s/(\rho_s - \rho_c)$ with ρ_s and ρ_c the foam and bulk densities, respectively. Intended for moderate shocks, whereas *P-*α and its descendents are intended for stronger shocks.

8. **Phase Transitions in Shocked Materials**

A. J. W. Bates, and D. C. Montgomery, "Some numerical studies of exotic shock wave behavior," *Phys. Fluids* **11**, 462 (1999).

Role of phase transitions and critical points when the shock Hugoniot passes close by. Application to ICF targets. Bates now at LANL.

B. G. Q. Chen, T. J. Ahrens, W. Yang, and J. K. Knowles, "Effect of irreversible phase change on shock-wave propagation," *J. Mech. Phys. Solids* **47**, 763 (1999).

Proximity of shock Hugoniot to model EOS critical points in P-V space for quartz and germanium dioxide.

C. G. E. Duvall and R. A. Graham, "Phase transitions under shock-wave loading," *Rev. Mod. Phys.* **49**, 523 (1977).

Comprehensive review of phase transitions induced by shock loading. Transitions reviewed include first-order polymorphic, second-order, melting, and freezing. Mostly metallic and salt systems.

D. M. E. Fisher, "The nature of criticality in ionic fluids," *J. Phys.: Condens. Matter* **8**, 9103 (1996).

Fundamental issues in criticality of ionic fluids.

E. B. F. Henson, B. W. Asay, R. F. Sander, S. F. Son, J. M. Robinson, and P. M. Dickson, "Dynamic measurement of the HMX β-γ phase transition by second-harmonic generation," *Phys. Rev. Lett.* **82**, 1213 (1999).
The β-γ phase transition in HMX studied by optical second-harmonic generation. Promoted as being key to understanding thermal decomposition in HMX. LANL.

F. E. S. Hertel, Jr., R. L. McIntosh, and B. C. Patterson, "A comparison of phase change phenomena in CTH with experimental data," *Int. J. Impact Engng.* **17**, 399 (1995).
Zn spheres impacting Zn plates modeled with CTH. See progression on debris pattern as in [8H]. Critical constants discussed in [1R].

G. W. M. Howard, P. C. Souers, and L. E. Fried, "Kinetic calculations of explosives with slow-burning constituents," *SHOCK97*, 349 (1998).
CHEETAH thermochemical simulation of explosive-binder mixtures. "Binder-as-bad-HE" concept. Gives an example of work at Naval Surface Warfare Center that uses such a strategy to model the binder.

H. R. J. Lawrence, L. N. Kmetyk, and L. C. Chhabildas, "The influence of phase changes on debris-cloud interactions with protected structures," *Int. J. Impact Engng.* **17**, 487 (1995).
Transition of release wave phase composition with impact speed. Steady progression from all-solid to all-vapor spall. Thin Ti and Al plates are the materials.

I. Z. H. Liu, X. D. Zhang, X. G. Zhu, Z. N. Qi, and F. S. Wang, "Effect of morphology on the brittle ductile transition of polymer blends: 1. A new equation for correlating morphological parameters," *Polymer* **38**, 5267 (1997). This article is the first in a six-part series that appeared in *Polymer* **38** and **39**.
Effects of particle size, distribution, and volume fraction on brittle-ductile transition in polymer blends. Sensitivity to particle size distribution noted especially. Relate toughness to "ligament thickness."

J. Z.-R. Liu, Y.-H. Shao, C.-M. Yin, and Y.-H. Kong, "Measurement of the eutectic composition and temperature of energetic materials. Part 1. The phase diagram of binary systems," *Thermochem. Acta* **250**, 65 (1995).
Comparison of two methods, differential scanning calorimetry and hot stage microscope, for constructing phase diagrams of energetic materials. Good agreement between the two methods is found.

K. A. J. Oshinski, H. Keskkula, and D. R. Paul, "The role of matrix molecular weight in rubber toughened nylon 6 blends: 3. Ductile-brittle transition temperature," *Polymer* **37**, 4919 (1996).
Study of ductile-brittle transition in rubber-toughened nylon. Part of another long series.

L. F. H. Ree, "Supercritical fluid phase separations: Implications for detonation properties of condensed explosives," *J. Chem. Phys.* **84**, 5845 (1986).
Argument for gas-phase phase separation in some explosives. Only get agreement when phase separation is allowed, and then the agreement is best when three phases are allowed. Transition conditions strongly dependent on parameter values; i.e., the system is sensitive.

M. P. X. Tran, D. W. Brenner, and C. T. White, "Complex route to chaos in velocity-driven atoms," *Phys. Rev. Lett.* **65**, 3219 (1990).
MD simulations showing chaotic behavior in dissociation of even a triatomic as a function of particle velocity of the "driver" atom. Pairwise interactions with molecule constrained to be linear.

N. C. Vega, B. Garzon, L. G. MacDowell, P. Padilla, S. Calero, and S. Lago, "The vapour-liquid equilibrium of n-alkanes," *J. Phys.: Condens. Matter* **8**, 9643 (1996).

Demonstrate that a hard-sphere model of normal alkanes can predict the maxima in critical constants as functions of chain length. The peak values of critical pressure occur at 5 or 6 carbon atoms (i. e. n-pentane or n-hexane) for the model and at 4 carbon atoms from experiment.

O. T. Vu-Khanh and Z. Yu, "Mechanics of brittle-ductile transition in toughened thermoplastics," *Theor. Appl. Mech.* **26**, 177 (1997).

Brittle-ductile transitions in two thermoplastics: rubber-toughened nylon and polystyrene. The transition in the nylon occurs close to a solid-solid phase change, whereas the transition in the polystyrene occurs at the rubber-glass transition.

P. C. T. White, S. B. Sinnott, J. W. Mintmire, D. W. Brenner, and D. H. Robertson, "Chemistry and phase transitions from hypervelocity impacts," *Int. J. Quantum Chem. Symp.* **28**, 129 (1994).

MD flyer-plate simulations show detonation and phase transition behaviors even for a diatomic solid.

9. **Multiphase Flow**

A. M. R. Baer and J. W. Nunziato, "A two-phase mixture theory for deflagration-to-detonation transition (DDT) in reactive granular materials," *Int. J. Multiphase Flow* **12**, 861 (1986).

Seminal article that underpins recent work of Asay et al. [3B, 9B].

B. J. B. Bdzil, R. Menikoff, S. F. Son, A. K. Kapila, and D. S. Stewart, "Two-phase modeling of deflagration-to-detonation transition in granular materials: A critical examination of modeling issues," *Phys. Fluids* **11**, 378 (1999).

Massive treatment of two-phase modeling of DDT. Modify a two-phase model for granular materials, originated by Baer and Nunziato [9A] of Sandia National Laboratories, Albuquerque, also formulated for this same problem. Two-phase treatment appears primarily in the preshock region of the front where compaction of grains and nozzling of gas flow make prominent contributions. Very complex model, not suitable for initial efforts, but probably where the program needs to end up.

C. V. M. Bioko, V. P. Kiselev, S. P. Kiselev, A. N. Papyrin, S. V. Poplavsky, and V. M. Fomin, "Shock-wave interaction with a cloud of particles," *Shock Waves* **7**, 275 (1997).

Shock waves propagating through mixtures of gas and solid particles. Here the solid particles are already dispersed uniformly before the arrival of the shock front. Particles build up in front of the shock, eventually producing a reflected shock wave separate from the primary front. As with most studies of this type, at least in subsonic regimes, Stokes flow of the gas around the particles is assumed.

D. M. Bürger, D. S. Kim, W. Schwalbe, H. Unger, H. Hohmann, and H. Schins, "Two phase description of hydrodynamic fragmentation processes within thermal detonation waves," *J. Heat Transfer* **106**, 728 (1984).

Background development for [9E].

E. M. Bürger, K. Müller, M. Buck, S.-H. Cho, A. Schatz, H. Schins, R. Zeyen, and H. Hohmann, "Examination of thermal detonation codes and included fragmentation models by means of triggered propagation experiments in a tin/water mixture," *Nucl. Eng. Des.* **131**, 61 (1991).

Application of IKE code to tin-water mixture explosion, which they characterize as a thermal explosion, as opposed to a chemical explosion. A tin-water mixture reacts violently (very high heat of reaction) to produce steam or vapor, which drives the explosion. Very concerned with fragmentation processes associated with this kind of explosion. Fragmentation still considered a mystery. From my perspective, the water is not in a supercritical state, and so fragmentation probably is not a shattering mode.

F. C. Carachalios, H. Unger, and M. Bürger, “Modeling of multiphase detonations with drop disintegration—description of thermal detonations,” *Chem. Eng. Technol.* **11**, 327 (1988).
Model of thermally generated, vapor-driven detonation. Fragmentation behind the shock front is a natural event in this type of detonation. Interest derives from the reactor safety community.

G. J. S. Duffield, G. Friz, and R. Nijsing, “Critical flow in a chemically reacting two-phase multicomponent mixture,” *Int. J. Multiphase Flow* **20**, 993 (1994).
Excellent discussion of when nonequilibrium models are required and the added difficulty in supplying the physical models of the exchange processes. Focus mostly on the limitations associated with assuming interphase equilibrium.

H. E. P. Fahrenthold, and C. H. Yew, “Hydrocode simulation of hypervelocity impact fragmentation,” *Int. J. Impact Engng.* **17**, 303 (1995).
Implementation of Grady-Kipp fragmentation model [4L] in CTH.

I. W. Gregor, “Theoretical aspects of critical flow and the velocity of sound in disperse two-phase flow,” *Chem. Eng. Sci.* **38**, 1971 (1986).
Derives an expression for a maximum pressure gradient in a two-phase system at a critical point for the system.

J. J. Jena and V. D. Sharma, “Self-similar shocks in a dusty gas,” *Int. J. Non-Lin. Mech.* **34**, 313 (1999).
Large class of self-similar solutions to shock propagation in dusty gases.

K. A. K. Kapila, S. F. Son, J. B. Bdzil, R. Menikoff, and D. S. Stewart, “Two-phase modeling of DDT: Structure of the velocity-relaxation zone,” *Phys. Fluids* **9**, 3885 (1997).
Nonconservative treatment of the relaxation zone behind the shock front intended to shed light on how jump-condition models of shocks should be more faithfully modeled. Nonconservative approach requires high resolution of physics at and behind the front. Offers some comments on the limitations to the Baer-Nunziato model [9A] and references more directly concerned with these limitations.

L. S. V. Kostin, A. G. Strunina, and V. V. Barzykin, “Initiation conditions in the composite charges of heterogeneous systems,” *Fiz. Goreniya Vzryva* (English) **22**, 93 (1986).
Initiation condition based on the “critical condition method,” defined as equalization between the heating from an external source and the HE reaction. For heterogeneous systems, oscillatory behavior in the initiation process is possible, depending on the heat loss and zone thickness of the components. Second component may be either solid byproduct or binder.

M. S. L. Passman, J. W. Nunziato, and E. K. Walsh, “A theory of multiphase mixtures,” in *Rational Thermodynamics*, C. Truesdell, Ed. (Springer-Verlag, New York, 1984), App. 5C.
Discussion of the role of entropy constraints in formulating multiphase flow models. The entropy of the whole system must always be increasing. EOSs and constitutive relations are all required to satisfy this constraint of entropy increase as the balance equations are evolved in time. Principle is stated by Truesdell in *Rational Thermodynamics*, (New York, McGraw-Hill, 1969). Also builds on founding work of Goodman and Cowin [*Archive for Rational Mechanics and Analysis* **51**, 249 (1972)]. The references cited in this paper start in 1823.

N. J. M. Powers, D. S. Stewart, and H. Krier, “Theory of two-phase detonation—Part I: Modeling” and “Part II: Structure,” *Combust. Flame* **80**, 264 and 280 (1980).
Early form of two-phase modeling underpinning Baer-Nunziato model [9A].

O. S. L. Soo, *Multiphase Fluid Dynamics* (Science Press, Beijing, 1990).
General text.

P. T. G. Trucano, and L. C. Chhabildas, "Computational design of hypervelocity launchers," *Int. J. Impact Engng.* **17**, 849 (1995).
Modeling of Sandia Hypervelocity Launcher with CTH code in a mode requiring multiphase release wave description.

Appendix A. References for Porous and/or Polymeric Materials

This list is a compilation of references from Sec. V most directly related to shocked porous materials and/or shocked polymeric materials.

Equations of State

[1G] R. Cauble, T. S. Perry, D. R. Bach, K. S. Budil, B. A. Hammel, G. W. Collins, D. M. Gold, J. Dunn, P. Celliers, L. B. Da Silva, M. E. Foord, R. J. Wallace, R. E. Stewart, and N. C. Woolsey, "Absolute equations-of-state data in the 10–40 Mbar (1–4 TPa) regime," *Phys. Rev. Lett.* **80**, 1248 (1998).

[1O] V. K. Gryaznov, V. E. Fortov, M. V. Zhernokletov, G. V. Simakov, R. F. Trunin, and L. I. Trusov, "Shock compression and thermodynamics of highly nonideal metallic plasma," *Sov. Phys. JETP* **87**, 678 (1998).

[1Q] K. V. Khishchenko, V. E. Fortov, and I. V. Lomonosov, "High-temperature, high-pressure equation of state for polymer materials," *SHOCK97*, 103 (1998).

[1V] C. E. Morris, J. N. Fritz, and R. G. McQueen, "The equation of state of polytetrafluoroethylene to 80 GPa," *J. Chem. Phys.* **80,** 5203 (1984).

[1DD] V. K. Sachdeva, P. C. Jain, and V. S. Nanda, "Equation of state of poly-di-methyl siloxane fluids," *Mater. Res. Soc. Symp. Proc.* **22**, 243 (1984).

[1JJ] M. E. van Leeuwen, "Deviation from corresponding-states behaviour for polar fluids," *Mol. Phys.* **82**, 383 (1994).

[1LL] D. A. Young and E. M. Corey, "A new global equation of state model for hot, dense matter," *J. Appl. Phys.* **78**, 3748 (1995).

Stress-Strain Constitutive Modeling

[2B] S. G. Bardenhagen, M. G. Stout, and G. T. Gray, "Three-dimensional, finite deformation, viscoplastic constitutive models for polymer materials," *Mech. Mater.* **25**, 235 (1997).

[2W] J. Zhang, N. Kikuchi, V. Li, A. Yee, and G. Nusholtz, "Constitutive modeling of polymeric foam material subjected to dynamic crash loading," *Int. J. Impact Engng.* **21**, 369 (1998).

Shock Dynamics and Hugoniot Behavior

[3B] B. W. Asay, S. F. Son, and J. B. Bdzil, "The role of gas permeation in convective burning," *Int. J. Multiphase Flow* **22**, 923 (1996).

[3D] C. S. Coffey, "Energy dissipation and the initiation of explosives during plastic flow," *SHOCK95*, 807 (1996).

[3K] K. A. Gonthier, R. Menikoff, S. F. Son, and B. W. Asay, "Modeling energy dissipation induced by quasi-static compaction of granular HMX," *SHOCK97*, 289 (1998).

[3S] J. Sharma and C. S. Coffey, "Nature of ignition sites and hot spots, studied by using an atomic force microscope," *SHOCK95*, 811 (1996).

[3T] G. H. Vineyard, "Simple model to explain inhomogeneous structures in shocked solids," *J. Appl. Phys.* **54**, 7198 (1983).

Fracture, Spall, and Strength

[4D] F. L. Addessio and J. N. Johnson, “Rate-dependent ductile fracture,” *J. Appl. Phys.* **74**, 1640 (1993).

[4P] J. N. Johnson and F. L. Addessio, “Tensile plasticity and ductile fracture,” *J. Appl. Phys.* **64**, 6699 (1988).

[4W] L. Seaman, M. Boustie, and T. de Resseguier, “Use of the Steinberg and Carroll-Holt model concepts in ductile fracture,” *SHOCK97*, 219 (1998).

Fragmentation

[5E] D. Boyer, G. Tarjus, and P. Viot, “Shattering transition in a multivariable fragmentation model,” *Phys. Rev. E* **51**, 1043 (1995).

[5I] D. E. Grady, “Fragment size prediction in dynamic fragmentation,” SHOCK81, 456 (1982).

[5N] F. Kun and H. J. Herrmann, “A study of fragmentation processes using a discrete element method,” *Comput. Methods Appl. Mech. Eng.* **138**, 3 (1996).

[5R] E. D. McGrady and R. M. Ziff, “‘Shattering’ transition in fragmentation,” *Phys. Rev. Lett.* **58**, 892 (1987).

[5W] P. Singh and G. J. Rodgers, “Kinetics of depolymerization,” *Phys. Rev. E* **51**, 3731 (1995).

Reaction Dynamics

[6D] M. D. Cook and P. J. Haskins, “The development of a new Arrhenius-based burn model for both homogeneous and heterogeneous explosives,” *SHOCK97*, 337 (1998).

[6F] G. Demol, J. C. Goutelle, and P. Mazel, “CHARME: A reactive model for pressed explosives using pore and grain size distributions as parameters,” *SHOCK97*, 353 (1998).

[6Q] J. Franken, S. A. Hambir, D. E. Hare, and D. D. Dlott, “Shock waves in molecular solids: Ultrafast vibrational spectroscopy of the first nanosecond,” *Shock Waves* **7**, 135 (1997).

[6Y] A. L. Nichols, “Nonequilibrium detonation of composite explosives,” *SHOCK97*, 345 (1998).

Shocked Porous Media

[7A] U. Alon, J. Hecht, D. Ofer, and D. Shvarts, "Power laws and similarity of Rayleigh-Taylor and Richtmyer-Meshkov fronts at all density ratios," *Phys. Rev. Lett.* **74**, 534 (1995).

[7B] M. R. Baer, “A numerical study of shock wave reflections on low density foam,” *Shock Waves* **2**, 212 (1992).

[7E] L. G. Bolkhovitinov and Yu. B. Khvostov, “The Rankine-Hugoniot relation for shock waves in very porous media,” *Nature* **274**, 882 (1978).

[7F] M. M. Carroll and A. C. Holt, “Static and dynamic pore-collapse relations for ductile porous materials,” *J. Appl. Phys.* **43**, 1627 (1972).

[7G] M. M. Carroll, K. T. Kim, and V. F. Nesterenko, “The effect of temperature on viscoplastic pore collapse,” *J. Appl. Phys.* **59**, 1962 (1986).

[7N] N. C. Holmes, “Shock compression of low density foams,” *SHOCK93*, 153 (1994).

[7V] M. Koenig, A. Benuzzi-Mounaix, F. Philippe, B. Faral, D. Batani, T. A. Hall, N. Grandjouan, W. Nazarov, J. P. Chieze, and R. Teyssier, "Laser driven shock wave acceleration experiments using plastic foams," *Appl. Phys. Lett.* **75**, 3026 (1999).

[7Y] Y. P. Lagutov, L. G. Gvozdeva, Y. L. Sharov, and N. B. Sherbak, “Experimental investigation of gas percolation through porous compressible material under the effect of shock wave,” *Physica A* **241**, 111 (1997).

[7EE] J. W. Mintmire, D. H. Robertson, M. L. Elert, D. W. Brenner, and C. T. White, “Molecular dynamics of void collapse mechanisms in shocked media,” *SHOCK93*, 969 (1994).

[7GG] V. F. Nesterenko, “Thermodynamics of shock compression of porous materials,” *Mater. Res. Soc. Symp. Proc.* **22**, 195 (1984).

[7KK] T. A. Peyser, P. L. Miller, P. E. Stry, K. S. Budil, E. W. Burker, D. A. Wojtowicz, D. L. Griswold, B. A. Hammel, and D. W. Phillion, "Measurement of radiation-driven shock-induced mixing from nonlinear initial perturbations," *Phys. Rev. Lett.* **75**, 2332 (1995).

[7OO] D. S. Stewart, B. Asay, and K. Prasad, “Simplified modeling of transition to detonation in porous energetic materials,” *Phys. Fluids* **6**, 2515 (1994).

[7PP] T. G. Trucano and D. E. Grady, “Impact shock and penetration fragmentation in porous media,” *Int. J. Impact Eng.* **17**, 861 (1995).

[7RR] J. Wang and J. Zhang, “Molecular dynamics simulation of ejection induced by reflection of shock wave at free surface of metals,” *SHOCK91*, 151 (1992).

[7SS] S. Xu and D. S. Stewart, “Deflagration-to-detonation transition in porous energetic materials: A comparative model study,” *J. Eng. Math.* **31**, 143 (1997).

[7UU] M. Yasuhara, S. Watanabe, K Kitagawa, T. Yasue, and M. Mizutani, “Experiment on effects of porosity in the interaction of shock wave and foam,” *JSME Int. J.* **39**, 287 (1996).

Appendix B. List of Acronyms

AFM	atomic force microscopy
AIP	American Institute of Physics
BKW	Becker-Kistiakowsky-Wilson
CH	Carroll-Holt pore collapse
CJ	Chapman-Jouguet
DDT	deflagration-to-detonation transition
DLA	diffusion-limited aggregation
EOS	equation of state
HE	high explosive
HMX	high-melting explosive
ICF	inertial confinement fusion
JCZ3	"JCZ" EOS, version 3
JWL	Jones-Wilkins-Lee
LANL	Los Alamos National Laboratory
LLNL	Lawrence Livermore National Laboratory
MD	molecular dynamics
NEZND	nonequilibrium Zel’dovich–von Neumann–Doring
PBX	plastic-bonded explosive
PMMA	polymethylmethacrylate
QEOS	quotidian equation of state
RDX	royal demolition explosive
RM	Richtmyer-Meshkov
RT	Rayleigh-Taylor
SDT	shock-to-detonation transition
VISAR	velocity interferometer system for any reflector
ZND	Zel’dovich–von Neumann–Doring

This report has been reproduced directly from the best available copy. It is available electronically on the Web (http://www.doe.gov/bridge).

Copies are available for sale to U.S. Department of Energy employees and contractors from—

Office of Scientific and Technical Information
P.O. Box 62
Oak Ridge, TN 37831
(423) 576-8401

Copies are available for sale to the public from—

National Technical Information Service
U.S. Department of Commerce
5285 Port Royal Road
Springfield, VA 22616
(800) 553-6847

Los Alamos
NATIONAL LABORATORY
Los Alamos, New Mexico 87545